

UNIVERSITÉ DU QUÉBEC

**PALÉOCÉANOGRAPHIE ET VARIABILITÉ CLIMATIQUE SUR LE TALUS
DU MACKENZIE (MER DE BEAUFORT, ARCTIQUE CANADIEN)
AU COURS DE L'HOLOCÈNE RÉCENT**

**MÉMOIRE
PRÉSENTÉ À
L'UNIVERSITÉ DU QUÉBEC À RIMOUSKI**

Comme exigence partielle de la maîtrise en Océanographie

**PAR
MANUEL BRINGUÉ**

Décembre 2009

UNIVERSITÉ DU QUÉBEC À RIMOUSKI
Service de la bibliothèque

Avertissement

La diffusion de ce mémoire ou de cette thèse se fait dans le respect des droits de son auteur, qui a signé le formulaire « *Autorisation de reproduire et de diffuser un rapport, un mémoire ou une thèse* ». En signant ce formulaire, l'auteur concède à l'Université du Québec à Rimouski une licence non exclusive d'utilisation et de publication de la totalité ou d'une partie importante de son travail de recherche pour des fins pédagogiques et non commerciales. Plus précisément, l'auteur autorise l'Université du Québec à Rimouski à reproduire, diffuser, prêter, distribuer ou vendre des copies de son travail de recherche à des fins non commerciales sur quelque support que ce soit, y compris l'Internet. Cette licence et cette autorisation n'entraînent pas une renonciation de la part de l'auteur à ses droits moraux ni à ses droits de propriété intellectuelle. Sauf entente contraire, l'auteur conserve la liberté de diffuser et de commercialiser ou non ce travail dont il possède un exemplaire.

AVANT-PROPOS

J'ai manifesté depuis le plus jeune âge une volonté insatiable de comprendre mon environnement. C'est la grande question du « Comment ? » qui m'a poussé à étudier les sciences de la Terre au niveau collégial, puis universitaire. Les premières réponses concrètes sont apparues dans mes cours de physique qui ont su créer en moi un pont tangible entre la formation de la matière dans l'infiniment petit et le monde perceptible à notre échelle humaine. Réaliser que la matière - tout comme la lumière - est soumise à des lois logiques et quantifiables, a été le point de départ d'une quête que je poursuivrai jusqu'à mon dernier soupir. Lorsque j'ai entamé un premier cycle universitaire en biologie et en géographie à l'Université du Québec à Rimouski (UQAR), je tentais, un peu naïvement, de tout apprendre sur la magie du Vivant et son évolution conjointe avec la matrice qui le supporte. Force a été de constater que chaque réponse contenait en elle-même le germe de dix autres questions! Je ne pouvais pas m'arrêter là...

Le baccalauréat à l'UQAR a été extrêmement profitable pour plusieurs raisons. En premier lieu, de nombreux professeurs et chargés de cours ont eu le génie de savoir transmettre des connaissances de base de qualité, ainsi qu'une passion contagieuse envers les sciences de la Terre. Je remercie à ce titre Richard Cloutier (paléontologie et évolution), Thomas Buffin-Bélanger (géographie, épistémologie), Pierre Blier (pour sa passion, tout simplement!) et Robert Chabot (la science du vivant), pour ne citer qu'eux.

Ensuite, j'y ai été initié aux méthodes et à la démarche scientifique, autrement dit l'art de répondre rigoureusement aux questions que l'on se pose. Et pour finir, c'est dans le cadre d'un projet de recherche au premier cycle que j'ai commencé à travailler avec André Rochon à l'été 2006. André m'a ouvert les yeux sur la paléocéanographie, domaine passionnant qui se trouve au carrefour de la biologie, la (micro-)paléontologie et la géologie marine. Ce projet m'a ouvert les portes sur la maîtrise en océanographie à l'Institut des sciences de la mer de Rimouski (ISMER-UQAR), avec, pour agrémenter le tout, une mission océanographique dans le golfe du St-Laurent (été 2006), une autre sur la côte pacifique mexicaine (2007) et une dernière dans l'est de l'Arctique canadien (2008). J'adresse donc un remerciement tout spécial à André, car il m'a aidé à trouver ma voie et à décrocher plusieurs bourses de prestige. Je le remercie pour tout le temps de qualité dont j'ai bénéficié, ses conseils constructifs, sa patience et sa constante bonne humeur.

Mon projet de maîtrise a donc l'avantage de réunir mes principaux champs d'intérêts, dans le cadre d'une problématique bien actuelle, celle des « changements climatiques ». L'Arctique, de surcroît, est un milieu complexe et fascinant au cœur d'enjeux politiques, économiques et environnementaux considérables. Se servir des enregistrements sédimentaires pour retracer la variabilité climatique passée constitue, à mon sens, un élément déterminant dans notre compréhension de la tendance actuelle au réchauffement global. J'espère que ma contribution pourra servir à mieux cerner la composante naturelle de la variabilité climatique arctique, et que le lecteur aura autant de plaisir à lire ce mémoire que j'en ai eu à l'écrire.

Je tiens à remercier particulièrement ma famille immédiate qui a toujours su me soutenir dans les différentes étapes qui ont mené à l'élaboration du présent mémoire, que ce soit à partir du sol européen (Nicole Cargouët, Daniel Choureaux, Éric Bringué) ou d'ici, au Québec (Gilbert Bringué, Constance de Champlain, Isabelle de Champlain-Bringué). Je dois beaucoup également à ma grande amie Isabelle Paquin, pour la multitude de ses petites attentions quotidiennes, ses précieux conseils et sa présence éclairante. L'énergique Jacques Labrie (Institut des Sciences de la Mer, Université de Québec à Rimouski: ISMER-UQAR) m'a aussi été d'un précieux soutien, grâce à ses remarquables compétences informatiques et techniques le jour, et à sa contrebasse le soir. Je remercie aussi Jean-François Hélie et Bassam Ghaleb (Centre de recherche en géochimie et en géodynamique: GEOTOP, UQAM) ainsi que Claude Belzile (ISMER-UQAR) pour leur grand professionnalisme dans la réalisation et/ou la supervision des analyses isotopiques et granulométriques, respectivement. J'ai eu la chance d'assister à des cours de micropaléontologie donnés par Anne de Vernal (GEOTOP, UQAM) et de la côtoyer à plusieurs reprises; je la remercie pour son enthousiasme et sa passion contagieuse, ainsi que pour les nombreuses lettres de référence qu'elle a accepté de rédiger. Guillaume St-Onge et Gwénaëlle Chaillou (ISMER-UQAR) m'ont aidé à plusieurs reprises pour répondre à mes innombrables questions, notamment au sujet du ^{210}Pb . C'est également le cas de Benoît Thibodeau qui m'a aidé dans l'interprétation des profiles d'isotopes stables. Je remercie également l'équipe administrative de l'ISMER qui a toujours été disposée à soutenir les étudiants dans les multiples démarches qui jalonnent deux années de maîtrise.

Merci aussi au Conseil de Recherche en Sciences Naturelles et en Génie (CRSNG) pour leur soutien financier (bourse ES-M) et le financement du programme CASES. André et moi-même sommes très reconnaissants de la contribution des officiers et de l'équipage du NGCC *Amundsen* lors de la collecte, du sous-échantillonnage et des analyses préliminaires des carottes sédimentaires (notamment David B. Scott et Trecia Schell de l'Université Dalhousie, Robbie Bennett de NRCAN - Dartmouth, Ursule Boyer-Villemaire et Hubert Gagné de Rimouski). Sur le plan professionnel aussi bien que sur le plan personnel, je tiens à souligner les qualités humaines et scientifiques de l'équipe du laboratoire de géologie marine: Francesco Barletta, Agathe Lisé-Pronovost, Marie-Pier St-Onge, Hervé Guyard, Ursule Boyer-Villemaire et Étienne Faubert, sans oublier David Leduc qui m'a tant appris. Merci pour vos conseils, vos rires, votre amitié. Enfin, je tiens à remercier chaleureusement Francine St-Cyr car elle m'a permis d'achever ma maîtrise dans des conditions idéales. Cette liste est loin d'être exhaustive; aussi j'adresse un dernier remerciement à toutes les personnes qui par leur présence, leurs conseils ou leur soutien, ont rendu possible la réalisation du présent mémoire.

RÉSUMÉ

Une séquence sédimentaire prélevée sur le talus du Mackenzie (station CASES 2004-804-803, mer de Beaufort, Arctique canadien) à 218 m de profondeur a permis de documenter la variabilité hydroclimatique au cours des derniers 4600 ans à cet emplacement clé de l'Arctique occidental. La sédimentation y est à la fois influencée par la gyre de Beaufort (impliquée dans le transport des glaces et dans les principaux modes de variabilité hydroclimatiques telle l'Oscillation arctique) et la décharge sédimentaire du Mackenzie, de loin le plus important tributaire de l'Océan Arctique.

La chronologie de la carotte à piston (longueur: ~ 6 m) a été déterminée sur la base de quatre datations AMS-¹⁴C sur des coquilles de bivalves. Le taux de sédimentation résultant est extrêmement similaire à celui estimé à partir de mesures d'activité de ²¹⁰Pb sur les premiers 20 cm de la carotte boîte. La carotte à gravité ayant été corrélée stratigraphiquement à la carotte à piston, on obtient une séquence composite complète couvrant les derniers 4600 ans, avec un taux d'accumulation constant de 140 cm ka⁻¹.

Les reconstitutions quantitatives des paramètres océaniques de surface (température et salinité de surface en août, durée du couvert de glace) ont été estimées à partir des assemblages de kystes de dinoflagellés dans les sédiments en utilisant des fonctions de transfert (méthode des meilleurs analogues modernes). Celles-ci indiquent des conditions de surface relativement stables au cours des derniers 4600 ans. Cependant, des refroidissements épisodiques d'environ 1,5°C sous la valeur actuelle (5,9°C) sont enregistrés entre 700 et 1820 AD, possiblement reliés à l'advection d'eau pacifique froide (valeurs négatives de l'index PDO – *Pacific Decadal Oscillation*). Nous associons le dernier et le plus long de ces refroidissements (1560-1820 AD) avec le Petit Âge Glaciaire. De 1920 à 2004 AD, des variations récurrentes de salinité de surface (oscillant entre ~21 et 27) peuvent être associées au mécanisme d'accumulation d'eau douce par la gyre de Beaufort pendant les régimes de circulation atmosphérique anticyclonique. Nos données indiquent également que des accumulations d'eau douce similaires (qui précèdent les anomalies de salinité documentées dans l'Atlantique Nord) ont pu survenir vers 1790 et 1860 AD.

Les données isotopiques ($\delta^{13}\text{C}$ et $\delta^{15}\text{N}$) indiquent une lente augmentation de l'influence marine (vs terrestre) dans l'origine de la matière organique au cours de l'Holocène récent. Cette variation est attribuable au rehaussement du niveau marin relatif dans la région du delta du Mackenzie, une région côtière particulièrement vulnérable à l'érosion. Nos données suggèrent également que le taux de transgression marine s'est intensifié depuis 1820 AD. Entre 4600 et 1300 cal avant aujourd'hui, des variations séculaires de l'Oscillation arctique sont enregistrées par les mesures de $\delta^{15}\text{N}$ qui mettent en évidence des modifications de l'influence de l'eau pacifique au site d'étude.

Ainsi, cette étude à haute résolution a permis de documenter la variabilité hydroclimatique arctique au-delà des mesures instrumentales récentes. Des changements hydrographiques importants ont pu être mis en évidence au sein de la stabilité climatique relative de l'Holocène récent.

TABLE DES MATIÈRES

AVANT-PROPOS	ii
RÉSUMÉ	vi
TABLE DES MATIÈRE	vii
LISTE DES TABLES	x
LISTE DES FIGURES	xi
LISTE DES ABRÉVIATIONS	xii
CHAPITRE I.....	1

INTRODUCTION ET DISCUSSION GÉNÉRALES

1.1 Introduction générale	2
1.2 Discussion générale	8
1.2.1 Chronologie	8
1.2.2 La technique des meilleurs analogues modernes	9
1.2.3 Analyses de transformées de Fourier et d'ondelettes	10
1.2.4 Variabilité hydroclimatique sur le talus du Mackenzie depuis 4,6 ka AA	11

CHAPITRE II	15
--------------------------	-----------

**LATE HOLOCENE PALEOCEANOGRAPHY AND CLIMATE VARIABILITY
OVER THE MACKENZIE SLOPE (BEAUFORT SEA, CANADIAN ARCTIC)**

Manuel Bringué and André Rochon

2.1 Introduction.....	16
2.2 Environmental settings	18
2.2.1 The Mackenzie Shelf	18
2.2.2 Hydrography of the shelf under riverine influence.....	19
2.2.3 Modes of climate variability	21
2.2.4 The Little Ice Age	22
2.2.5 Relative sea-level rise in the southern Beaufort Sea since the LGM.....	23
2.3 Material and methods.....	24
2.3.1 Sampling	24
2.3.2 Palynological preparation and count.....	25
2.3.3 Dinoflagellate cysts as paleoenvironmental proxies.....	26
2.3.4 Quantitative reconstruction of sea-surface parameters	28
2.3.5 Carbon and nitrogen content, stable isotopes and grain size analyses.....	29
2.4 Chronology of the composite sequence	31
2.5 Results.....	35
2.5.1 Lithology and geochemical properties.....	35
2.5.2 Palynological data.....	37
2.5.3 Quantitative reconstructions	42
2.6 Discussion.....	43
2.6.1 Late Holocene hydrological and climate stability over the Mackenzie Slope.....	43
2.6.2 Relative sea-level rise	44

2.6.3 Variations in Pacific water inflow (zones D1 and D2).....	46
2.6.4 Constraining the Little Ice Age (zone D3).....	48
2.6.5 Hydrological and atmospheric forcing upon sea-ice cover	49
2.6.6 Recent hydrological changes (zone D4)	50
2.7 Summary and conclusions	53
2.8 Acknowledgements.....	55
CHAPITRE III.....	56
CONCLUSIONS GÉNÉRALES	
3.1 Conclusions générales.....	57
RÉFÉRENCES	60
ANNEXE 1	78
ANNEXE 2	79
ANNEXE 3	82
ANNEXE 4	85
ANNEXE 5	86
ANNEXE 6	89

LISTE DES TABLES

Table 1. Radiocarbon dates for core 803PC.....	31
Table 2. Décomptes des dinokystes dans les carottes sédimentaires de la station 803.....	79
Table 3. Concentrations des principaux palynomorphes dans les carottes sédimentaires de la station 803.....	82
Table 4. Liste meilleurs analogues modernes et de leurs distances statistiques pour chacun des assemblages fossiles des carottes de la station 803	86

LISTE DES FIGURES

Fig. 1. Study area.....	19
Fig. 2. Age model for core 803PC.....	32
Fig. 3. Boxcore SR determination from ^{210}Pb data.....	34
Fig. 4. Grain size composition and geochemical parameters of station 803 cores	36
Fig. 5. Concentrations of the main organic-walled microfossils in station 803 cores.....	38
Fig. 6. Dinocyst concentration, proportion of autotrophs (gonyaulacales) vs heterotrophs (peridiniales), relative abundance of the main dinocyst taxa and reconstructed sea-surface parameters from station 803 cores.....	41
Fig. 7. Image du 3.5 kHz <i>subbottom profiler</i> (station 2004-804-803).....	78
Fig. 8. Résultats des exercices de validation	85
Fig. 9. Circulation des eaux pacifiques et atlantiques pendant les phases de circulation atmosphérique anticyclonique / phases négatives de l'Oscillation arctique.....	89
Fig. 10. Circulation des eaux pacifiques et atlantiques pendant les phases de circulation atmosphérique cyclonique / phases positives de l'Oscillation arctique.....	90

LISTE DES ABRÉVIATIONS

CODE	SIGNIFICATION
AA	Avant aujourd’hui (avant 1950)
ACCR	Anticyclonic circulation regime
AD	Anno Domini
AMS	Accelerator mass spectrometry
ANN	Artificial neural network
AO	Arctic Oscillation
BC	Boxcore
BP	Before present (before 1950)
ca.	<i>Circa</i> (environ)
cal	Calibrated year(s)
CASES	Canadian Arctic Shelf Exchange Study
CCGS	Canadian Coast Guard Ship
CCR	Cyclonic circulation regime
cf.	<i>Confer</i> (se réfère à / se compare à)
C_{total} , C_{org} , C_{inorg}	Total, organic and inorganic carbon
D1, D2, D3 and D4	Dinocyst zones 1, 2, 3 and 4

$\delta^{13}\text{C}$	Rapport isotopique $^{13}\text{C}/^{12}\text{C}$
$\delta^{15}\text{N}$	Rapport isotopique $^{15}\text{N}/^{14}\text{N}$
$\delta^{18}\text{O}$	Rapport isotopique $^{18}\text{O}/^{16}\text{O}$
dpm	Disintegrations per minute
e.g.	<i>Exempli gratia</i> (par exemple)
et al.	<i>Et alii</i> (et collaborateurs)
ENSO	El Niño-Southern Oscillation
FOE	Fonction orthogonale empirique
GISP2	Greenland Ice Sheet Project 2
GRIP	Greenland Ice Core Project
GSA	Great salinity anomaly (anomalies)
HCl	Hydrochloric acid
HF	Hydrofluoric acid
HTM	Holocene Thermal Maximum
ISMER	Institut des sciences de la mer de Rimouski
ka	Millier(s) d'années
LGM	Last Glacial Maximum
ln	Logarithme népérien (ou naturel)

MAT	Modern Analogue Technique
NGCC	Navire de la Garde côtière canadienne
NRCAN	Natural Resources Canada
N_{total}	Total nitrogen
OA	Oscillation arctique
PC	Piston core
PDO	Pacific Decadal Oscillation
σ	Standard deviation
SR	Sedimentation rate
SSS	Sea-surface salinity (salinities)
SST	Sea-surface temperature(s)
TWC	Trigger weight core
UQAM	Université du Québec à Montréal
UQAR	Université du Québec à Rimouski
V-PDB	Vienna Pee-Dee Belemnite
vs	<i>Versus</i> (par rapport à)
WA-PLS	Weighted averaging – partial least-square

CHAPITRE I

INTRODUCTION ET DISCUSSION GÉNÉRALES

1.1 Introduction générale

À l'heure où les « changements » climatiques préoccupent la population mondiale, les composantes atmosphériques et océanographiques du milieu arctique, intimement liées, apparaissent comme des éléments clés dans la compréhension des variations climatiques passées, contemporaines et à venir (2004). La tendance actuelle au réchauffement, accompagnée par des inégalités croissantes dans les régimes de précipitations, se manifeste à l'échelle globale (GIEC 2007). C'est cependant dans l'Arctique que le réchauffement anticipé par les modèles climatiques globaux sera le plus prononcé (hausse de 5°C ou plus au pôle d'ici 2100) et que les changements environnementaux sont les plus préoccupants (Manabe et al. 1992, Mitchell et al. 1995, Serreze et al. 2003, McBean et al. 2004).

Le cas du couvert de glace de mer pérenne en est un exemple frappant: les récentes mesures satellitaires indiquent que l'étendue minimale de la glace de mer observée le 14 septembre 2007 était de 38% inférieure aux moyennes historiques (1978-2000 AD; Comiso 2002, Comiso et al. 2008). La diminution de l'étendue des glaces altère le bilan radiatif de la planète par un mécanisme de rétroaction positive dû à l'albédo plus faible de l'eau de mer par rapport à une surface de glace et de neige (Holland and Bitz 2003). Par ailleurs, une décharge d'eau douce plus importante de l'Océan Arctique vers l'Atlantique Nord tend à ralentir la circulation thermohaline, ce qui affecte le climat au niveau planétaire (Häkkinen 1999, Alley and Agustsdottir 2005). Cet exemple illustre bien la position centrale de l'Arctique vis-à-vis du réchauffement global.

Cependant, notre connaissance de la variabilité naturelle du climat de l'Arctique demeure extrêmement limitée. Jusqu'au début des années 1990, l'Arctique était communément considéré comme un milieu relativement stable (Macdonald et al. 2005). De nos jours, cette vision a été remplacée par celle d'un milieu où des changements majeurs peuvent survenir en un laps de temps très court. La variabilité à court terme des conditions climatiques et hydrographiques semble répondre aux variations naturelles du champ de pression atmosphérique associées à l'Oscillation arctique (Rigor et al. 2000, 2002, Steele et al. 2004, Darby et al. 2006, Houssais et al. 2007). L'Oscillation arctique explique en effet 20% de la variance du champ de pression (Thompson and Wallace 1998); elle explique aussi la moitié des variations de températures de l'air en surface (Rigor et al. 2000). Elle est définie comme le premier mode de variabilité d'une fonction orthogonale empirique (FOE) des pressions atmosphériques au niveau de la mer en hiver (octobre à mars) de l'hémisphère Nord (Thompson and Wallace 1998). L'Oscillation arctique (ou plus rigoureusement « Northern-hemisphere Annular Mode ») présente une structure annulaire associée au vortex polaire (Macdonald et al. 2005). L'Anomalie Dipolaire (second mode de variabilité de la FOE; ~ 13% de la variance) présente une structure davantage méridionale (Wu et al. 2006). Dans la mer de Béring et le sud de la mer de Beaufort, les modes de variabilité climatique du Pacifique Nord exercent aussi une certaine influence en raison de leur proximité géographique et de l'advection de masses d'eau pacifique par le détroit de Béring. C'est le cas de la *Pacific Decadal Oscillation* (Niebauer and Day 1989, Bjornsson et al. 1995) et du phénomène *El Niño-Southern Oscillation* (ENSO; Liu et al. 2004). Mais ces modes de variabilité

climatique sont-ils apparus récemment ou ont-ils au contraire gouverné le climat arctique depuis sa stabilisation?

Afin de comprendre la tendance actuelle au réchauffement du climat global, ainsi que pour fournir une base solide aux simulations climatiques, il est essentiel de documenter la variabilité naturelle de l'Arctique à plus long terme. Le manque de données instrumentales historiques antérieures à 1950 AD ne permet pas d'étudier les variations climatiques aux échelles séculaires et millénaires; selon McBean et al. (2004), elles permettent à peine de distinguer si l'Arctique connaît actuellement des « variations » ou des « changements » climatiques. Pour accéder à de plus longues séries temporelles, il faut donc se tourner vers des indicateurs indirects capables d'enregistrer les variations climatiques passées. Les compositions isotopiques de formations minérales (e.g., $\delta^{13}\text{C}$ des spéléothèmes, $\delta^{18}\text{O}$ des carottes de glace groenlandaises et antarctiques) ou de restes fossiles d'organismes vivants (e.g., $\delta^{18}\text{O}$ des récifs coralliens, des cernes d'arbres) peuvent être utilisées à cette fin. En milieu aquatique, les sédiments accumulés sur les fonds lacustres et marins offrent une grande variété de traceurs minéralogiques, géochimiques et micropaléontologiques. Le prélèvement de carottes sédimentaires à des endroits clés (voir annexe 1) permet alors l'accès à des séries temporelles pouvant atteindre des millions d'années (cas d'un faible taux de sédimentation) ou très détaillées (cas d'un taux d'accumulation sédimentaire élevé).

L'objectif de la présente étude consiste à documenter la variabilité hydroclimatique sur le talus du Mackenzie au cours de l'Holocène récent (4600 dernières années). L'Holocène, ou dernier interglaciaire (derniers 10 000 ans) est une période qui a été

qualifiée d'« extrêmement stable » (Dansgaard et al. 1993). Les changements climatiques qui ont accompagné la dernière déglaciation (ca. 18 – 12 ka avant aujourd’hui (AA); Darby et al. 2002, 2006) sont en effet considérables par rapport aux variations mesurées instrumentalement, avec un réchauffement de 5 à 10°C (estimé par le $\delta^{18}\text{O}$ de la carotte de glace GRIP; Anklin et al. 1993, Dansgaard et al. 1993) et un rehaussement du niveau marin global de l’ordre de 130 m (e.g., Peltier 2002, Tarasov and Peltier 2004). Pour l’Arctique, cela implique la submergence des énormes plateaux continentaux (> 50% de l’Océan Arctique actuel; Darby et al. 2006) ainsi que la reprise des échanges avec le Pacifique Nord par le détroit de Béring (England and Furze 2008). Le niveau marin global se serait stabilisé vers 10 ka AA (Darby et al. 2006). La mise en place du régime actuel de circulation des eaux atlantiques et pacifiques dans l’Océan Arctique aurait eu lieu vers 8 ka AA (Hillaire-Marcel et al. 2004, de Vernal et al. 2005a, Ledu et al. 2008), et la stabilisation de l’advection d’eau atlantique par le détroit de Fram et la mer de Barents est estimée à 4,7 ka AA (Lubinski et al. 2001, Voronina et al. 2001, Duplessy et al. 2005). L’Holocène est aussi marqué par un optimum thermique (températures supérieures de $1,6 \pm 0,8^\circ\text{C}$ à la moyenne du XX^e siècle) documenté entre 11 ka AA dans l’ouest et 5 ka AA dans l’est de l’Arctique (Kaufman et al. 2004, de Vernal and Hillaire-Marcel 2006). En comparaison, les conditions hydroclimatiques au cours de l’Holocène récent sont relativement semblables aux conditions modernes; l’étude des fluctuations depuis cette relative stabilisation peut donc nous renseigner sur la variabilité naturelle à long terme dans un contexte très similaire à l’actuel (e.g., Macdonald et al. 2005).

Les carottes sédimentaires qui font l'objet de la présente étude ont été récoltées dans le cadre du Leg 8 du programme CASES (Canadian Arctic Shelf Exchange Study) à bord du Navire de la Garde côtière canadienne (NGCC) *Amundsen* (Rochon and onboard participants 2004). Le lecteur pourra se référer à la section 2.3.1 du présent mémoire pour les détails concernant le prélèvement des carottes à boîte, à gravité et à piston de la station 2004-804-803 (station 803; Fig. 1). À cet emplacement clé du talus du Mackenzie, la sédimentation est à la fois influencée par le gyre anticyclonique de Beaufort (impliquée dans les oscillations climatiques arctiques et le transport des glaces), ainsi que par le fleuve Mackenzie, le plus important tributaire de l'Océan Arctique en termes de charge sédimentaire (Macdonald et al. 1998, Carson et al. 1998).

Les traceurs utilisés pour reconstituer le paléoenvironnement marin sont les kystes de dinoflagellés (ou dinokystes). Leur potentiel et leur utilisation en tant qu'indicateurs des conditions de surface sont détaillés dans les sections 2.3.3. et 2.3.4. Rappelons simplement qu'aux hautes latitudes, ils constituent des traceurs de choix dans la mesure où ils présentent une forte diversité spécifique, alors que d'autres indicateurs couramment utilisés aux basses et moyennes latitudes (e.g., diatomées, coccolithophores) présentent des assemblages quasi-monospécifiques au-delà de l'isotherme de 5°C. Leur paroi étant constituée d'un polymère extrêmement résistant, la dinosporine, les dinokystes ne sont pas affectés par la dissolution (Kokinos et al. 1998), comme c'est le cas pour les organismes à test silicaté (e.g., diatomées, radiolaires et silicoflagellés) et à test carbonaté (e.g., foraminifères, coccolithophores; e.g., de Vernal et al. 2005b, Scott et al. 2008). Outre les assemblages de dinokystes, tous les

palynomorphes (i.e. microfossiles à paroi organique) identifiables ont été dénombrés (voir sections 2.3.2 et 2.3.3). Des analyses granulométriques et géochimiques (carbone total, organique et inorganique, azote total, $\delta^{13}\text{C}$ et $\delta^{15}\text{N}$) ont également été effectuées en vue d'acquérir des éléments d'interprétation complémentaires (voir sections 2.3.5, 2.6.2 et 2.6.3). L'hypothèse de travail est que les conditions hydroclimatiques sont demeurées stables au cours des derniers 4600 ans.

À ce jour, cette étude de la mer de Beaufort est la première à fournir des reconstitutions quantitatives à aussi haute résolution (carottes à gravité et à piston: résolution temporelle de ~ 70 ans; carotte boîte: ~ 7 ans) couvrant l'ensemble de l'Holocène récent. Afin de pouvoir partager les fruits de cette étude avec la communauté scientifique, un article scientifique (présenté au chapitre II) a été rédigé en anglais, selon les normes de présentation de la revue *Canadian Journal of Earth Sciences* (CJES). L'article intitulé « Late Holocene paleoceanography and climate variability over the Mackenzie Slope (Beaufort Sea, Canadian Arctic) » sera soumis pour publication à l'automne 2009.

1.2 Discussion générale

1.2.1 Chronologie

La chronologie des carottes de la station 803 a été estimée à partir de quatre âges AMS-¹⁴C et de mesures d'activité du ²¹⁰Pb sur les 20 centimètres supérieurs de la carotte à boîte. Les modèles d'âge indiquent que la séquence composite couvre les 4600 dernières années, avec un taux de sédimentation élevé ($\sim 140 \text{ cm.ka}^{-1}$; voir section 2.4). Un tel taux d'accumulation confirme que la station 803 se trouve sous l'influence de la plume du Mackenzie (Backman et al. 2004, Richerol et al. 2008a) et permet des reconstitutions paléocéanographiques à haute résolution. Les carottes à gravité et à piston ont été sous-échantillonnées aux 10 cm (résolution temporelle de ~ 70 ans) et la carotte boîte à chaque centimètre (~ 7 ans).

De tels modèles d'âge (Figs. 2-3) représentent bien entendu une approximation de la réalité. En effet, un taux de sédimentation constant sur les 4600 dernières années peut apparaître contradictoire avec les interprétations d'apports d'eau douce variables via le Mackenzie (e.g., section 2.6.5). Nous avons tout simplement appliqué le principe de parcimonie (en accord avec Barletta et al. 2008) qui permet une interprétation simple des signaux présents dans notre séquence sédimentaire.

À noter que la carotte à gravité (dans laquelle aucun matériel datable n'a pu être échantillonné) a été corrélée stratigraphiquement avec la carotte à piston grâce à des mesures de densité (*wet bulk density*) et de susceptibilité magnétique sur les deux carottes

(Barletta et al. 2008). Cet exemple illustre bien l'utilité des études paléomagnétiques dans la détermination de chronologies problématiques.

1.2.2 La technique des meilleurs analogues modernes

Les reconstitutions des paramètres océanographiques de surface (température et salinité de surface en août, durée du couvert de glace) sont établies sur la base des assemblages fossiles de dinokystes à l'aide de fonctions de transfert (de Vernal et al. 2005b). La méthode utilisée est une technique de similarité directe appelée technique des analogues modernes (*modern analogue technique*: MAT; Guiot and de Vernal 2007). À ce sujet, certains éclaircissements s'imposent.

À l'inverse des techniques de calibration (e.g., WA-PLS: *Weighted averaging – Partial least-square*, ANN: *Artificial neural network*), les techniques de similarité n'utilisent pas d'équations établies empiriquement entre des assemblages et un paramètre environnemental; elles ne nécessitent pas de calibration (Guiot and de Vernal 2007). Les assemblages fossiles sont directement comparés à la base de données de référence, ne faisant intervenir qu'un simple calcul de distance (d) donné par la formule:

$$d = \sum_{j=1}^n [\ln f_{ij} - \ln f_{tj}]^2$$

où f = fréquence relative de chaque taxon « j » (exprimée en %)

ij = taxon dans la base de données moderne

tj = taxon dans l'assemblage fossile

n = 63 taxons (dans notre base de données comprenant 1198 sites de référence).

Cependant, l'utilisation de la technique « MAT » repose sur le postulat qu'un assemblage donné se développe sous une combinaison de conditions environnementales identiques à celles qui caractérisent son analogue moderne (Guio et al. 2007). On considère donc que l'écologie des espèces n'a pas changé au cours de la période étudiée, ce qui est raisonnable dans le cas de l'Holocène récent. Les résultats des exercices de validation (voir section 2.3.4) sont présentés en annexe 4.

Le choix du nombre d'analogues est également à justifier. Kucera et al. (2005) considèrent que plus la base de données de référence est grande (et représentative des différents environnements), plus on peut utiliser d'analogues pour les reconstitutions. Selon Peros and Gajewski (2009) qui travaillent sur des assemblages polliniques avec de vastes bases de données de référence, un nombre supérieur à trois analogues comporte l'inconvénient d'augmenter l'intervalle de confiance des reconstitutions. Nous avons donc limité le nombre d'analogues à cinq, ce qui est généralement le cas dans les études utilisant les dinokystes comme paléoindicateurs (e.g., de Vernal et al. 2005a, b, McKay et al. 2008, Ledu et al. 2008).

1.2.3 Analyses de transformées de Fourier et d'ondelettes

Dans le devis de maîtrise figure un type d'analyses absent du présent mémoire: les transformées de Fourier et les ondelettes (*wavelet* en anglais). L'objectif consistait à documenter les *cycles* hydroclimatiques sur la base des différents signaux identifiés dans la séquence sédimentaire étudiée. Nous avons décidé de ne pas poursuivre cet objectif

pour deux raisons. Le fait de corréler trois carottes qui se chevauchent résulte en un pas d'échantillonnage inégal si on les représente en une seule séquence composite. En considérant les séquences individuellement, le nombre de sous-échantillons (carotte boîte: 34; carotte à gravité: 12; carotte à piston: 63) ne permet pas de documenter efficacement les cycles hydroclimatiques, compte tenu de l'« effet bord ». En second lieu, nous jugeons le nombre de datations au ^{14}C insuffisant pour servir de base à des analyses de traitement du signal aussi détaillées (quatre datations pour ~ 6 m de sédiments). Les interprétations auraient été approximatives, ce qui aurait remis en cause la qualité générale du mémoire. Cela n'altère en rien la complétude et la pertinence de l'étude finale dans la mesure où l'objectif principal, celui de documenter la variabilité hydroclimatique des 4600 dernières années sur le talus du Mackenzie, est pleinement atteint.

1.2.4 Variabilité hydroclimatique sur le talus du Mackenzie depuis 4,6 ka AA

Cette section présente les principaux éléments caractérisant la variabilité hydroclimatique à la station 803 au cours de l'Holocène récent (pour une argumentation complète, se référer à la section 2.6).

Les décomptes de dinokystes et les concentrations des principaux palynomorphes présents dans les carottes de la station 803 figurent en annexes 2 et 3, respectivement. Les assemblages de dinokystes (Fig. 6) sont dominés par *Operculodinium centrocarpum* (abondance relative moyenne de 38,1%), *Brigantedinium* spp. (17,7%), les kystes de

Pentapharsodinium dalei (17,6%) et *Islandinum minutum* (16,8%). Les variations des abondances relatives des principaux taxons ont mené à la détermination de quatre zones d'assemblage (Bennett 1996, Juggins 2005). De 4600 à 2700 cal AA (zone D1), les assemblages sont clairement dominés par le taxon autotrophe *O. centrocarpum* (moyenne de 49,0%). Cette dominance est moins nette en zone D2 (2700-1500 cal AA), alors que les taxons hétérotrophes *Brigantedinium* spp. (28,8%) et les kystes de *Polykrikos* sp. var. *arctic/quadratus* (2,8%) sont plus fortement représentés. Les fortes abondances relatives de *I. minutum* (19,9%) caractérisent la zone D3 (1500-30 cal AA ou 450-1920 AD). Enfin, la zone D4 (de 1920 à 2004 AD) est de nouveau dominée par *O. centrocarpum* (44,5%), alors que les taxons *Brigantedinium* spp. et cf. *Echinidinium karaense* y sont presque absents.

Les reconstitutions quantitatives des paramètres océaniques de surface indiquent des conditions relativement stables depuis 4,6 ka AA. L'amplitude maximale des variations de température de surface et de la durée du couvert de glace sont de l'ordre de 1,5°C et 1 mois par année, respectivement (Fig. 6). Cette relative stabilité concorde avec la littérature existante (reconstitutions dans la mer de Beaufort: Rochon et al. 2006; conditions post-HTM: Kaufman et al. 2004; organisation des masses d'eaux comme à l'actuel: Hillaire-Marcel et al. 2004; stabilisation de l'advection d'eau atlantique: Duplessy et al. 2005) mais contraste avec des variations de plus forte amplitude enregistrées dans la mer de Chukchi (de Vernal et al. 2005a, McKay et al. 2008) et la fosse du Mackenzie (Richerol et al. 2008b). Ces variations fines révèlent cependant une série de refroidissements épisodiques d'environ 1,5°C sous la valeur actuelle (5,9°C)

s'étalant de 700 à 1820 AD (Fig. 6). Ces refroidissements sont possiblement la conséquence d'advection d'eau pacifique relativement froide en lien avec des valeurs fortement négatives de l'index PDO (Kim et al. 2004). Nous associons le dernier et le plus long de ces refroidissements (1560-1820 AD) avec le Petit Âge Glaciaire tel que documenté sur le continent eurasien (Solomina and Alverson 2004), dans les carottes de glace groenlandaises (Fischer et al. 1998), dans la Cordillère canadienne (Menounos et al. 2009) et dans l'Arctique canadien (Smol et al. 2005, Podritske and Gajewski 2007, Richerol et al. 2008b).

Les données isotopiques ($\delta^{13}\text{C}$ et $\delta^{15}\text{N}$; Fig. 4) indiquent une lente augmentation de l'influence marine (vs terrestre) dans l'origine de la matière organique au cours de l'Holocène récent. Cette variation est attribuable au rehaussement du niveau marin relatif dans la région du delta du Mackenzie (Hill et al. 1993, 1996, Héquette et al. 1995, Campeau et al. 2000, Manson and Solomon 2007, Lesack and Marsh 2007), une région côtière particulièrement vulnérable à l'érosion (Shaw et al. 1998). Nos données suggèrent également que l'influence marine s'est intensifiée depuis 1820 AD.

Les mesures de $\delta^{15}\text{N}$ enregistrées entre 4600 et 1300 cal AA suggèrent des variations de l'influence d'eau pacifique au site d'étude (Calvert et al. 1992, Meyers 1997). Sous les conditions actuelles, l'advection accrue d'eau pacifique dans le sud de la mer de Beaufort est observée pendant les phases négatives de l'Oscillation arctique (ou régime de circulation atmosphérique anticyclonique; McLaughlin et al. 2002, 2005, Steele et al. 2004, Macdonald et al. 2005). Le profil de $\delta^{15}\text{N}$ suggère donc des variations séculaires de l'OA entre 4600 et 1300 cal AA.

Finalement, les oscillations de salinité de surface depuis 1920 AD (Fig. 6) peuvent être associées au mécanisme d'accumulation d'eau douce par la gyre de Beaufort décrit par Proshutinsky et al. (2002). L'accumulation de glace de mer (essentiellement en épaisseur) et d'eau relativement douce ($< 34,8$) dans la gyre de Beaufort se produit durant les phases de circulation atmosphérique anticyclonique, puis cette eau douce est évacuée vers l'Atlantique Nord pendant les régimes cycloniques. Les phases de circulation atmosphérique anticyclonique et cyclonique alternent sur une base décennale (Proshutinsky and Johnson 1997). Ce phénomène est reconnu comme étant à l'origine des anomalies de salinité (*Great Salinity Anomalies*) observées dans l'Atlantique Nord dans les années 1970 (Dickson et al. 1988), 1980 et 1990 (Belkin et al. 1998, Belkin 2004). Les reconstitutions de salinité de surface suggèrent également que de telles anomalies ont pu avoir lieu autour de 1860 et 1790 AD.

CHAPITRE II

LATE HOLOCENE PALEOCEANOGRAPHY AND CLIMATE VARIABILITY

OVER THE MACKENZIE SLOPE (BEAUFORT SEA, CANADIAN ARCTIC)

Manuel Bringué and André Rochon

Introduction

Recent observations and model experiments confirm that Arctic environments lie in the vanguard of climate change (Serreze et al. 2003, McBean et al. 2004). Significant decrease in sea-ice extent and thickness (Comiso et al. 2008), permafrost thawing (Schuur et al. 2008), coastal erosion (Manson and Solomon 2007) and altered distribution of Arctic species (Derocher et al. 2004) constitute major physical, ecological, sociological, and economic issues (IPCC 2007). Moreover, variations in freshwater export from the Arctic Ocean to the North Atlantic alter the global thermohaline circulation, thus affecting climate on a global scale (Häkkinen 1999, Alley and Agustsdottir 2005). However, the origin of such climate forcings remains unclear. The paucity of observations prior to 1950 AD makes it difficult to distinguish with confidence whether the Arctic undergoes natural climate variability or human induced climate change (McBean et al. 2004). On the basis of recent instrumental data, several modes of climate variability have been identified, such as the Arctic Oscillation (AO). The AO explains 20% of the variance in the northern hemispheric atmospheric pressure field, with strong regional discrepancies (Thompson and Wallace 1998, Macdonald et al. 2005). With regard to long-term variability, paleoceanographic, limnological or driftwood studies (e.g., Dyke et al. 1997, de Vernal et al. 2005a, Smol et al. 2005) could provide useful insights on Holocene climate variability in the Arctic. For instance, Darby and Bischof (2004) and Ledu et al. (2008) have documented AO shifts at centennial and millennial time scales, respectively.

In order to provide a basis for future climate simulations, we need to better constrain long-term climatic patterns that might explain the actual climate trend. For this purpose, the 2004 CASES (Canadian Arctic Shelf Exchange Study) participants collected sedimentary cores covering the Holocene time period in the Canadian Arctic (Rochon and onboard participants 2004). A piston core, its companion trigger weight core and a boxcore were collected at site 2004-804-803 (henceforth station 803; 70°37.976 N / 135°52.815 W; 218 m water depth) over the upper Mackenzie Slope. Sedimentation at this particular location is influenced by both the Beaufort gyre and the Mackenzie River, whose sedimentary discharge is by far the largest among all other Arctic rivers (Macdonald et al. 1998, Carson et al. 1998).

This study focuses on late Holocene hydrological changes over the upper Mackenzie Slope and their implications for past climate variability. Station 803 cores were analysed for their palynological and geochemical content. Organic-walled dinoflagellate cysts (dinocysts) were used as paleoenvironmental proxies since dinoflagellates show high species diversity in high latitude environments, they thrive in surface waters and their cysts are well preserved in the sediments (Kokinos et al. 1998). Following de Vernal et al. (2005b), reconstructions of past sea-surface parameters (temperature, salinity and duration of sea-ice cover) were estimated using transfer functions (modern analogue technique; Guiot and de Vernal 2007). We provide reconstructions of sea-surface parameters at multidecadal (~ 70 years) resolution over the last 4.6 ka and decadal (~ 7 years) resolution over the last 250 yrs.

2.2 Environmental settings

2.2.1 The Mackenzie shelf

The Mackenzie Shelf is a shallow, rectangular platform located along the northwestern Canadian coast, in the southeastern Beaufort Sea (western Arctic Ocean, Fig. 1). It is bordered to the west by the Mackenzie Trough and to the east by the Amundsen Gulf. The Mackenzie Slope constitutes the northern limit of the shelf as the sea floor drops sharply to reach the deep Canada Basin (Carmack and Macdonald 2002, O'Brien et al. 2006).

The ice cover shows great annual and interannual variability over the shelf and slope. Freeze-up usually starts in September/October, with landfast ice forming from the coastline to the 20 m isobath (Carmack et al. 2004). As drifting pack ice is advected by wind and surface currents, a stamukhi (i.e. continuous rubble fields containing ice and sediments) forms at the outer edge of the landfast ice (Macdonald et al. 1995). Break up begins around May with the formation of flaw leads seaward of the stamukhi. Freshet from the Mackenzie River, wind forcing and rising air temperatures result in ice-free conditions over the shelf in late July and the slope in August (Carmack et al. 2004, Wang et al. 2005, O'Brien et al. 2006, Ogi et al. 2008).

2.2.2 Hydrography of the shelf under riverine influence

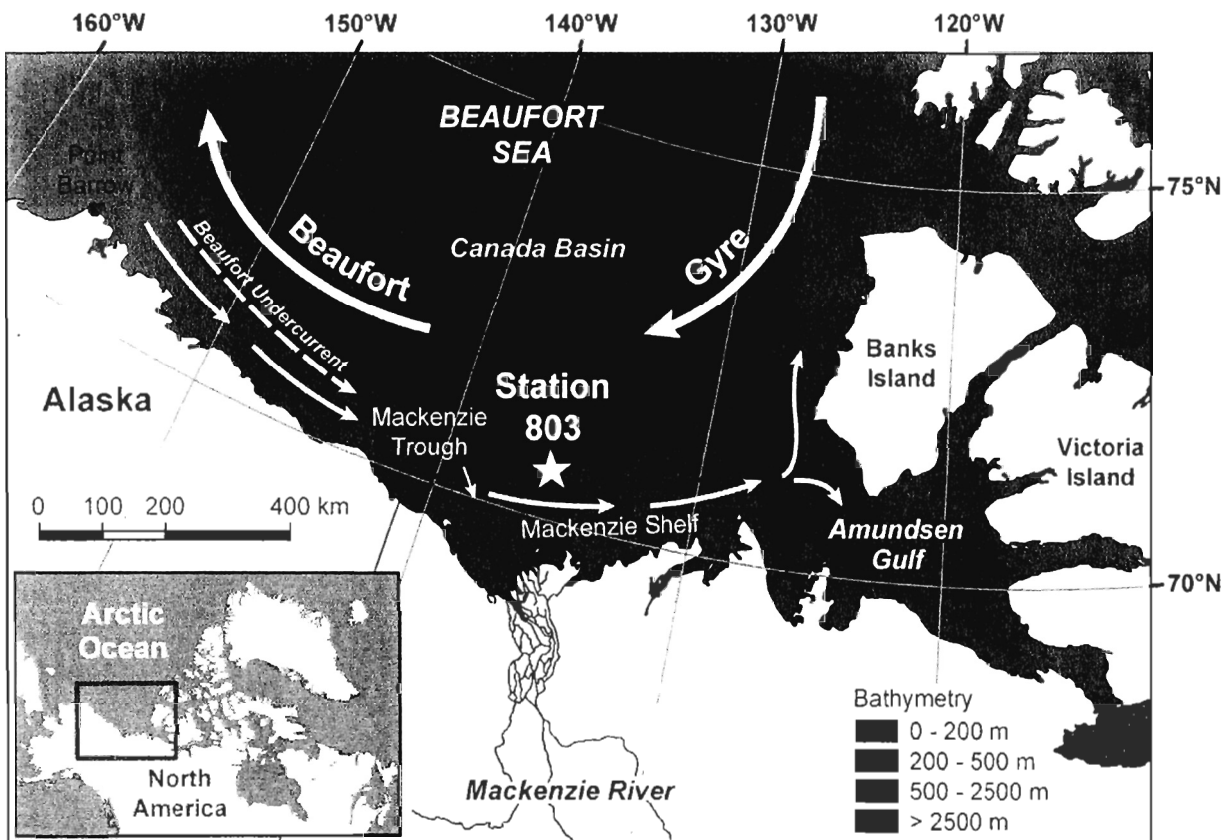


Fig. 1. Study area, located in the southeastern Beaufort Sea. Station 803 lies at 218 m depth on the Mackenzie Slope, at the edge of the Mackenzie plume influence (dashed black line). The Beaufort gyre (thick grey arrows) dominates offshore surface currents, as coastal surface circulation (thin grey arrows) is driven by wind direction (here represented under westerlies influence).

The Mackenzie is the third largest Arctic river in terms of freshwater flow (typical inflow of $3.2 \times 10^{11} \text{ m}^3.\text{yr}^{-1}$; Hirst et al. 1987). Its drainage basin covers an area of $1.8 \times 10^6 \text{ km}^2$, with contributing rivers carrying sediments mostly from the northern Rockies and Mackenzie Mountains (Hill et al. 2001, Abdul Aziz and Burn 2006). Eroding steeply sloping alluvial strata (Matthiessen et al. 2000), the Mackenzie

sedimentary discharge to the Arctic Ocean is by far the largest among all other great rivers, with $\sim 127 \times 10^6$ Mt.yr $^{-1}$ (Macdonald et al. 1998, O'Brien et al. 2006, Carson et al. 1998).

The Mackenzie River inflow to the Beaufort Sea is relatively low in winter (~ 4000 m $^3.s^{-1}$) compared to the flow of summer (30000 m $^3.s^{-1}$; Dunton et al. 2006). During winter (November–April), the stamukhi acts as an inverted dam which entraps the Mackenzie discharge on the inner shelf, leading to the formation of the ‘floating freshwater’ lake Herlinveaux (Carmack et al. 2004). A deep mixed layer of ~ 100 m depth takes place over the rest of the shelf, with temperatures of about -1.7 °C and salinity ~ 32 (Mudie and Rochon 2001). In summer, freshet from the Mackenzie River peaks over a two weeks period between the end of May and early July (Dunton et al. 2006, O'Brien et al. 2006). Together with sea-ice melt, this inflow leads to the formation of the warm (1-10°C) and fresh (salinity in the range of 5 to 30) upper mixed layer (~ 0 -30 m depth), providing strong stratification to the water column. Down to ~ 200 m depth, halocline waters formed by the nutrient rich Bering Sea summer and winter waters, as well as Alaskan Coastal Waters, are of Pacific origin. Relatively warm ($> 0^\circ\text{C}$), salty (> 34.9) Atlantic water is found downslope at depths greater than 200 m (Carmack et al. 1989, Macdonald et al. 1989, Mudie and Rochon 2001, McLaughlin et al. 2002, 2005, Carmack et al. 2004).

Surface water circulation is strongly influenced by the anticyclonic Beaufort gyre that drives the offshore currents westward at the shelf break (Macdonald et al. 1995, Mudie and Rochon 2001). However, below 50 m, the Beaufort Undercurrent transports

Pacific waters eastward along the slope (Fig. 1; Pickart 2004). In ice-free conditions, summer winds drive surface currents along the coast, influencing the Mackenzie plume spread as well as upwelling (under easterly) and downwelling (under westerly) events in the troughs along the Mackenzie Slope (Mudie and Rochon 2001, Carmack et al. 2004, Williams et al. 2006). Over station 803, present summer surface temperature and salinity are 5.8°C and 20.6, respectively. Sea-ice cover lasts for 10 months per year.

2.2.3 Modes of climate variability

On the basis of recent instrumental data, several high-frequency modes of climate variability have been brought to light, showing strong regional discrepancies. The Arctic Oscillation (AO), closely related to the North Atlantic Oscillation, is a robust pattern of the surface manifestation of the strength of the polar vortex (Macdonald et al. 2005). It is defined as the first leading mode of variability from empirical orthogonal function of Northern Hemisphere sea-level pressure (the Dipole Anomaly being the second leading mode; Thompson and Wallace 1998, Wu et al. 2006). In particular, the AO is known to influence sea-ice motion (e.g., Kwok 2000, Rigor et al. 2002) and the freshwater export to the North Atlantic (Houssais et al. 2007). In addition, the inflow of Pacific water through the Bering Strait is enhanced during positive phases of the AO¹ (McLaughlin et al. 2002). Positive (negative) AO phases are associated with wind-driven cyclonic

¹ L'annexe 6 (figures 9 et 10) illustre la circulation des eaux pacifiques et atlantiques dans l'Arctique, sous influence des régimes de circulation atmosphérique anticyclonique (AO⁻) et cyclonique (AO⁺), respectivement. Cette situation est illustrée en annexe 6 (Fig. 9).

(anticyclonic) circulation regimes described by Proshutinsky and Johnson (1997)².

Influence of El Niño-Southern Oscillation (ENSO) has also been documented in the Arctic (Liu et al. 2004), whereas impacts of the Pacific Decadal Oscillation (major mode of North Pacific climate variability) seem to be restricted to the western Arctic (Carmack et al. 2006).

2.2.4 The Little Ice Age

In the western Arctic, the temporal extent of the period known as the Little Ice Age (LIA: generally ~ 1550 to 1850 AD) is yet to be determined. This brief, cold period has been documented in numerous sites throughout the northern hemisphere, either from Eurasian tree-rings, marine and lake sediments (Solomina and Alverson 2004), Greenland ice cores (Fischer et al. 1998), and shifts of diatom and pollen assemblages in lakes from the Canadian Arctic (Rühland et al. 2003, Smol et al. 2005, Rühland and Smol 2005, Michelutti et al. 2006, Peros and Gajewski 2008). In the western Arctic, evidence from varve thickness in lake Iceberg (southcentral Alaska) fed by glacier melt water suggests a cool period spanning from 1500 to 1850 AD (Loso et al. 2006). On the other hand, tree ring and lichenometric dating studies held in the Canadian Cordillera showed that glaciers began their advances as early as the 11th century and reached their maximum Holocene extent during the early 18th or mid-19th centuries (Menounos et al. 2009, and references therein). Closer to our study site, a limnological study held on a small lake on

² Pour une analyse détaillée de la relation entre Oscillation Arctique et régimes de circulation atmosphérique, le lecteur peut se référer à Proshutinsky and Johnson (1997), Serreze et al. (2000) et Macdonald et al. (2005).

western Victoria Island indicate that the LIA could have begun as soon as 1150 AD, and ended ca. 1800 AD (Podritske and Gajewski 2007). Finally, Richerol et al. (2008a) have shown a spatio-temporal nearshore-offshore gradient in the timing of the end of the LIA, associated with the gradual decrease in the influence of the Mackenzie River along the Mackenzie Trough.

2.2.5 Relative sea-level rise in the southern Beaufort Sea since the Last Glacial Maximum

According to Peltier (2002) and Tarasov and Peltier (2004), most of the eustatic (global) sea-level rise in the southern Beaufort Sea since the Last Glacial Maximum (which lies in the range of 130 m) occurred during the late Pleistocene and early Holocene, but post-glacial and deltaic isostatic adjustments result in variable regional relative sea-level changes. In the case of the Mackenzie delta region, the relative sea-level has been rising over the last 10 ka (Hill et al. 1993, 1996, Manson and Solomon 2007, Lesack and Marsh 2007). On the basis of sidescan sonar records and high-resolution seismic reflection profiles, Hill et al. (1993) and Héquette et al. (1995) estimated that the Canadian Beaufort Sea relative sea level rose of approximately 70 m during the Holocene, at variable rates (early Holocene: 4 to 5 mm.yr⁻¹; mid-Holocene: 7 to 14 mm.yr⁻¹; last 3 ka: < 3 mm. yr⁻¹). Another study using diatom-based transfer functions suggests a transgression rate of 1.1 mm.yr⁻¹ for the last millennium in the Mackenzie delta region (Campeau et al. 2000).

2.3 Material and methods

2.3.1 Sampling

Sampling at station 803 (Fig. 1) occurred in 2004 during Leg 8 of the *Canadian Arctic Shelf Exchange Study* (CASES), onboard the Canadian Coast Guard Ship (CCGS) *Amundsen* (Rochon and onboard participants 2004). The site was chosen on the basis of multibeam sonar data (EM300) and 3.5 kHz subbottom profiler in order to select undisturbed sediments³. Boxcore (803BC) was sampled at 218 m depth on July 2nd at 70°38.169 N / 135°55.041W, and trigger weight core (803TWC) and piston core (803PC) were sampled on July 8th at 70°37.976 N / 135°52.815 W (less than 1 nautical mile away from 803BC). Core 803BC (length of 35 cm) was then subsampled every centimetre, whereas cores 803TWC (106 cm) and 803PC (614 cm) were subsampled every 10 cm. All cores were split and described onboard the CCGS *Amundsen*, except a 16 cm long, top section of the piston core, which was split later at the Bedford Institute of Oceanography (BIO), Dartmouth, Nova Scotia. Samples of approximately 5 cm³ were processed for palynological analysis following standard procedure described by Rochon et al. (1999).

³ L'image du 3.5 kHz subbottom profiler à la verticale de la station 803 est présentée en annexe 1.

2.3.2 Palynological preparation and count

The weight of each 5 cm³ subsample was measured and the exact volume was determined by water displacement in a graduated cylinder. A small amount of wet sediment was collected and weighted before and after >12 hours in an incubator, in order to determine the percentage of water in each sample.

Palynomorph concentrations were determined using the marker grain method (Matthews 1969) and expressed as individuals per cubic centimetre of wet sediment. A tablet of *Lycopodium clavatum* of known concentration (12100 ± 1892 spores/tablet) was added to each sample prior to sieving. After 3 to 5 min of sonication, wet sieving was performed using Nytex® sieves of 100 and 10 µm mesh to eliminate coarse sands, fine silts and clays. The coarse (>100 µm) fraction was dried and kept stored. The fraction between 10 and 100 µm was then processed with repeated hot 10% HCl and hot 49% HF treatments, to remove carbonates and silicates, respectively. After proper rinse and a final sieving at 10 µm (to remove remaining fine particles and fluorosilicates), a drop of treated material was mounted between slide and cover slip in a glycerine gel.

Dinoflagellate cysts, pollen grains, spores, foraminiferal organic linings, acritarchs, copepod eggs, tintinnids and freshwater palynomorphs were systematically counted using a light microscope (Nikon Eclipse 80 – I, transmitted light, magnification factor of 400x). Reworked palynomorphs (i.e. pre-Quaternary fossil pollen grains, spores and dinocysts) were also counted. A minimum of 300 dinocysts was counted in most samples, with only five exceptions (>250 dinocysts) for which no more than two complete slides were

counted. The nomenclature of dinocyst taxa follows Rochon et al. (1999), Head et al. (2001) and the Lentin and Williams index (Fensome and Williams 2004)⁴.

2.3.3 Dinoflagellate cysts as paleoenvironmental proxies

Dinoflagellates are microscopic biflagellate protists found in most aquatic environments. Even at high latitude, they show great diversity in terms of morphology and feeding behaviour (auto-, hetero- and mixotrophy), which makes them one of the main primary producers (Taylor 1987). For ~ 15-20 % of the species, sexual reproduction leads to the formation of non-motile, resting cysts (dinocysts). Their organic wall is made of dinosporine, a highly resistant polymer that does not suffer dissolution (Kokinos et al. 1998), allowing good preservation of the cysts' wall in the sediments.

Most of the autotrophic cyst-forming species belong to the orders of Gonyaulacales, as Peridiniales (defined as protoperidinioides plus polykrikoid species; Mudie and Rochon 2001) have heterotrophic behaviour, yet mixotrophy is widespread among dinoflagellates (Stoecker 1999). Dinoflagellates thrive in surface waters since autotrophic taxa depend on light availability and heterotrophic taxa feed mainly on diatom (e.g., Jacobson and Anderson 1986). The dinocyst assemblages in the sediments thus reflect sea-surface conditions that prevailed at the time of their deposition. Many studies have shown the close relationship between dinocyst assemblages in modern sediment samples and present sea-surface conditions, regardless of latitude

⁴ Les décomptes de dinokystes et les concentrations des principaux palynomorphes dénombrés dans les carottes de la station 803 sont présentés en annexes 2 et 3 (tables 2 et 3, respectivement).

(e.g., Zonneveld 1997, Radi et al. 2001). Sea-surface temperature and salinity, seasonality and duration of sea-ice cover at high latitudes have been shown to be determinant factors on the distribution of dinocyst taxa (e.g., Rochon et al. 1999, de Vernal et al. 2005b).

Dinocysts are thus excellent paleoenvironmental proxies especially for high latitude environments (e.g., Rochon 2009), with respect to calcareous (e.g., foraminifers, coccolithophores) and siliceous (e.g., diatoms) microfossils which undergo severe dissolution in cold environments (Mudie et al. 2001, de Vernal et al. 2005b). *In situ* preservation of dinocysts at station 803 are assumed to be not affected by oxygen availability in the sediments. Indeed, studies from Zonneveld et al. (1997, 2001) and Zonneveld and Brummer (2000) showed that cysts formed by *Protoperidinium* species are the most sensitive to aerobic degradation. In our case, high sedimentation rate and observed excellent preservation of *Brigantedinium* cysts (produced by the *Protoperidinium* species) allow us to assume that no selective degradation occurred at station 803.

Apart from dinoflagellate cysts, numerous other palynomorphs provide useful information on past environments. Pollen grains and spores are terrestrial palynomorphs transported by wind and/or water masses. In marine environments, organic linings of foraminifers are considered to be good indicators of benthic productivity, and copepod eggs (as well as dinocysts) indicate past pelagic productivity (de Vernal et al. 1992). Tintinnids are ciliates associated with brackish environments that have high suspended loads, and could therefore be associated with turbid river runoff waters (Schell et al. 2008, Scott et al. 2008). Freshwater input indicators also include the acritarch

Halodinium (Rochon et al. 2006, Richerol et al. 2008b), the colonial green algae *Pediastrum* and *Zygnema*-type spores, hereafter grouped as ‘freshwater protists’. Finally, reworked palynomorphs are indicators of riverine (and coastal) erosion.

2.3.4 Quantitative reconstruction of sea-surface parameters

Quantitative reconstructions of past sea-surface parameters (i.e. August sea-surface temperature: SST, August sea-surface salinity: SSS, and duration of sea-ice cover) have been assessed on the basis of dinocyst assemblages in station 803 cores using transfer functions. The modern analogue technique (MAT), a technique of direct similarity (Guiot and de Vernal 2007), was used following the procedure described by de Vernal et al. (2005b). MAT was performed using the software R and the latest version of the evergrowing reference database (1189 sites, 63 taxa) developed at GEOTOP by de Vernal et al. (1997, 2001, 2005) and Rochon et al. (1999). The best estimates (averages weighted inversely to the distance) and the associated confidence interval (minimal and maximal possible values) were calculated with respect to a set of five best modern analogues. Modern environmental data used for statistical analysis consist in sea-surface temperature and salinity values at 10 m depth provided by the 2001 version of the World Ocean Atlas (NODC 2001). Seasonal duration of sea-ice cover, defined as the number of months per year with sea-ice concentration greater than 50%, was compiled after the 1953-1990 data set provided by the National Climate Data Centre in Boulder, Colorado.

Validation tests performed on the ‘ $n=1189$ ’ database indicate good reliability of the reconstructed parameters⁵. Indeed, relationships between estimates and observations are linear, with high correlation coefficients (August SST: $R^2 = 0.95$; August SSS: 0.74; sea-ice cover: 0.90). Standard deviation of the residuals (RMSE: Root Mean Square Error) provides an estimation of the accuracy of reconstructed parameters. They are ± 1.7 , ± 2.5 and ± 1.2 for August SST, August SSS and sea-ice cover, respectively. As pointed out by Richerol et al. (2008b), reconstructed salinity should always be interpreted with caution.

2.3.5 Carbon and nitrogen content, stable isotopes and grain size analyses

Total carbon, organic carbon and total nitrogen content (C_{total} , C_{org} and N_{total} , respectively) were determined by high temperature catalytic combustion analysis, using a Carlo-Erba elemental analyser at GEOTOP, Montreal, Quebec. Two aliquots were taken from each sample, and one of them was treated with HCl (1N) to remove inorganic carbon. Both aliquots were dried, grounded and analysed for their carbon and nitrogen content. Inorganic carbon content (C_{inorg}) was indirectly determined from C_{total} and C_{org} measurements (Hélie 2009).

Stable isotopic data ($\delta^{13}\text{C}$, $\delta^{15}\text{N}$) were obtained using a Micromass IsoprimeTM mass spectrometer in continuous-flow mode, coupled to the Carlo-Erba elemental analyser. Raw data were corrected using a calibration slope built on the basis of two internal reference materials. Carbon and nitrogen contents are expressed as percentage of

⁵ Les graphiques résultants des exercices de validation sont présentés en annexe 4.

dry sediment. All $\delta^{13}\text{C}$ values are given in ‰ versus Vienna Pee-Dee Belemnite (V-PDB, $\pm 0.1\text{‰}$ at 1σ), and $\delta^{15}\text{N}$ values are expressed as ‰ versus air ($\pm 0.2\text{‰}$ at 1σ).

Grain size analyses were performed using a Beckman Coulter LS 13320 laser diffraction analyser at the Institut des sciences de la mer de Rimouski (ISMER), Rimouski, Quebec. We used the software Gradistat to calculate standard statistical parameters (Blott and Pye 2001).

2.4 Chronology of the composite sequence

Chronology of cores 803PC and 803TWC has been determined by Barletta et al. (2008). Chronology of the piston core was assessed using four accelerator mass spectrometry (AMS) ^{14}C measurements on calcareous pelecypod shells (Table 1) performed at Beta Analytic Inc., Miami, Florida. Conventional radiocarbon dates were calculated using Libby's half life (5568 yrs) and normalized for a $\delta^{13}\text{C}$ value of -25‰ versus V-PDB (Stuiver and Polach 1977). Calibration was performed using the online software CALIB version 5.0.2 (Stuiver et al. 2005) and the Hughen et al. (2004) marine dataset. In addition to a global reservoir (400 yrs), a regional reservoir correction (ΔR) of 400 yrs was applied (total: 800 yrs) based on the average ΔR values derived from the dates measured on five pelecypod shells collected in the Amundsen Gulf prior to nuclear testing (Andrews and Dunhill 2004, McNeely et al. 2006, Barletta et al. 2008).

Table 1. Radiocarbon dates for core 803PC (modified from Barletta et al. 2008).

Depth (cm) ^a	Corrected depth (cm) ^b	Date (yr BP) ^c	Calibrated date (cal BP) ^d	Dated material	Lab number ^e
66	108	1530±40	693 (621-765)	<i>Yoldia myalis</i>	Beta-201958
290	332	3000±40	2249 (2140-2358)	<i>Buccinum</i> sp.	Beta-201959
376	418	3540±40	2928 (2800-3056)	Shell fragments	Beta-201960
566	608	4560±40	4242 (4105-4378)	Shell fragments	Beta-201961

^a A 16 cm top section was not available in the study from Barletta et al. (2008); there is hence a 16 cm lag between these depths and those provided by Barletta et al. (2008).

^b Depth corrected for the missing top sediment (see text for details).

^c All dates were determined by the AMS method (using Libby's half life: 5568 yrs) and normalized for a $\delta^{13}\text{C}$ value of -25‰ versus VPDB. Statistical uncertainties are given as 1σ (Stuiver and Polach 1977).

^d Dates were calibrated using the online software CALIB version 5.0.2 (Stuiver et al. 2005) and the Hughen et al. (2004) marine dataset. Regional reservoir correction (ΔR) is 400 yrs (total correction: 800 yrs). Date ranges are given as 2σ .

^e Beta: Beta Analytic Inc., Miami, Florida.

Chronology of core 803BC was determined from ^{210}Pb data on the top 20 cm (Fig. 3). Raw ^{210}Pb measurements were corrected for salt content (Sorgente et al. 1999) and the time lag between sampling and analysis. We used a constant rate of supply model (Appleby and Oldfield 1983) to determine the SR of recent sediments. ^{210}Pb total activity profile (Fig. 3A) indicates biological mixing limited to the first centimetre, with a supported ^{210}Pb activity of 2.6 dpm (disintegrations per minute).

Note that boxcore sample ‘5 to 6 cm’ had to be removed from the model (as well as from subsequent palynological analysis) since we found evidence of a slight sediment remobilisation event in grain size and palynological data. Indeed, the finest particles ($<0.064 \mu\text{m}$) are missing at that depth (Fig. 3B), suggesting higher than normal kinetic energy in the nepheloid layer. Abundances of foraminiferal organic linings are low (487 linings. cm^{-3}) in comparison with the rest of the boxcore (mean of 1071 linings. cm^{-3}), suggesting low content of fresh organic matter. We tentatively associate this event with the huge 1963 storm, documented from Point Barrow (Alaska) to the Canadian Arctic Archipelago, with winds $> 25 \text{ m.s}^{-1}$ (e.g., Lynch et al. 2003). We put forth the hypothesis of a slight event remobilizing upslope sediment, associated with the rapid deposition of a layer of $\sim 1 \text{ cm}$ thick of coarser sediment (lacking the finest particles that would have been transported further downslope) at station 803.

Neperian logarithm of the excess ^{210}Pb plotted against corrected depth (i.e. without the ‘5 to 6 cm’ sample; Fig. 3C) indicate a SR of 139.1 cm.ka^{-1} . This SR is similar to that calculated in the piston core (141.5 cm.ka^{-1}); therefore we assume a constant SR in the complete sequence. For the boxcore, a constant SR implies a temporal coverage of 250 yrs,

from ~ 1750 to 2004 AD (Fig. 3D). Since Barletta et al. (2008) have stratigraphically correlated the TWC with the PC, we obtain a complete composite sequence covering the last 4600 yrs cal BP. Based on this SR and the sampling intervals, we estimate the temporal resolution of ~ 70 yrs in cores 803PC and TWC, and ~ 7 yrs in core 803BC.

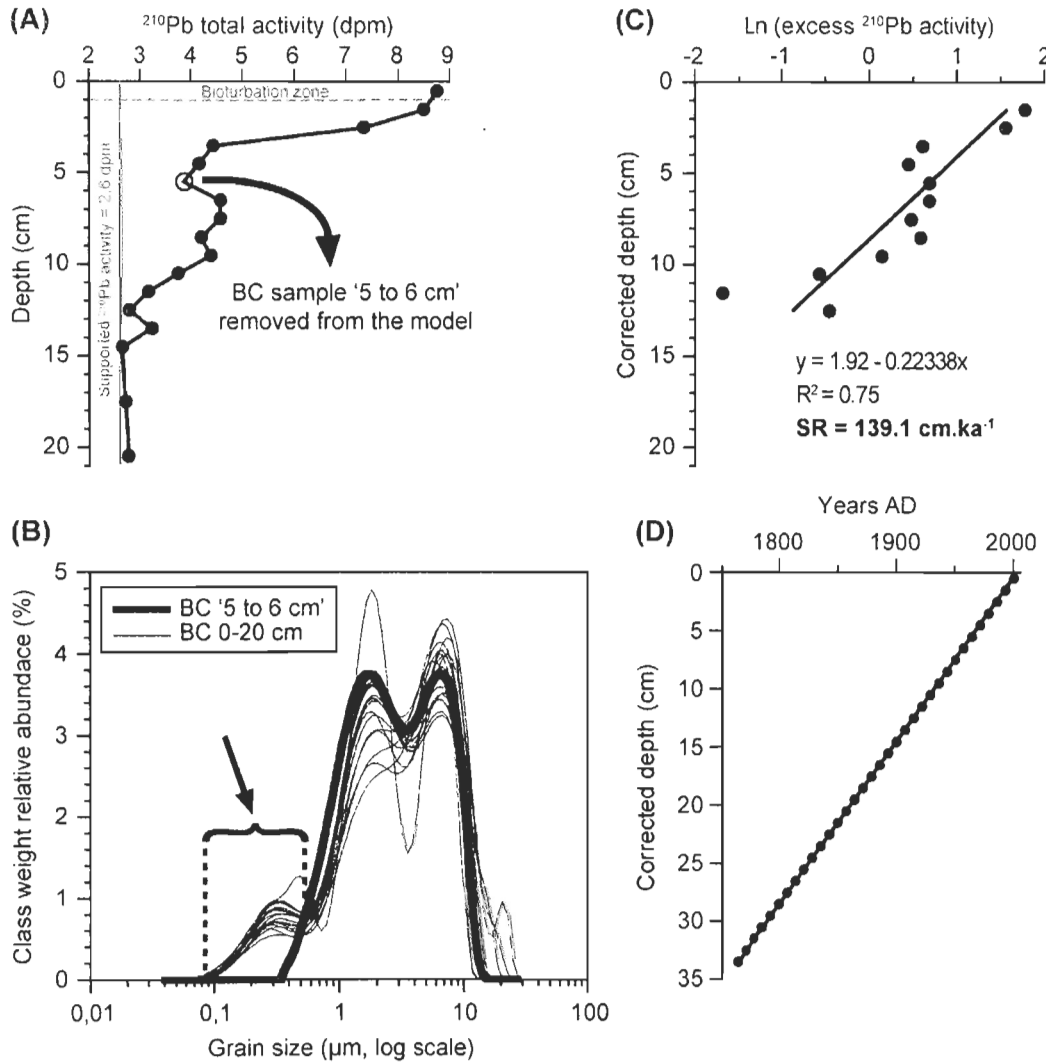


Fig. 3. Boxcore SR determination from ^{210}Pb data. (A) ^{210}Pb total activity (dpm: disintegration per minute) in the top 20 cm. The supported ^{210}Pb activity is illustrated by the vertical gray line (asymptote = 2.6 dpm), as the dotted horizontal grey line indicates the bioturbation zone. (B) Grain size evidence of a slight gravity flow at station 803 (the arrow and brace point out the particles <0.064 μm that are missing in BC sample '5 to 6 cm'; see text for details). (C) Neperian logarithm of excess ^{210}Pb activity used for the estimation of SR. (D) BC age model, extrapolated assuming constant SR.

2.5 Results

2.5.1 Lithology and geochemical properties

All cores are composed of olive-grey silty clays (Munsell colour 5Y 4/1) with variable degree of bioturbation, except the top 4 cm of the boxcore which is dark yellowish brown in colour (10YR 4/6). Slightly darker layers (5Y 3/2) occur between PC depths 46 and 71 cm. Occasional black horizons and laminations are also observed throughout the trigger weight and piston cores. Grain size analysis also reveal sparse occurrences of fine ice rafted debris (sand particles < 250 µm) that seem to decrease gradually upward the piston core (Fig. 4). As suggested by the ^{14}C dates and the homogenous sedimentary facies of the cores, the entire cores are composed of postglacial sediments. The porosity profile shows typical high values (> 0.72) in the upper 4 cm of the boxcore, with a constant decreasing trend (down to ~ 0.60) toward the base of the sequence.

Geochemical analyses (Fig. 4) indicate relatively constant values of total carbon (~ 1.8%), organic carbon (~ 1%), total nitrogen (~ 0.14%) and C/N ratio of organic matter (~ 8.6%) throughout the entire sequence. However, stable isotopic data reveal a slight, gradual increase in $\delta^{13}\text{C}$ values, ranging from ~ -27.1‰ at the base of the PC to ~ -25.8‰ at the top of the BC. As recorded by the boxcore, the period ranging from 1820 AD to present is subject to a more pronounced increase in $\delta^{13}\text{C}$ values. The $\delta^{15}\text{N}$ profile shows values fluctuating around 4.2‰ with centennial-scale oscillations,

especially between 3500 and 1500 cal BP. The boxcore records a trend toward higher $\delta^{15}\text{N}$ values that reach 5‰ at the very top.

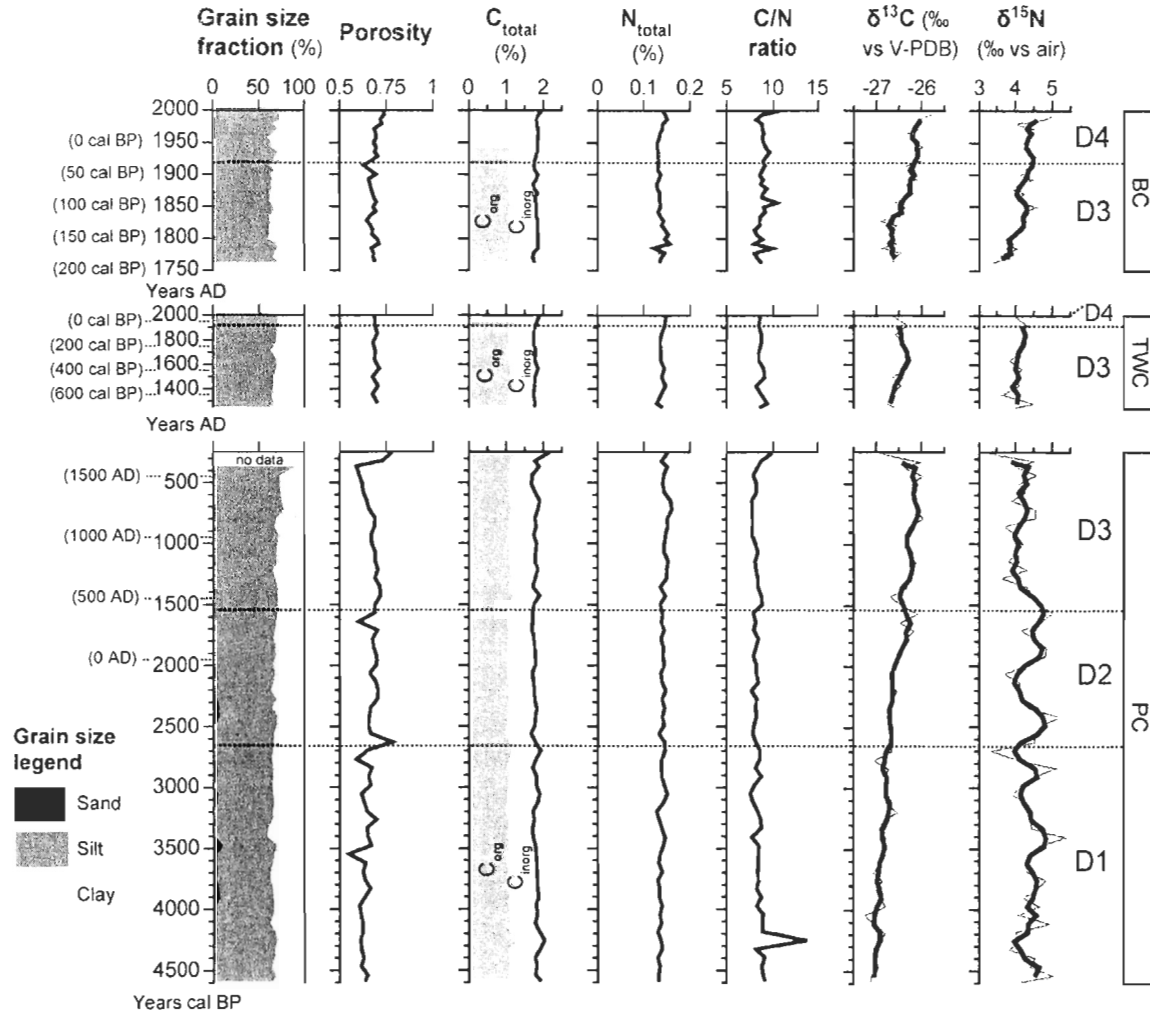


Fig. 4. Grain size composition and geochemical parameters of station 803 cores (BC = boxcore; TWC = trigger weight core; PC = piston core). BC and TWC ages are given in years AD with the equivalent in cal BP in parenthesis; conversely, dates in the PC graphs are expressed in years cal BP. Temporal resolutions are 1 sample every ~ 70 years (TWC and PC) and 1 sample every ~ 7 years (BC). Note that PC scale starts at 250 cal BP. The grey area within the total carbon curve illustrates the proportion of organic carbon. 3-points moving averages are shown as thick, black curves on stable isotopic (organic δ¹³C and δ¹⁵N) data. Dinocyst zones D1 to D4 are delimited with dashed lines (see text for details).

2.5.2 Palynological data

Amongst all organic-walled microfossils, the most abundant were reworked palynomorphs (reworked spores, pollen and dinocysts: mean of ~ 4000 grains.cm $^{-3}$; Fig. 5). Together with the high sedimentation rate of ~ 140 cm.ka $^{-1}$, this suggests that the Mackenzie River load accounts for a large part of the sedimentation at station 803. Dinocysts, foraminifer organic linings and pollen grains were also well represented, with means of 1165, 1106 and 400 individuals.cm $^{-3}$, respectively. Abundances of spores, freshwater eukaryotes and copepod eggs were about one order of magnitude lower than dinocyst abundances. Tintinnid concentrations never exceeded 60 individuals.cm $^{-3}$.

Terrestrial palynomorph concentrations (pollen grains and spores) remained relatively constant throughout the entire sequence (Fig. 5), suggesting no major shift in land plants production over the last 4.6 ka. Pollen assemblages were dominated by *Picea* (overall mean of 42.4%), accompanied by *Alnus* (17.7%), *Pinus* (12.3%) and *Betula* (11.2%). Numerous other pollen grains were recovered at low relative abundances (< 3.6%), such as *Salix* and pollen produced by the families Compositeae, Cyperaceae, Ericaceae and Caryophyllaceae. This pollen record is consistent with previous work in the Mackenzie delta area (e.g., Ritchie and Hare 1971) and on Victoria Island (Peros and Gajewski 2008). Periods of high freshwater discharge and high productivity are recorded between 4600 and 2700 cal BP, and from 1500 cal BP to the top of the sequence, as revealed by the high abundances of freshwater input indicators (reworked palynomorphs,

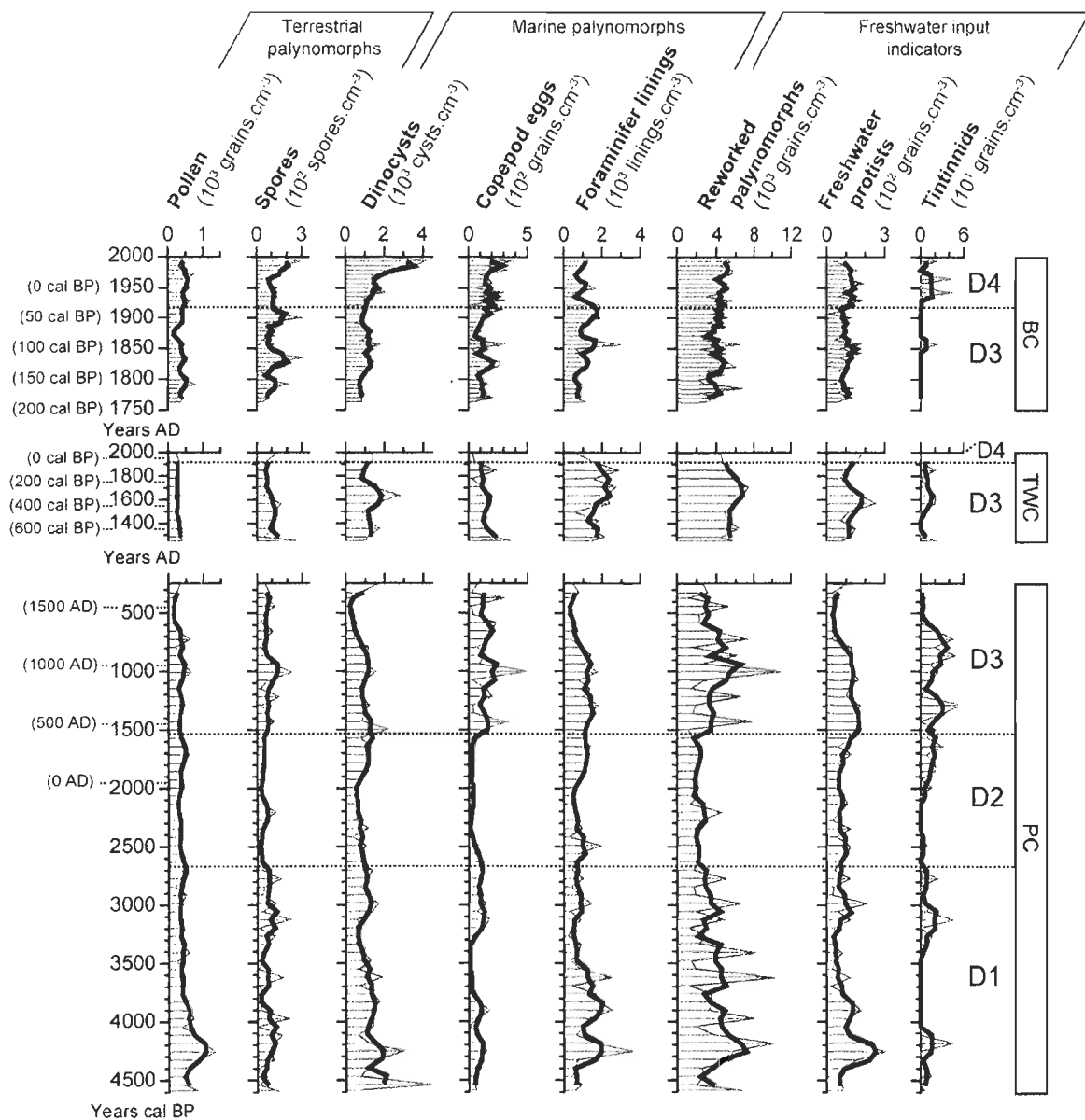


Fig. 5. Concentrations of the main organic-walled microfossils in station 803 cores.

Reworked palynomorphs consist in eroded pre-Quaternary microfossils (spores, pollen grains and dinocysts). Freshwater protists include *Halodinium*, *Pediastrum* colonies and *Zygnema*-type spores. The thick, black curves represent 3-points running averages. Dinoflagellate cyst zones D1 to D4 are also shown. Note that the X axis scale differs from one palynomorph type to another. See text for the significance of each type of microfossil and the determination of dinocyst zones.

freshwater protists and tintinnids) and marine palynomorphs (dinocysts, copepod eggs and organic linings of foraminifer; Fig. 5).

A total of 15 species of dinocysts have been identified in our samples, which is consistent with previous work in the Canadian Arctic Ocean (Mudie and Rochon 2001, Richerol et al. 2008a). The palynomorphs were generally well preserved. In this study, *Operculodinium centrocarpum* refers to all morphotypes (*O. centrocarpum* sensu Wall & Dale 1966, *O. centrocarpum*-short processes and *O. centrocarpum*-arctic morphotype); *Brigantedinium* spp. include *B. simplex*, *B. cariacoense* as well as round brown cysts with smooth surface that could not be identified to the species level (archeopyle not visible and/or damaged).

All dinocyst assemblages are dominated by four taxa: *O. centrocarpum* (mean of 38.1%), *Brigantedinium* spp. (17.7%), cysts of *Pentapharsodinium dalei* (17.6%) and *Islandinium minutum* (16.8%). The mean relative abundances of *Spiniferites elongatus/frigidus*, cf. *Echinidinium karaense*, *Islandinium minutum* var. *cezare* and cysts of *Polykrikos* sp. var. *arctic/quadratus* range between 3.0 and 1.5%. Other taxa (*Echinidinium aculeatum*, *Impagidinium pallidum*, cysts of *Protoperidinium americanum*, *Spiniferites ramosus*, *Spiniferites* spp., cysts of *Polykrikos schwartzii* and *Nematospaeropsis labyrinthus*) are rare but present ($\leq 0.1\%$).

Following Bennett (1996), the composite sequence has been divided into four zones determined on the basis of dinocyst relative abundances (Fig. 6) using the free software ZONE (version 1.2, ‘Optimal Sum of Square Partition’ method; Juggins 2005). All subsamples from the three cores were pooled and ordinated according to their

estimated date of deposition (see section 2.4) prior to zonation. Thus, a single ‘dinocyst zone’ could encompass assemblages from more than one core⁶.

Dinocyst assemblage zone 1 (D1), from 4600 to 2700 cal BP, is dominated by the autotrophic taxa *O. centrocarpum* (mean of 49.0%). In zone D2 (2700-1500 cal BP), the relative abundances of *O. centrocarpum* decrease (34.4%) in favour of the opportunistic, heterotrophic taxa *Brigantedinium* spp. (28.8%) and cysts of *Polykrikos* sp. var. *arctic/quadratus* (2.8%). This shift is also illustrated by the diminution of gonyaulacales versus peridiniales, a trend observed in both zones D2 and D3. In fact, dinocyst zone D3 (1500-30 cal BP or 450-1920 AD) is characterized by the high relative abundance of the peridinioid taxa *I. minutum* (19.9%). The last zone (D4), spanning from 1920 to 2004 AD, is again dominated by *O. centrocarpum* (44.5%), and shows low relative abundances of *Brigantedinium* spp. and cf. *Echinidinium karaense*. Note that the limits of zones D1, D2 and D3 correspond to shifts in marine palynomorphs and freshwater input indicators (Fig. 5).

⁶ C'est le cas de la zone D3 qui recoupe les trois carottes de la station 803. La zone D4 se retrouve également dans les carottes à boite et à gravité (voir Fig. 6).

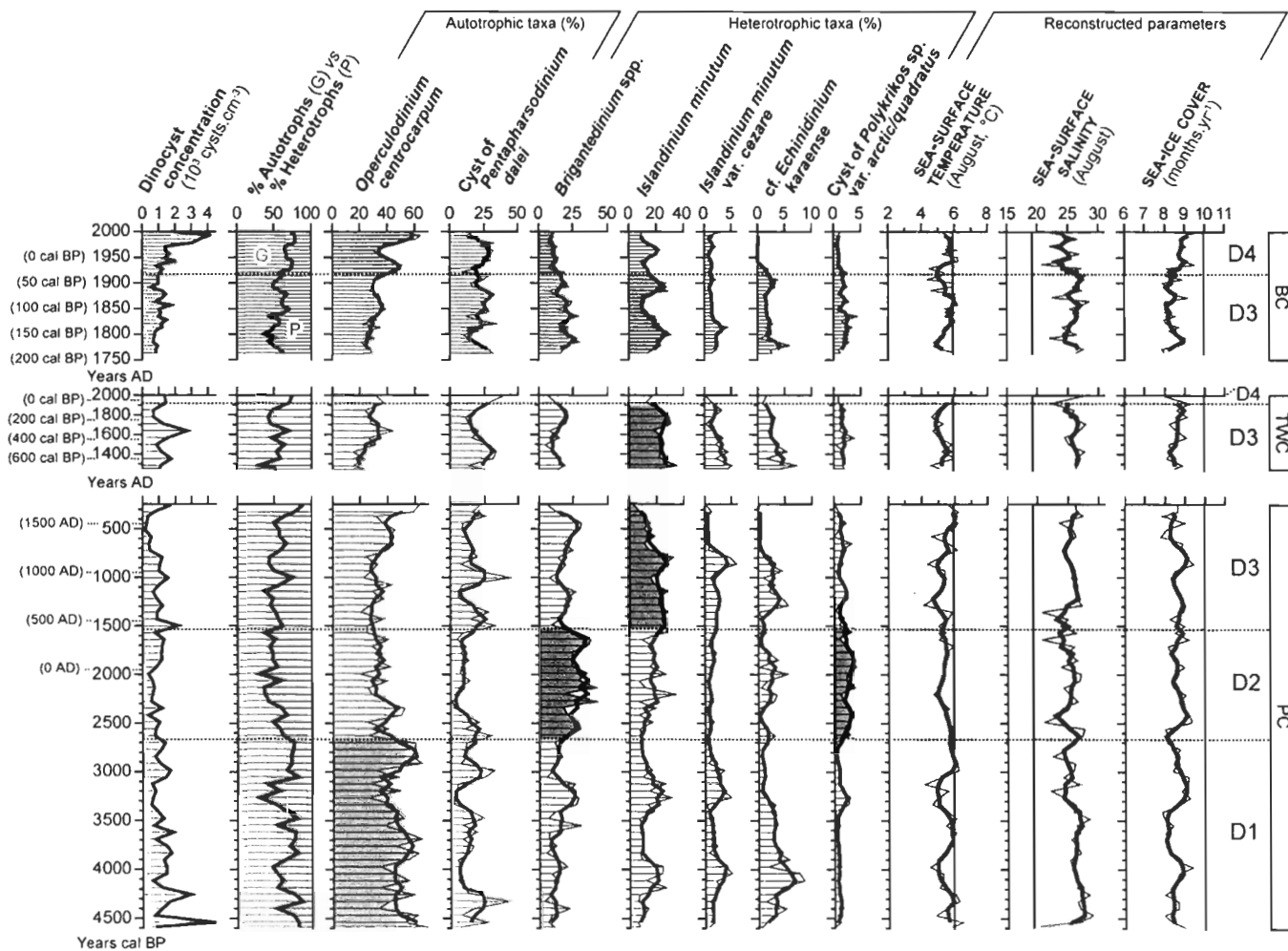


Fig. 6. Dinocyst concentration, proportion of autotrophs (gonyaulacales, in green) vs heterotrophs (peridiniales, in brown), relative abundance of the main dinocyst taxa and reconstructed sea-surface parameters from station 803 cores. The thick, black curves illustrate 3-points moving averages. Dark, shaded areas point out key taxa that characterize the four dinocyst assemblage zones (dotted horizontal lines). Lightly shaded areas show the confidence interval of reconstructed parameters (minima and maxima among the five best modern analogues). Solid, vertical lines indicate the values of modern sea-surface conditions.

2.5.3 Quantitative reconstructions

Quantitative reconstructions of past sea-surface parameters⁷ reveal relatively stable conditions over the last 4600 years in the Mackenzie Slope area (Fig. 6). In dinocyst zones D1, D2 and D3 (from ca. 4600 cal BP to 1920 AD), reconstructed SST remains close to the modern value (5.9°C) with occasional cooling events in zones D1 and D3. The amplitude of these cooling events (4200 - 3800, 3400 - 3000 cal BP for zone D1; around 700 AD and 1500 - 1800 AD in zone D3) do not exceed 1.5°C. Sea-surface salinity reconstructions suggest a more saline environment until 1920 AD (modern value = 19.2), with reconstructed values fluctuating around 26. The duration of sea-ice cover also shows little variation in zones D1 to D3 (all values between 8 and 9 months per year), but remained 1 to 2 months below the modern value of 10 months.yr⁻¹.

Conversely, dinocyst zone D4 (1920-2004 AD) is marked by several hydroclimatic changes well documented by the boxcore record (sampling interval of 7 years). SST in D4 increases from 4.5°C at the base to the actual value (5.9°C) within 20 years, and remained stable since 1940 AD. A shift in SSS toward fresher values is observed near the base of D4, with decadal-scale oscillations centered on 24. The last 80 years are marked by an increase in duration of sea-ice cover, which is recorded around 8 months.yr⁻¹ at the base of D4, stabilizes close to 9 from ca. 1940 to 1990 AD, and finally reaches the modern value (10 months.yr⁻¹) at the very top of the sequence.

⁷ La liste des meilleurs analogues modernes pour chaque assemblage fossile, utilisés pour les reconstitutions quantitatives, sont présentés dans la table 4 (en annexe 5). Les distances statistiques y figurent également.

2.6 Discussion

2.6.1 Late Holocene hydrological and climate stability over the Mackenzie Slope

Both palynological and geochemical data in station 803 cores depict relatively stable hydrological conditions over the last 4.6 ka. The sedimentary facies and grain size properties remain extremely similar throughout the whole three cores, suggesting no significant variation in the depositional environment.

From 4600 cal BP to 1920 AD, the amplitude of variations in reconstructed sea-surface parameters does not exceed 1.5°C (SST), 8 salinity units (SSS), with sea-ice cover variations of about 1 month.yr⁻¹. This contrasts with considerably larger environmental changes associated, for instance, with the end of the Last Glacial Maximum (LGM; de Vernal et al. 2005b). In terms of Holocene climate variability, Kaufman et al. (2004) have constrained the timing of a warmer than present period in the Canadian Arctic, the Holocene thermal maximum (HTM). On the basis of 120 Holocene records from the western Arctic (showing similar timing between sites of marine and terrestrial settings), they estimated that the HTM ended ca. 6 ka BP at our study site. Another major paleoceanographic feature is the penetration of warm Atlantic water in the Arctic Ocean that underlies the halocline waters of Pacific origin. The onset of the current circulation pattern began ~ 8 ka BP as documented in marine cores from the Chukchi Sea (Hillaire-Marcel et al. 2004, de Vernal et al. 2005a) and the Canadian Arctic Archipelago (Ledu et al. 2008). Detailed studies of the Barents Sea Holocene paleoceanography also constrain

the inception of modern hydrological pattern, characterized by a stabilized inflow of Atlantic water, around 4.7 ka cal BP (Lubinski et al. 2001, Voronina et al. 2001, Duplessy et al. 2005).

However, the post-HTM climate stability recorded in our cores appears to be restricted to the upper Mackenzie Slope, excluding its western trough. Indeed, much higher variability has been recorded during the late Holocene in the western Arctic, even close to the study site. For instance, variations in SST of $\sim 6^{\circ}\text{C}$ in the Chukchi Sea have been reported for the last 6 ka (de Vernal et al. 2005a, McKay et al. 2008), and a warming of $\sim 4^{\circ}\text{C}$ was documented in the Mackenzie Trough within the last few hundreds of years (Richerol et al. 2008b). This is consistent with foraminiferal and dinocyst assemblages in numerous cores from the Mackenzie Shelf, slope and trough suggesting that the influence of the Mackenzie River was limited to the trough and surrounding areas during the mid- and late Holocene (Rochon et al. 2006, Scott et al. 2007, Schell et al. 2008, Richerol et al. 2008b).

2.6.2 Relative sea-level rise

Stable isotopic data in our cores suggest a slight, gradual increase in the marine (vs terrestrial) influence on the origin of organic matter. $\delta^{13}\text{C}$ measurements along the three cores show values rising from $\sim -27.1\text{\textperthousand}$ at the base to $\sim -25.8\text{\textperthousand}$ at the top (Fig. 4). A similar trend is observed in the $\delta^{15}\text{N}$ values, although the profile shows some fluctuations from the base of the sequence up to ~ 600 AD (i.e. approximately in dinocyst zones D1 and

D2). These relatively low values in comparison to surface sediment samples from the Chuckchi and Beaufort Seas indicate the clear dominance of terrigenous organic matter, as a result of long ice-cover duration, low nutrient availability and high supply of terrestrial materials from the Mackenzie River (Chen et al. 2006, Schell et al. 2008, Scott et al. 2009). According to Naidu et al. (2000), the modern cross-shelf seaward increase in $\delta^{13}\text{C}$ values observed in the Beaufort Sea is most simply explained by the mixing of the terrestrial ($\sim -27\text{\textperthousand}$ for the Beaufort Sea) and marine (typically between -20 and -22‰; Meyers 1997) end members.

Therefore, we associate the increase of $\delta^{13}\text{C}$ values in station 803 cores with an increase of marine influence due to the rise of the relative sea-level in the southern Beaufort Sea area. Since ice-rafted debris are of terrestrial origin, their gradual decrease along the sequence (Fig. 4) also seems to corroborate this hypothesis. Our data suggest that the recent (1820 AD to present) rate of increase in $\delta^{13}\text{C}$ values is quite higher than the average rate that prevailed prior to 1820 AD (Fig. 4). This constitutes a major concern with regard to present and future coastal erosion. In fact, due to the predominance of ice-rich unconsolidated sediments and wide spread thermokarst erosion, the southeastern Beaufort Sea coast has been classified as highly sensitive to a future rise in sea level (Shaw et al. 1998).

2.6.3 Variations in Pacific water inflow (zones D1 and D2)

$\delta^{15}\text{N}$ data is most commonly used to distinguish algal vs land plants sources of organic matter (Meyers 1997). In our stable isotopic data, the general co-variation of $\delta^{15}\text{N}$ and $\delta^{13}\text{C}$ values and the consistency with previous work indicate a good reliability of these proxies (see the above section ‘Relative sea-level rise’). However, fluctuations in $\delta^{15}\text{N}$ profile between 3.6 ka and 1300 cal BP are absent from the $\delta^{13}\text{C}$ records (Fig. 4), suggesting that other(s) mechanism(s) might be involved in the control of nitrogen isotopic ratio. Denitrification of dissolved NO_3^- is very unlikely to have occurred at station 803 since bottom waters are not oxygen-depleted (e.g., Simpson et al. 2008, Macdonald et al. 1987) and our surface (dinocysts and copepod eggs) and benthic (organic linings of foraminifera) productivity indicators do not suggest periods of extremely high productivity, especially in zone D2 (Fig. 5). Alternatively, Calvert et al. (1992) demonstrated that low $\delta^{15}\text{N}$ values might record periods of enhanced nitrate availability that allowed greater algal discrimination in favor of ^{14}N . In our case, nitrogen is known to limit primary production over the middle and outer shelf (Carmack et al. 2004). Indeed, the Mackenzie River waters contain high amounts of silicates but are relatively poor in nitrates, the latter being mostly advected by nutrient rich water masses of Pacific origin (Macdonald et al. 1987, McLaughlin et al. 2005). In addition, dinocyst zone D2 is marked by a decrease of both pelagic and benthic productivity (Fig. 5) associated with reduced freshwater runoff. This period is hence subject to greater limitation of river-adverted nutrients, leaving the Pacific water masses the major source of nitrates.

Thus, we interpret the $\delta^{15}\text{N}$ variations from 3.6 ka to 1300 cal BP as fluctuations in the inflow of Pacific-originated water masses. The onset of these fluctuations around 3.6 ka cal BP corresponds to a shift in the inflow of Pacific water through the Bering Strait, as suggested by the decrease of the proportion of chlorite (a clay mineral used as a tracer of Pacific waters; Ortiz et al. 2009) and paleomagnetic properties (median destructive field of the Natural Remanent Magnetization; Brachfeld et al. 2009) in Holocene sedimentary sequences from the Chukchi-Alaskan margin. Increases in Pacific water influence at station 803 could be either due to larger Bering Sea water inflow (Häkkinen and Proshutinsky 2004), weaker stratification (de Vernal et al. 2005a) or enhanced frequency, intensity, and/or duration of upwelling events that bring halocline waters to the surface, as observed over the Mackenzie Trough (Macdonald et al. 1987, Carmack et al. 2006, Williams et al. 2006). In particular, periods of high Pacific water influence (low $\delta^{15}\text{N}$ values) could be the consequence of past atmospheric circulation pattern analogous to negative AO phases (anticyclonic regimes). In modern climatic conditions, Pacific water inflow to the Arctic Ocean increases under negative AO phases⁸; halocline waters circulate in the Canada Basin and the strengthened Beaufort Gyre confines the eastward surface currents over the shelf (McLaughlin et al. 2002, 2005, Steele et al. 2004, Macdonald et al. 2005). Therefore, our data suggest that variations of the AO from 4.6 ka to \sim 1300 cal BP have occurred with centennial scale oscillations.

⁸ Voir annexe 6 (figures 9 et 10).

2.6.4 Constraining the Little Ice Age (zone D3)

At station 803, core 803TWC records a cooler period spanning from ~ 1560 to 1850 AD. Indeed, reconstructed SSTs indicate a decrease of ~ 1.5°C in comparison to surface temperatures that prevailed right before and after this interval (~ 6°C at 1500 and 1900 AD). Owing to a sampling interval of 7 years, the boxcore record draws a more accurate picture of the LIA termination. The latter appears to have taken place around 1820 AD, consistent with Richerol et al. (2008b) data with regard to the distance of our coring site to the Mackenzie mouth. However, as revealed by the piston core, the period ranging from 700 to 1500 AD is characterized by three shorter cooling events of the same amplitude than the LIA. Alkenone-derived SST records and model simulations indicate cool sea-surface temperatures in the northeastern Pacific between ~ 900 and 1300 AD (Kim et al. 2004), associated with strong negative PDO index values (Macdonald and Case 2005). Colder Pacific waters during this interval might explain the cooling events recorded in zone D3, illustrating how the PDO indirectly influences the western Arctic. Taken together, these colder periods could be seen as one feature and related to the early onset of the LIA described by Podritske and Gajewski (2007) on Victoria Island. We conclude by constraining the LIA from 1560 to 1820 AD over the Mackenzie Slope, but we also consider the LIA as the last (as well as the longest) of a series of cooling events that took place between 700 and 1820 AD.

2.6.5 Hydrological and atmospheric forcing upon sea-ice cover

The duration of sea-ice cover over the Mackenzie Shelf and Slope is subject to considerable interannual variability (see Fig. 2c in O'Brien et al. 2006). For instance, historical data from the National Climate Data Centre (Boulder, Colorado) over the period 1954-2004 AD indicate a relatively high standard deviation of 1.41 month per year over station 803 (average duration of 9.96 months.yr⁻¹). A flaw lead has also been observed as early as late February (year 1991; Macdonald et al. 1995), whereas break up usually begins in May (Carmack et al. 2004). In station 803 cores, cross correlations between reconstructed duration of sea-ice cover vs SSS ($r^2=0.43$) and SST ($r^2=0.12$) suggest that surface salinity exerts a dominant role in controlling the duration of sea-ice cover. Indeed, owing to the large amounts of freshwater delivered by the Mackenzie River, this relatively narrow shelf (~ 100 km) is considered to be the most estuarine of all Arctic shelves (O'Brien et al. 2006). Less saline surface waters allow sea-ice to form more rapidly, while enhanced stratification also facilitates new ice formation. This is consistent with Manak and Mysak (1989) who found a positive correlation between sea-ice cover and discharge anomalies in the Beaufort Sea region for the period 1953-1984 AD, with discharge leading by 12 months.

In dinocyst zone D4, the opposite trend between SSS and duration of sea-ice cover is particularly well illustrated. Freshwater runoff indicators (Fig. 5) suggest relatively high discharge of fresh, warm waters from the Mackenzie River, associated with a shift in surface salinity toward lower values (from ~ 26 to ~ 24) and higher SST values (from ~ 5 to

$\sim 6^{\circ}\text{C}$) at the base of D4 (Fig. 6). As expected, this shift in SSS is accompanied by an increase of $\sim 1 \text{ month.yr}^{-1}$ in sea-ice cover duration.

Nevertheless, this overall control of surface salinity upon sea-ice cover must be interpreted with caution. The hydrological forcing appears to be different in zone D3. Freshwater input indicators also suggest high discharge from the Mackenzie River, whereas reconstructed SST indicate colder sea-surface conditions (series of cooling events, including the LIA). This suggests a supra-local scale hydrological or atmospheric forcing, which would explain the related cold period recorded on Victoria Island by Podritske and Gajewski (2007), i.e. away from the zone of influence of the Mackenzie River.

2.6.6 Recent hydrological changes (zone D4)

Dinocyst zone D4 records the most relevant variations of the entire sequence. Sea-surface temperatures in zone D4 are characterized by a brief cool period (August SST of $\sim 5^{\circ}\text{C}$ from 1880 to 1930 AD) followed by a warming with SST reaching the modern value (5.9°C ; Fig. 6). A similar cooling event at 0.1 ka has been recorded in both Greenland GISP2 ice cores (Stuiver 1999) and the Barents Sea (Voronina et al. 2001). Limnological data from lake KR02 (Victoria Island) also suggest a warming of $\sim 0.5^{\circ}\text{C}$ in the last 100 years (Peros and Gajewski 2008). Although weak in our records, this recent warming trend in the western Canadian Arctic has been instrumentally measured and observed in numerous lake and marine cores, as opposed to a cooling trend recorded in the eastern

Arctic (Koerner and Fisher 1990, Bourgeois et al. 2000, Rochon et al. 2006, Zabenskie and Gajewski 2007).

We observe an increase of ~ 1 month.yr $^{-1}$ in sea-ice cover duration since 1920 AD (Fig. 6), which is surprising for two reasons. First, one would expect more ice-free conditions (thus light availability) with high relative abundances of the autotrophic taxa *Operculodinium centrocarpum* (Fig. 6). Yet, Radi et al. (2001) have shown that the distribution of *O. centrocarpum* is positively correlated with sea-ice cover ($R=0.912$) in the Bering Sea. More sea-ice is also surprising with regard to recent instrumental observations that report dramatic decreases in Arctic summer sea-ice extent and thickness (e.g., McBean et al. 2004, Serreze et al. 2007). However, submarine-based observations suggest that ice thickness in the Arctic Ocean remained constant during the 1990s (Winsor 2001). Similarly, Melling et al. (2005) observed a slight increase in seasonal pack ice concentrations close to station 803 (< 100 km upslope) since 1991, and little evidence for any trend in ice-covered area over the continental shelf from a 36 years long ice-chart record. In addition, more sea-ice is recorded in the last 100 years over the Mackenzie Trough and Slope by foraminiferal and dinocyst assemblages (Scott et al. 2007, Schell et al. 2008, Richerol et al. 2008b). Our data is thus consistent with previous work, but this apparent contradiction points out the need of an integrative, multi-proxy approach considering several records to encompass supra-local sea-ice changes.

Finally, we venture the hypothesis that the SSS decadal oscillations in zone D4 are associated with the accumulation of freshwater by the Beaufort Gyre described by

Proshutinsky et al. (2002). Surface salinities alternate between high (~ 27) and low (~ 21) values every 14 years (period = 28 years), accompanied by slight variations in sea-ice cover (Fig. 6). Proshutinsky and Johnson (1997) brought to light that two wind-driven circulation regimes are possible in the Arctic (a cyclonic: CCR, and an anticyclonic: ACCR), alternating at 5-7 year intervals (period of 10-15 years). During ACCR, the Beaufort Gyre accumulates a significant amount of freshwater (in both sea-ice and low salinity waters), which is then released to the North Atlantic during CCR through Fram Strait and the Canadian Arctic Archipelago (Belkin et al. 1998, Macdonald et al. 1999, Proshutinsky et al. 2002). This mechanism is believed to explain the origin of the Great Salinity Anomalies (GSAs) observed in the North Atlantic in the 1970's (Dickson et al. 1988), 1980's and 1990's (Belkin et al. 1998, Belkin 2004). GSAs are of major concern since they tend to reduce the formation of Labrador Sea deep water, hence weakening the global thermohaline circulation (Darby and Bischof 2004, Zhang and Vallis 2006).

These SSS oscillations in zone D4 are not recorded in SST reconstructions; nor could they be linked with freshwater palynomorphs and instrumentally measured discharges from the Mackenzie River. Although our sampling interval (7 years) does not allow to document such high frequency features, the ACCR/CCR period (10-15 years) lies in the range of the second harmonic of SSS oscillations recorded in our data (period: 28 years = 2 times that of ACCR/CCR shifts). In addition, our boxcore record shows two other low salinity events prior to 1920 AD (SSS ~ 22 in 1860 and 1790 AD). If our hypothesis is valid, these low salinity events could have preceded similar GSAs, as suggested by Dickson et al. (1988), Walsh and Chapman (1990) and Schmitt and Hansen (2003).

2.7 Summary and conclusions

Sedimentary cores collected at station 2004-804-803 (upper Mackenzie Slope, 218 m depth) provide a high resolution record of surface hydrological changes over the last 4600 years. A sedimentation rate of ~ 140 cm.ka $^{-1}$ has been constrained on the basis of four calibrated AMS- ^{14}C measurements, in addition to ^{210}Pb activity on the top 20 cm of the sequence, which suggests an important contribution of the Mackenzie River sedimentary discharge. Palynological and geochemical analyses reveal numerous features in this post-HTM sequence, summarized as follows:

- Four zones have been determined on the basis of dinocyst assemblages, the dominant taxa being *Operculodinium centrocarpum* (overall mean of 38.1%), *Brigantedinium* spp. (17.7%), cysts of *Pentapharsodinium dalei* (17.6%) and *Islandinum minutum* (16.8%);
- Quantitative reconstructions indicate that sea-surface conditions remained relatively stable over the last 4.6 ka;
- Sea-surface salinity seems to exert a dominant role in controlling the duration of sea-ice cover; however some variations in reconstructed sea-ice cover must imply supra-local scale hydrological and/or atmospheric forcing;

- The $\delta^{15}\text{N}$ profile might have recorded variations in Pacific water influence from 4600 to \sim 1300 cal BP, probably associated with centennial scale shifts of the Arctic Oscillation phases;
- We associate a cool period recorded between 1560 and 1820 AD (sea-surface temperature of $\sim 1.5^\circ\text{C}$ below the modern value of $\sim 6^\circ\text{C}$) with the Little Ice Age, but we also consider the LIA as the last and the longest of episodic cooling events that took place between 700 and 1820 AD;
- Stable isotopic data suggest that the rate of relative sea-level rise in the southern Beaufort Sea increased since 1820 AD. Thus, this highly sensitive coastal area might continue to undergo severe erosion in the next decades;
- Reconstructed sea-surface salinity shows decadal oscillations since 1920 AD that we associate with the accumulation of freshwater by the Beaufort Gyre and the subsequent Great Salinity Anomalies. Our data suggest that similar salinity anomalies could have occurred ca. 1860 and 1790 AD.

2.8 Acknowledgements

This work is a contribution to the Canadian Arctic Shelf Exchange Study program (CASES) and was funded by the Natural Sciences and Engineering Research Council of Canada (NSERC), the International Polar Year project, Natural climate variability and forcings in Canadian Arctic and Arctic Ocean – NSERC Special Research Opportunity – International Polar Year and the Canadian Foundation for Innovation. Manuel Bringué was funded through a NSERC PGS-M scholarship. We are grateful to the officers and crew of the CCGS *Amundsen* who helped during the collection and analyses of the cores, in addition to David B. Scott and Trecia Schell, Dalhousie University; Kate Jarrett and Robbie Bennett, Bedford Institute of Oceanography; Jean-François Hélie and Bassam Ghaleb, GEOTOP, UQAM; Claude Belzile, Ursule Boyer-Villemaire and Hubert Gagné, Institut des sciences de la mer de Rimouski, UQAR. Many thanks to Jacques Labrie, Francesco Barletta, David Ledu and Gwénaëlle Chaillou (ISMER-UQAR) for their technical support and advises. Finally, we wish to express our gratitude to Guillaume St-Onge (ISMER-UQAR) and Fabienne Marret (University of Liverpool) who helped to improve the manuscript.

CHAPITRE III

CONCLUSIONS GÉNÉRALES

3.1 Conclusions générales

L'étude des carottes sédimentaires de la station CASES 2004-804-803 (carottes à boîte, à gravité et à piston) a permis de documenter la variabilité hydroclimatique sur le talus du Mackenzie au cours des derniers 4600 ans. Le taux de sédimentation de 140 cm ka⁻¹ (estimé à partir de quatre datations AMS-¹⁴C sur des coquilles de bivalves et de mesures d'activité de ²¹⁰Pb sur les premiers 20 cm de la carotte boîte) suggère une contribution substantielle des apports sédimentaires du Mackenzie.

Quatre zones d'assemblage de dinokystes ont été déterminées sur la base des variations des abondances relatives des principaux taxons. De 4600 à 2700 cal AA (zone D1), les assemblages sont dominés par le taxon autotrophe *Operculodinium centrocarpum* (moyenne de 49,0%). En zone D2 (2700-1500 cal AA), les taxons hétérotrophes *Brigantedinium* spp. (28,8%) et les kystes de *Polykrikos* sp. var. *arctic/quadratus* (2,8%) sont plus fortement représentés. Les fortes abondances relatives de *Islandinium minutum* (19,9%) caractérisent la zone D3 (1500-30 cal AA ou 450-1920 AD). Au sommet de la séquence, la zone D4 (de 1920 à 2004 AD) est de nouveau dominée par *O. centrocarpum* (44,5%), avec des abondances relatives de *Brigantedinium* spp. et cf. *Echinidinium karaense* presque nulles.

Les reconstitutions quantitatives des paramètres océaniques de surface (température et salinité de surface en août, durée du couvert de glace) ont été estimées à partir des assemblages de kystes de dinoflagellés dans les sédiments en utilisant des fonctions de transfert (méthode des meilleurs analogues modernes). Celles-ci indiquent des conditions

de surface relativement stables au cours des derniers 4600 ans. Cette relative stabilité concorde avec la littérature existante (notamment concernant les conditions post-*Holocene Thermal Maximum* et la stabilisation de l'advection d'eau atlantique dans l'Océan Arctique) mais contraste avec des variations de plus forte amplitude enregistrées dans la mer de Chukchi et la fosse du Mackenzie. On note tout de même des refroidissements épisodiques d'environ 1,5°C sous la valeur actuelle (5,9°C) entre 700 et 1820 AD, possiblement reliés à l'advection d'eau pacifique froide (valeurs négatives de l'index PDO – *Pacific Decadal Oscillation*). Nous associons le dernier et le plus long de ces refroidissements (1560-1820 AD) avec le Petit Âge Glaciaire.

Les données d'isotopes stables ($\delta^{13}\text{C}$ et $\delta^{15}\text{N}$) indiquent une lente augmentation de l'influence marine (vs terrestre) dans l'origine de la matière organique au cours de l'Holocène récent. Cette variation est attribuable au rehaussement du niveau marin relatif dans la région du delta du Mackenzie, une région côtière particulièrement vulnérable à l'érosion. Nos données suggèrent également que le taux de transgression marine s'est intensifié depuis 1820 AD. Entre 4600 et 1300 cal avant aujourd'hui, des variations séculaires de l'Oscillation arctique sont enregistrées par les mesures de $\delta^{15}\text{N}$ qui mettent en évidence des modifications de l'influence de l'eau pacifique au site d'étude.

De 1920 à 2004 AD, des variations récurrentes de salinité de surface (oscillant entre ~21 et 27) peuvent être associées au mécanisme d'accumulation d'eau douce par la gyre de Beaufort pendant les régimes de circulation atmosphérique anticyclonique. Nos données indiquent également que des accumulations d'eau douce similaires (qui précèdent les

anomalies de salinité documentées dans l'Atlantique Nord) ont pu survenir vers 1790 et 1860 AD.

Ainsi, des changements hydrographiques importants ont pu être observés au sein de la stabilité relative de l'Holocène récent (Dansgaard et al. 1993, Macdonald et al. 2005). Les sédiments du talus du Mackenzie constituent des enregistrements paléoenvironmentaux de qualité. En effet, le fort taux de sédimentation permet des études à haute résolution temporelle, et sa position géographique permet de documenter les principaux modes de variabilité climatique de l'Arctique canadien occidental. Des études utilisant d'autres traceurs des conditions de surface pourront contribuer à documenter la variabilité passée en confirmant ou en infirmant les reconstitutions et les hypothèses avancées dans le présent mémoire. En particulier, il serait intéressant de détailler certaines périodes clés (e.g., entre 3500 et 1300 AD pour les transitions séculaires de l'Oscillation arctique) à plus haute résolution afin de pouvoir documenter plus efficacement les modes de variabilité hydroclimatiques à l'échelle multi-annuelle.

RÉFÉRENCES

- Abdul Aziz, O.I. and Burn, D.H. 2006. Trends and variability in the hydrological regime of the Mackenzie River Basin. *Journal of Hydrology*, 319(1-4): 282-294. doi: 10.1016/j.jhydrol.2005.06.039.
- Alley, R.B. and Agustsdottir, A.M. 2005. The 8k event: cause and consequences of a major Holocene abrupt climate change. *Quaternary Science Reviews*, 24(10-11): 1123-1149. doi: 10.1016/j.quascirev.2004.12.004.
- Andrews, J.T. and Dunhill, G. 2004. Early to mid-Holocene Atlantic water influx and deglacial meltwater events, Beaufort Sea slope, Arctic Ocean. *Quaternary Research*, 61(1): 14-21. doi: 10.1016/j.yqres.2003.08.003.
- Anklin, M., Barnola, J.M., Beer, J., Blunier, T., Chappellaz, J., Clausen, H.B., Dahljensen, D., Dansgaard, W., Deangelis, M., Delmas, R.J., Duval, P., Fratta, M., Fuchs, A., Fuhrer, K., Gundestrup, N., Hammer, C., Iversen, P., Johnsen, S., Jouzel, J., Kipfstuhl, J., Legrand, M., Lorius, C., Maggi, V., Miller, H., Moore, J.C., Oeschger, H., Orombelli, G., Peel, D.A., Raisbeck, G., Raynaud, D., Schotthvidberg, C., Schwander, J., Shoji, H., Souchez, R., Stauffer, B., Steffensen, J.P., Stievenard, M., Sveinbjornsdottir, A., Thorsteinsson, T. and Wolff, E.W. 1993. Climate instability during the last interglacial period recorded in the GRIP ice core. *Nature*, 364(6434): 203-207.
- Appleby, P.G. and Oldfield, F. 1983. The assessment of ^{210}Pb data from sites with varying sediment accumulation rates. *Hydrobiologia*, 103: 29-35. doi: 10.1007/BF00028424.
- Backman, J., Jakobsson, M., Lovlie, R., Polyak, L. and Febo, L.A. 2004. Is the central Arctic Ocean a sediment starved basin? *Quaternary Science Reviews*, 23(11-13): 1435-1454. doi: 10.1016/j.quascirev.2003.12.005.
- Barletta, F., St-Onge, G., Channell, J.E.T., Rochon, A., Polyak, L. and Darby, D. 2008. High-resolution paleomagnetic secular variation and relative paleointensity records from the western Canadian Arctic: implication for Holocene stratigraphy and

- geomagnetic field behaviour. Canadian Journal of Earth Sciences, 45(11): 1265-1281. doi: 10.1139/e08-039.
- Belkin, I.M. 2004. Propagation of the "Great Salinity Anomaly" of the 1990s around the northern North Atlantic. Geophysical Research Letters, 31(8). doi: 10.1029/2003 gl019334.
- Belkin, I.M., Levitus, S., Antonov, J. and Malmberg, S.-A. 1998. "Great Salinity Anomalies" in the North Atlantic. Progress in Oceanography, 41(1): 1-68.
- Bennett, K.D. 1996. Determination of the number of zones in a biostratigraphical sequence. New Phytologist, 132(1): 155-170.
- Bjornsson, H., Mysak, L.A. and Brown, R.D. 1995. On the interannual variability of precipitation and runoff in the Mackenzie drainage-basin. Climate Dynamics, 12(1): 67-76.
- Blott, S.J. and Pye, K. 2001. GRADISTAT: A grain size distribution and statistics package for the analysis of unconsolidated sediments. Earth Surface Processes and Landforms, 26(11): 1237-1248.
- Bourgeois, J.C., Koerner, R.M., Gajewski, K. and Fisher, D.A. 2000. A holocene ice-core pollen record from Ellesmere Island, Nunavut, Canada. Quaternary Research, 54(2): 275-283. doi: 10.1006/qres.2000.2156.
- Brachfeld, S., Barletta, F., St-Onge, G., Darby, D. and Ortiz, J.D. 2009. Impact of diagenesis on the environmental magnetic record from a Holocene sedimentary sequence from the Chukchi-Alaskan margin, Arctic Ocean. Global and Planetary Change, 68(1-2): 100-114. doi: 10.1016/j.gloplacha.2009.03.023.
- Calvert, S.E., Nielsen, B. and Fontugne, M.R. 1992. Evidence from nitrogen isotope ratios for enhanced productivity during formation of eastern Mediterranean sapropels. Nature, 359(6392): 223-225.
- Campeau, S., Héquette, A. and Pienitz, R. 2000. Late Holocene diatom biostratigraphy and sea-level changes in the southeastern Beaufort Sea. Canadian Journal of Earth Sciences, 37(1): 63-80.

- Carmack, E.C. and Macdonald, R.W. 2002. Oceanography of the Canadian shelf of the Beaufort Sea: A setting for marine life. *Arctic*, 55: 29-45.
- Carmack, E.C., Macdonald, R.W. and Papadakis, J.E. 1989. Water mass structure and boundaries in the Mackenzie Shelf estuary. *Journal of Geophysical Research*, 94(C12): 18043-18055.
- Carmack, E.C., Macdonald, R.W. and Jasper, S. 2004. Phytoplankton productivity on the Canadian Shelf of the Beaufort Sea. *Marine Ecology Progress Series*, 277: 37-50.
- Carmack, E., Barber, D., Christensen, J., Macdonald, R., Rudels, B. and Sakshaug, E. 2006. Climate variability and physical forcing of the food webs and the carbon budget on panarctic shelves. *Progress in Oceanography*, 71(2-4): 145-181. doi: 10.1016/j.pocean.2006.10.005.
- Carson, M.A., Jasper, J.N. and Conly, F.M. 1998. Magnitude and sources of sediment input to the Mackenzie Delta, Northwest Territories, 1974-94. *Arctic*, 51(2): 116-124.
- Chen, Z.H., Shi, X.F., Cai, D.L., Han, Y.B. and Yang, Z.H. 2006. Organic carbon and nitrogen isotopes in surface sediments from the western Arctic Ocean and their implications for sedimentary environments. *Acta Oceanologica Sinica*, 25(5): 39-54.
- Comiso, J.C. 2002. A rapidly declining perennial sea ice cover in the Arctic. *Geophysical Research Letters*, 29(20). doi: 10.1029/2002gl015650.
- Comiso, J.C., Parkinson, C.L., Gersten, R. and Stock, L. 2008. Accelerated decline in the Arctic sea ice cover. *Geophysical Research Letters*, 35. doi: 10.1029/2007gl031972.
- Dansgaard, W., Johnsen, S.J., Clausen, H.B., Dahljensen, D., Gundestrup, N.S., Hammer, C.U., Hvidberg, C.S., Steffensen, J.P., Sveinbjornsdottir, A.E., Jouzel, J. and Bond, G. 1993. Evidence for general instability of past climate from a 250-kyr ice-core record. *Nature*, 364(6434): 218-220.
- Darby, D.A. and Bischof, J.F. 2004. A Holocene record of changing Arctic Ocean ice drift analogous to the effects of the Arctic Oscillation. *Paleoceanography*, 19(1). PA1027.

- Darby, D.A., Bischof, J.F., Spielhagen, R.F., Marshall, S.A. and Herman, S.W. 2002. Arctic ice export events and their potential impact on global climate during the late Pleistocene. *Paleoceanography*, 17(2). doi: 10.1029/2001pa000639.
- Darby, D.A., Polyak, L. and Bauch, H.A. 2006. Past glacial and interglacial conditions in the Arctic Ocean and marginal seas - a review. *Progress in Oceanography*, 71(2-4): 129-144.
- de Vernal, A. and Hillaire-Marcel, C. 2006. Provincialism in trends and high frequency changes in the northwest North Atlantic during the Holocene. *Global and Planetary Change*, 54(3-4): 263-290.
- de Vernal, A., Bilodeau, G., Hillaire-Marcel, C. and Kassou, N. 1992. Quantitative assessment of carbonate dissolution in marine sediments from foraminifer linings vs. shell ratios; Davis Strait, Northwest North Atlantic. *Geology*, 20(6): 527-530.
- de Vernal, A., Rochon, A., Turon, J.L. and Matthiessen, J. 1997. Organic-walled dinoflagellate cysts: Palynological tracers of sea-surface conditions in middle to high latitude marine environments. *Geobios*, 30(7): 905-920.
- de Vernal, A., Henry, M., Matthiessen, J., Mudie, P.J., Rochon, A., Boessenkool, K.P., Eynaud, F., Grosfeld, K., Guiot, J., Hamel, D., Harland, R., Head, M.J., Kunz-Pirring, M., Levac, E., Loucheur, V., Peyron, O., Pospelova, V., Radi, T., Turon, J.L. and Voronina, E. 2001. Dinoflagellate cyst assemblages as tracers of sea-surface conditions in the northern North Atlantic, Arctic and sub-Arctic seas: the new 'n=677' data base and its application for quantitative palaeoceanographic reconstruction. *Journal of Quaternary Science*, 16(7): 681-698.
- de Vernal, A., Hillaire-Marcel, C. and Darby, D.A. 2005a. Variability of sea ice cover in the Chukchi Sea (western Arctic Ocean) during the Holocene. *Paleoceanography*, 20(4): 18. doi: 10.1029/2005pa001157.
- de Vernal, A., Eynaud, F., Henry, M., Hillaire-Marcel, C., Londeix, L., Mangin, S., Matthiessen, J., Marret, F., Radi, T., Rochon, A., Solignac, S. and Turon, J.L. 2005b. Reconstruction of sea-surface conditions at middle to high latitudes of the Northern Hemisphere during the Last Glacial Maximum (LGM) based on dinoflagellate cyst assemblages. *Quaternary Science Reviews*, 24(7-9): 897-924.

- Derocher, A.E., Lunn, N.J. and Stirling, I. 2004. Polar bears in a warming climate. In Integrative and Comparative Biology, Vol. 44: pp. 163-176.
- Dickson, R.R., Meincke, J., Malmberg, S.-A. and Lee, A.J. 1988. The "great salinity anomaly" in the Northern North Atlantic 1968-1982. Progress in Oceanography, 20(2): 103-151.
- Dunton, K.H., Weingartner, T. and Carmack, E.C. 2006. The nearshore western Beaufort Sea ecosystem: Circulation and importance of terrestrial carbon in arctic coastal food webs. Progress in Oceanography, 71(2-4): 362-378. doi: 10.1016/j.pocean.2006.09.011.
- Duplessy, J.C., Cortijo, E., Ivanova, E., Khusid, T., Labeyrie, L., Levitan, M., Murdmaa, I. and Paterne, M. 2005. Paleoceanography of the Barents Sea during the Holocene. Paleoceanography, 20(4): 14. doi: 10.1029/2004pa001116.
- Dyke, A.S., England, J., Reimnitz, E. and Jette, H. 1997. Changes in driftwood delivery to the Canadian Arctic Archipelago: The hypothesis of postglacial oscillations of the transpolar drift. Arctic, 50(1): 1-16.
- England, J.H. and Furze, M.F.A. 2008. New evidence from the western Canadian Arctic Archipelago for the resubmergence of Bering Strait. Quaternary Research, 70(1): 60-67. doi: 10.1016/j.yqres.2008.03.001.
- Fensome, R.A. and Williams, G.L. 2004. The Lentin and Williams Index of Fossil Dinoflagellates. Contribution Series Number 42. American Association of Stratigraphic Palynologists Foundation, Dallas, TX.
- Fischer, H., Werner, M., Wagenbach, D., Schwager, M., Thorsteinsson, T., Wilhelms, F., Kipfstuhl, J. and Sommer, S. 1998. Little Ice Age Clearly Recorded in Northern Greenland Ice Cores. Geophysical Research Letters, 25(10): 1749-1752. doi: 10.1029/98gl01177.
- Groupe d'experts intergouvernemental sur l'évolution du climat (GIEC) 2007. Changements Climatiques 2007: Rapport de Synthèse. Available from http://www.ipcc.ch/publications_and_data/publications_ipcc_fourth_assessment_report_synthesis_report.htm [accessed May 2009].

- Guiot, J. and de Vernal, A. 2007. Chapter thirteen. Transfer functions: Methods for Quantitative Paleoceanography Based on Microfossils. In *Developments in Marine Geology*, Volume 1. Edited by H. Chamley. Elsevier. pp. 523-563.
- Häkkinen, S. 1999. A simulation of thermohaline effects of a great salinity anomaly. *Journal of Climate*, 12(6): 1781-1795.
- Häkkinen, S. and Proshutinsky, A. 2004. Freshwater content variability in the Arctic Ocean. *Journal of Geophysical Research-Oceans*, 109(C3).
- Head, M.J., Harland, R. and Matthiessen, J. 2001. Cold marine indicators of the late Quaternary: the new dinoflagellate cyst genus *Islandinium* and related morphotypes. *Journal of Quaternary Science*, 16(7): 621-636.
- Hélie, J.F. 2009. Elemental and stable isotopic approaches for studying the organic and inorganic carbon components in natural samples. In *From Deep-sea to Coastal Zones: Methods and Techniques for Studying Paleoenvironments*. IOP Conference Series: Earth and Environmental Science, Vol. 5. doi: 10.1088/1755-1307/5/1/012005.
- Héquette, A., Ruz, M.H. and Hill, P.R. 1995. The effects of the Holocene sea-level rise on the evolution of the southeastern coast of the Canadian Beaufort Sea. *Journal of Coastal Research*, 11(2): 494-507.
- Hill, P.R. 1996. Late quaternary sequence stratigraphy of the Mackenzie Delta. *Canadian Journal of Earth Sciences*, 33(7): 1064-1074.
- Hill, P.R., Héquette, A. and Ruz, M.H. 1993. Holocene sea-level history of the Canadian Beaufort Shelf. *Canadian Journal of Earth Sciences*, 30(1): 103-108.
- Hill, P.R., Lewis, C.P., Desmarais, S., Kauppaymuthoo, V. and Rais, H. 2001. The Mackenzie Delta: sedimentary processes and facies of a high-latitude, fine-grained delta. *Sedimentology*, 48(5): 1047-1078.
- Hillaire-Marcel, C., de Vernal, A., Polyak, L. and Darby, D. 2004. Size-dependent isotopic composition of planktic foraminifers from Chukchi Sea vs. NW Atlantic sediments - implications for the Holocene paleoceanography of the western Arctic. *Quaternary Science Reviews*, 23(3-4): 245-260. doi: 10.1016/j.quascirev.2003.08.006.

- Hirst, S.M., Miles, M., Blachut, S.P., Goulet, L.A. and Taylor, R.E. 1987. Quantitative syntheses of the Mackenzie Delta ecosystem; main volume. Report to Inland Waters Directorate., Environment Canada, Yellowknife, NWT.
- Holland, M.M. and Bitz, C.M. 2003. Polar amplification of climate change in coupled models. *Climate Dynamics*, 21(3-4): 221-232. doi: 10.1007/s00382-003-0332-6.
- Houssais, M.N., Herbaut, C., Schlichtholz, P. and Rousset, C. 2007. Arctic salinity anomalies and their link to the North Atlantic during a positive phase of the Arctic Oscillation. *Progress in Oceanography*, 73(2): 160-189. doi: 10.1016/j.pocean.2007.02.005.
- Hughen, K.A., Baillie, M.G.L., Bard, E., Beck, J.W., Bertrand, C.J.H., Blackwell, P.G., Buck, C.E., Burr, G.S., Cutler, K.B., Damon, P.E., Edwards, R.L., Fairbanks, R.G., Friedrich, M., Guilderson, T.P., Kromer, B., McCormac, G., Manning, S., Ramsey, C.B., Reimer, P.J., Reimer, R.W., Remmele, S., Southon, J.R., Stuiver, M., Talamo, S., Taylor, F.W., van der Plicht, J. and Weyhenmeyer, C.E. 2004. Marine04 marine radiocarbon age calibration, 0-26 cal kyr BP. *Radiocarbon*, 46(3): 1059-1086.
- Intergovernmental Panel on Climate Change (IPCC) 2007. Climate Change 2007: Synthesis Report. Available from http://www.ipcc.ch/publications_and_data/publications_ipcc_fourth_assessment_report_synthesis_report.htm [accessed May 2009].
- Jacobson, D.M. and Anderson, D.M. 1986. Thecate heterotrophic dinoflagellates: feeding behavior and mechanisms. *Journal of Phycology*, 22(3): 249-258.
- Juggins, S. 2005. Software. Available from <http://www.staff.ncl.ac.uk/staff/stephen.juggins/software.htm> [accessed April 2009].
- Kaufman, D.S., Ager, T.A., Anderson, N.J., Anderson, P.M., Andrews, J.T., Bartlein, P.J., Brubaker, L.B., Coats, L.L., Cwynar, L.C., Duvall, M.L., Dyke, A.S., Edwards, M.E., Eisner, W.R., Gajewski, K., Geirsdottir, A., Hu, F.S., Jennings, A.E., Kaplan, M.R., Kerwin, M.N., Lozhkin, A.V., MacDonald, G.M., Miller, G.H., Mock, C.J., Oswald, W.W., Otto-Bliesner, B.L., Porinchu, D.F., Rühland, K., Smol, J.P., Steig, E.J. and Wolfe, B.B. 2004. Holocene thermal maximum in the western Arctic (0-180 degrees W). *Quaternary Science Reviews*, 23(5-6): 529-560. doi: 10.1016/j.quascirev.2004.06.001.

- Kim, J.H., Rimbu, N., Lorenz, S.J., Lohmann, G., Nam, S.I., Schouten, S., Ruhlemann, C. and Schneider, R.R. 2004. North Pacific and North Atlantic sea-surface temperature variability during the Holocene. *Quaternary Science Reviews*: 2141-2154. doi: 10.1016/j.quascirev.2004.08.010.
- Koerner, R.M. and Fisher, D.A. 1990. A record of Holocene summer climate from a Canadian high-Arctic ice core. *Nature*, 343: 630-631.
- Kokinos, J.P., Eglinton, T.I., Goni, M.A., Boon, J.J., Martoglio, P.A. and Anderson, D.M. 1998. Characterization of a highly resistant biomacromolecular material in the cell wall of a marine dinoflagellate resting cyst. *Organic Geochemistry*, 28(5): 265-288.
- Kucera, M., Weinelt, M., Kiefer, T., Pflaumann, U., Hayes, A., Chen, M.T., Mix, A.C., Barrows, T.T., Cortijo, E., Duprat, J., Juggins, S. and Waelbroeck, C. 2005. Reconstruction of sea-surface temperatures from assemblages of planktonic foraminifera: multi-technique approach based on geographically constrained calibration data sets and its application to glacial Atlantic and Pacific Oceans. *Quaternary Science Reviews*, 24(7-9): 951-998. doi: 10.1016/j.quascirev.2004.07.014.
- Kwok, R. 2000. Recent changes in Arctic Ocean sea ice motion associated with the North Atlantic Oscillation. *Geophysical Research Letters*, 27(6): 775-778.
- Ledu, D., Rochon, A., de Vernal, A. and St-Onge, G. 2008. Palynological evidence of Holocene climate change in the eastern Arctic: a possible shift in the Arctic oscillation at the millennial time scale. *Canadian Journal of Earth Sciences*, 45(11): 1363-1375. doi: 10.1139/e08-043.
- Lesack, L.F.W. and Marsh, P. 2007. Lengthening plus shortening of river-to-lake connection times in the Mackenzie River Delta respectively via two global change mechanisms along the arctic coast. *Geophysical Research Letters*, 34(23): 6. doi: 10.1029/2007gl031656.
- Liu, J.P., Curry, J.A. and Hu, Y.Y. 2004. Recent Arctic Sea Ice Variability: Connections to the Arctic Oscillation and the ENSO. *Geophysical Research Letters*, 31(9): 4. doi: 10.1029/2004gl019858.

- Loso, M.G., Anderson, R.S., Anderson, S.P. and Reimer, P.J. 2006. A 1500-year record of temperature and glacial response inferred from varved Iceberg Lake, southcentral Alaska. *Quaternary Research*, 66(1): 12-24.
- Lubinski, D.J., Polyak, L. and Forman, S.L. 2001. Freshwater and Atlantic water inflows to the deep northern Barents and Kara seas since ca 13 C-14 ka: foraminifera and stable isotopes. *Quaternary Science Reviews*, 20(18): 1851-1879.
- Lynch, A.H., Cassano, E.N., Cassano, J.J. and Lestak, L.R. 2003. Case studies of high wind events in Barrow, Alaska: Climatological context and development processes. *Monthly Weather Review*, 131(4): 719-732.
- Macdonald, G.M. and Case, R.A. 2005. Variations in the Pacific Decadal Oscillation over the past millennium. *Geophysical Research Letters*, 32(8). doi: 10.1029/2005gl022478.
- Macdonald, R.W., Wong, C.S. and Erickson, P.E. 1987. The distribution of nutrients in the Southeastern Beaufort Sea: Implications for water circulation and primary production. *Journal of Geophysical Research*, 92(C3): 2939-2952.
- Macdonald, R.W., Carmack, E.C., McLaughlin, F.A., Iseki, K., MacDonald, D.M. and O'Brien, M.C. 1989. Composition and modification of water masses in the Mackenzie Shelf Estuary. *Journal of Geophysical Research*, 94: 18057-18070.
- Macdonald, R.W., Paton, D.W., Carmack, E.C. and Omstedt, A. 1995. The fresh-water budget and under-ice spreading of Mackenzie River water in the Canadian Beaufort Sea based on salinity and O-18/O-16 measurements in water and ice. *Journal of Geophysical Research-Oceans*, 100(C1): 895-919.
- Macdonald, R.W., Solomon, S.M., Cranston, R.E., Welch, H.E., Yunker, M.B. and Gobeil, C. 1998. A sediment and organic carbon budget for the Canadian Beaufort Shelf. *Marine Geology*, 144(4): 255-273.
- Macdonald, R.W., Carmack, E.C., McLaughlin, F.A., Falkner, K.K. and Swift, J.H. 1999. Connections among ice, runoff and atmospheric forcing in the Beaufort Gyre. *Geophysical Research Letters*, 26(15): 2223-2226.

- Macdonald, R.W., Harner, T. and Fyfe, J. 2005. Recent climate change in the Arctic and its impact on contaminant pathways and interpretation of temporal trend data. *Science of the Total Environment*, 342(1-3): 5-86.
- Manabe, S., Spelman, M.J. and Stouffer, R.J. 1992. Transient responses of a coupled ocean atmosphere model to gradual changes of atmospheric CO₂. *Journal of Climate*, 5(2): 105-126.
- Manak, D.K. and Mysak, L.A. 1989. On the relationship between Arctic sea-ice anomalies and fluctuations in northern Canadian air-temperature and river discharge. *Atmosphere-Ocean*, 27(4): 682-691.
- Manson, G.K. and Solomon, S.M. 2007. Past and future forcing of Beaufort sea coastal change. *Atmosphere-Ocean*, 45(2): 107-122. doi: 10.3137/ao.450204.
- Matthiessen, J., Kunz-Pirrung, M. and Mudie, P.J. 2000. Freshwater chlorophycean algae in recent marine sediments of the Beaufort, Laptev and Kara Seas (Arctic Ocean) as indicators of river runoff. *International Journal of Earth Sciences*, 89(3): 470-485.
- Matthews, J. 1969. The assessment of a method for the determination of absolute pollen frequencies. *The New Phytologist*, 68: 161-166. doi: 10.1111/j.1469-8137.1969.tb06429.x.
- McBean, G., Alekseev, G., Chen, D., Førland, E., Fyfe, J., Y.Groisman, P., King, R., Melling, H., Vose, R. and H.Whitfield, P. 2004. Chapter 2. Arctic Climate: Past and Present. In Impacts of a Warming Arctic: Arctic Climate Impact Assessment (ACIA). Cambridge University Press. pp. 21-60.
- McKay, J.L., de Vernal, A., Hillaire-Marcel, C., Not, C., Polyak, L. and Darby, D. 2008. Holocene fluctuations in Arctic sea-ice cover: dinocyst-based reconstructions for the eastern Chukchi Sea. *Canadian Journal of Earth Sciences*, 45(11): 1377-1397. doi: 10.1139/e08-046.
- McLaughlin, F., Carmack, E., Macdonald, R., Weaver, A.J. and Smith, J. 2002. The Canada Basin, 1989-1995: Upstream events and far-field effects of the Barents Sea. *Journal of Geophysical Research-Oceans*, 107(C7). doi: 10.1029/2001jc000904.

- McLaughlin, F., Shimada, K., Carmack, E., Itoh, M. and Nishino, S. 2005. The hydrography of the southern Canada Basin, 2002. *Polar Biology*, 28(3): 182-189. doi: 10.1007/s00300-004-0701-6.
- McNeely, R., Dyke, A.S. and Southon, J.R. 2006. Canadian marine reservoir ages, preliminary data assessment. Geological Survey Canada, Open file 5049.
- Melling, H., Riedel, D.A. and Gedalof, Z. 2005. Trends in the draft and extent of seasonal pack ice, Canadian Beaufort Sea. *Geophysical Research Letters*, 32(24). doi: 10.1029/2005gl024483.
- Menounos, B., Osborn, G., Clague, J.J. and Luckman, B.H. 2009. Latest Pleistocene and Holocene glacier fluctuations in western Canada. *Quaternary Science Reviews*, 28(21-22): 2049-2074. doi: 10.1016/j.quascirev.2008.10.018.
- Meyers, P.A. 1997. Organic geochemical proxies of paleoceanographic, paleolimnologic, and paleoclimatic processes. *Organic Geochemistry*, 27(5-6): 213-250.
- Michelutti, N., Douglas, M.S.V., Wolfe, A.P. and Smol, J.P. 2006. Heightened sensitivity of a poorly buffered high arctic lake to late-Holocene climatic change. *Quaternary Research*, 65(3): 421-430. doi: 10.1016/j.yqres.2006.02.001.
- Mitchell, J.F.B., Johns, T.C., Gregory, J.M. and Tett, S.F.B. 1995. Climate response to increasing levels of greenhouse gases and sulfate aerosols. *Nature*, 376(6540): 501-504.
- Mudie, P.J. and Rochon, A. 2001. Distribution of dinoflagellate cysts in the Canadian Arctic marine region. *Journal of Quaternary Science*, 16(7): 603-620.
- Mudie, P.J., Harland, R., Matthiessen, J. and de Vernal, A. 2001. Marine dinoflagellate cysts and high latitude Quaternary paleoenvironmental reconstructions: an introduction. *Journal of Quaternary Science*, 16(7): 595-602.
- Naidu, A.S., Cooper, L.W., Finney, B.P., Macdonald, R.W., Alexander, C. and Semiletov, I.P. 2000. Organic carbon isotope ratios (δ C-13) of Arctic Amerasian Continental shelf sediments. *International Journal of Earth Sciences*, 89(3): 522-532.

- Niebauer, N.J. and Day, R.H. 1989. Causes of interannual variability in the sea ice cover of the eastern Bering Sea. *GeoJournal*, 18: 45-59.
- National Oceanographic Data Center (NODC) 2001. World Ocean Atlas, 2001. National Oceanic and Atmospheric Administration (NOAA). Available from http://nodc.noaa.gov/OC5/WOD01/pr_wod01.html [accessed January 2009].
- O'Brien, M.C., Macdonald, R.W., Melling, H. and Iseki, K. 2006. Particle fluxes and geochemistry on the Canadian Beaufort Shelf: Implications for sediment transport and deposition. *Continental Shelf Research*, 26(1): 41-81. doi: 10.1016/j.csr.2005.09.007.
- Ogi, M., Rigor, I.G., McPhee, M.G. and Wallace, J.M. 2008. Summer retreat of Arctic sea ice: Role of summer winds. *Geophysical Research Letters*, 35(24): 5. doi: 10.1029/2008gl035672.
- Ortiz, J.D., Polyak, L., Grebmeier, J.M., Darby, D., Eberl, D.D., Naidu, S. and Nof, D. 2009. Provenance of Holocene sediment on the Chukchi-Alaskan margin based on combined diffuse spectral reflectance and quantitative X-Ray Diffraction analysis. *Global and Planetary Change*, 68(1-2): 71-84. doi: 10.1016/j.gloplacha.2009.03.020.
- Peltier, W.R. 2002. On eustatic sea level history: Last Glacial Maximum to Holocene. *Quaternary Science Reviews*, 21(1-3): 377-396.
- Peros, M.C. and Gajewski, K. 2008. Holocene climate and vegetation change on Victoria Island, western Canadian Arctic. *Quaternary Science Reviews*, 27(3-4): 235-249.
- Peros, M.C. and Gajewski, K. 2009. Testing the reliability of pollen-based diversity estimates. GC71A-04. In AGU-CGU Joint Assembly, Toronto, Canada.
- Pickart, R.S. 2004. Shelfbreak circulation in the Alaskan Beaufort Sea: Mean structure and variability. *Journal of Geophysical Research-Oceans*, 109(C4). doi: 10.1029/2003jc001912.
- Podritske, B. and Gajewski, K. 2007. Diatom community response to multiple scales of Holocene climate variability in a small lake on Victoria Island, NWT, Canada. *Quaternary Science Reviews*, 26(25-28): 3179-3196. doi: 10.1016/j.quascirev.2007.06.009.

- Proshutinsky, A.Y. and Johnson, M.A. 1997. Two circulation regimes of the wind driven Arctic Ocean. *Journal of Geophysical Research-Oceans*, 102(C6): 12493-12514.
- Proshutinsky, A., Bourke, R.H. and McLaughlin, F.A. 2002. The role of the Beaufort Gyre in Arctic climate variability: Seasonal to decadal climate scales. *Geophysical Research Letters*, 29(23).
- Radi, T., De Vernal, A. and Peyron, O. 2001. Relationships between dinoflagellate cyst assemblages in surface sediment and hydrographic conditions in the Bering and Chukchi seas. *Journal of Quaternary Science*, 16(7): 667-680.
- Richerol, T., Rochon, A., Blasco, S., Scott, D.B., Schell, T.M. and Bennett, R.J. 2008a. Distribution of dinoflagellate cysts in surface sediments of the Mackenzie Shelf and Amundsen Gulf, Beaufort Sea (Canada). *Journal of Marine Systems*, 74(3-4): 825-839. doi: 10.1016/j.jmarsys.2007.11.003.
- Richerol, T., Rochon, A., Blasco, S., Scott, D.B., Schell, T.M. and Bennett, R.J. 2008b. Evolution of paleo sea-surface conditions over the last 600 years in the Mackenzie Trough, Beaufort Sea (Canada). *Marine Micropaleontology*, 68(1-2): 6-20.
- Rigor, I.G., Colony, R.L. and Martin, S. 2000. Variations in surface air temperature observations in the Arctic, 1979-97. *Journal of Climate*, 13(5): 896-914.
- Rigor, I.G., Wallace, J.M. and Colony, R.L. 2002. Response of sea ice to the Arctic oscillation. *Journal of Climate*, 15(18): 2648-2663.
- Ritchie, J.C. and Hare, F.K. 1971. Late-quaternary vegetation and climate near the arctic tree line of northwestern North America. *Quaternary Research*, 1(3): 331-342.
- Rochon, A. 2009. The ecology and biological affinity of Arctic dinoflagellates and their paleoceanographical significance in the Canadian High Arctic. In *From Deep-sea to Coastal Zones: Methods and Techniques for Studying Paleoenvironments*. IOP Conference Series: Earth and Environmental Science, Vol. 5. doi: 10.1088/1755-1307/5/1/012003.

Rochon, A. and onboard participants 2004. CASES Leg 8 cruise report - 2.8 Millennial-decadal variability in sea ice and carbon fluxes (June 23 - August 5, 2004), CCGS Amundsen. p. 11.

Rochon, A., de Vernal, A., Turon, J.L., Matthiessen, J. and Head, M.J. 1999. Distribution of recent dinoflagellate cysts in surface sediments from the North Atlantic Ocean and adjacent seas in relation to sea-surface parameters. American Association of Stratigraphic Palynologists Foundation. Contribution series no. 35, Dallas, TX.

Rochon, A., Scott, D.B., Schell, T.M., Blasco, S., Bennett, R. and Mudie, P.J. 2006. Evolution of sea surface conditions during the Holocene: comparison between Eastern (Baffin Bay and Hudson Strait) and Western (Beaufort Sea) Canadian Arctic. In American Geophysical Union Annual Meeting, San Francisco, Calif. U34B, p. 867.

Rühland, K. and Smol, J.P. 2005. Diatom shifts as evidence for recent Subarctic warming in a remote tundra lake, NWT, Canada. *Palaeogeography Palaeoclimatology Palaeoecology*, 226(1-2): 1-16. doi: 10.1016/j.palaeo.2005.05.001.

Rühland, K., Priesnitz, A. and Smol, J.P. 2003. Paleolimnological evidence from diatoms for recent environmental changes in 50 lakes across Canadian Arctic treeline. *Arctic Antarctic and Alpine Research*, 35(1): 110-123.

Schell, T.M., Scott, D.B., Rochon, A. and Blasco, S. 2008. Late Quaternary paleoceanography and paleo-sea ice conditions in the Mackenzie Trough and Canyon, Beaufort Sea. *Canadian Journal of Earth Sciences*, 45(11): 1399-1415. doi: 10.1139/e08-054.

Schmitt, T. and Hansen, C. 2003. Fram Strait ice export during the nineteenth and twentieth centuries reconstructed from a multiyear sea ice index from southwestern Greenland. *Journal of Climate*, 16(16): 2782-2791.

Schuur, E.A.G., Bockheim, J., Canadell, J.G., Euskirchen, E., Field, C.B., Goryachkin, S.V., Hagemann, S., Kuhry, P., Lafleur, P.M., Lee, H., Mazhitova, G., Nelson, F.E., Rinke, A., Romanovsky, V.E., Shiklomanov, N., Tarnocai, C., Venevsky, S., Vogel, J.G. and Zimov, S.A. 2008. Vulnerability of permafrost carbon to climate change: Implications for the global carbon cycle. *Bioscience*, 58(8): 701-714. doi: 10.1641/b580807.

- Scott, D.B., Schell, T., Rochon, A. and Blasco, S. 2008. Benthic foraminifera in the surface sediments of the Beaufort Shelf and slope, Beaufort Sea, Canada: Applications and implications for past sea-ice conditions. *Journal of Marine Systems*, 74(3-4): 840-863. doi: 10.1016/j.jmarsys.2008.01.008.
- Scott, D.B., Schell, T.M., St-Onge, G., Rochon, A. and Blasco, S. 2007. Isotopic and sedimentological evidence for sea ice conditions and paleoceanography in last 15,000 years on the Beaufort Sea Slope and Amundsen Gulf, Canada. In *Geological Society of America Abstracts with Programs*, Vol. 39: p. 583.
- Scott, D.B., Schell, T., St-Onge, G., Rochon, A. and Blasco, S. 2009. Foraminiferal assemblage changes over the last 15,000 years on the Mackenzie-Beaufort Sea Slope and Amundsen Gulf, Canada: Implications for past sea ice conditions. *Paleoceanography*, 24: 20. doi: 10.1029/2007pa001575.
- Serreze, M.C., Walsh, J.E., Chapin, F.S., Osterkamp, T., Dyurgerov, M., Romanovsky, V., Oechel, W.C., Morison, J., Zhang, T. and Barry, R.G. 2000. Observational evidence of recent change in the northern high-latitude environment. *Climatic Change*, 46(1-2): 159-207.
- Serreze, M.C., Maslanik, J.A., Scambos, T.A., Fetterer, F., Stroeve, J., Knowles, K., Fowler, C., Drobot, S., Barry, R.G. and Haran, T.M. 2003. A record minimum arctic sea ice extent and area in 2002. *Geophysical Research Letters*, 30(3). doi: 10.1029/2002gl016406.
- Serreze, M.C., Holland, M.M. and Stroeve, J. 2007. Perspectives on the Arctic's shrinking sea-ice cover. *Science*, 315(5818): 1533-1536. doi: 10.1126/science.1139426.
- Shaw, J., Taylor, R.B., Solomon, S., Christian, H.A. and Forbes, D.L. 1998. Potential impacts of global sea-level rise on Canadian coasts. *The Canadian Geographer*, 42(4): 365-379.
- Simpson, K.G., Tremblay, J.-É., Gratton, Y. and Price, N.M. 2008. An annual study of inorganic and organic nitrogen and phosphorus and silicic acid in the southeastern Beaufort Sea. *J. Geophys. Res.*, 113. doi: 10.1029/2007jc004462.

- Smol, J.P., Wolfe, A.P., Birks, H.J.B., Douglas, M.S.V., Jones, V.J., Korhola, A., Pienitz, R., Rühland, K., Sorvari, S., Antoniades, D., Brooks, S.J., Fallu, M.A., Hughes, M., Keatley, B.E., Laing, T.E., Michelutti, N., Nazarova, L., Nyman, M., Paterson, A.M., Perren, B., Quinlan, R., Rautio, M., Saulnier-Talbot, E., Siitoneni, S., Solovieva, N. and Weckstrom, J. 2005. Climate-driven regime shifts in the biological communities of arctic lakes. *Proceedings of the National Academy of Sciences of the United States of America*, 102(12): 4397-4402. doi: 10.1073/pnas.0500245102.
- Solomina, O. and Alverson, K. 2004. High latitude Eurasian paleoenvironments: introduction and synthesis. *Palaeogeography Palaeoclimatology Palaeoecology*, 209(1-4): 1-18. doi: 10.1016/j.palaeo.2004.02.027.
- Sorgente, D., Frignani, M., Langone, L. and Ravaioli, M. 1999. Chronology of marine sediments- Interpretation of activity-depth profiles of ^{210}Pb and other radioactive tracers. Part I. Technical Report n. 54., Consiglio Nazionale Delle Ricerche, Istituto Per La Geologia Marina, Bologna. p. 29.
- Steele, M., Morison, J., Ermold, W., Rigor, I., Ortmeyer, M. and Shimada, K. 2004. Circulation of summer Pacific halocline water in the Arctic Ocean. *Journal of Geophysical Research-Oceans*, 109(C2): 18. doi: 10.1029/2003jc002009.
- Stoecker, D.K. 1999. Mixotrophy among dinoflagellates. *Journal of Eukaryotic Microbiology*, 46(4): 397-401.
- Stuiver, M. 1999. GISP2 Oxygen Isotope Data. Available from http://depts.washington.edu/qil/datasets/gisp2_main.html [accessed May 2009].
- Stuiver, M. and Polach, H.A. 1977. Discussion: Reporting of ^{14}C data. *Radiocarbon*, 19: 355-363.
- Stuiver, M., Reimer, P.J. and Reimer, R.W. 2005. CALIB version 5.0. Available from <http://radiocarbon.pa.qub.ac.uk/calib/> [accessed March 2008].
- Tarasov, L. and Peltier, W.R. 2004. A geophysically constrained large ensemble analysis of the deglacial history of the North American ice-sheet complex. *Quaternary Science Reviews*, 23(3-4): 359-388. doi: 10.1016/j.quascirev.2003.08.004.

- Taylor, F.J.R. 1987. Ecology of dinoflagellates: A.General and marine ecosystems. In The Biology of Dinoflagellates. Edited by F.J.R. Taylor. Blackwell Scientific Publications, Oxford. pp. 398-502.
- Thompson, D.W.J. and Wallace, J.M. 1998. The Arctic Oscillation signature in the wintertime geopotential height and temperature fields. *Geophysical Research Letters*, 25(9): 1297-1300.
- Voronina, E., Polyak, L., de Vernal, A. and Peyron, O. 2001. Holocene variations of sea-surface conditions in the southeastern Barents Sea, reconstructed from dinoflagellate cyst assemblages. *Journal of Quaternary Science*, 16(7): 717-726.
- Walsh, J.E. and Chapman, W.L. 1990. Arctic contribution to upper-ocean variability in the North-Atlantic. *Journal of Climate*, 3(12): 1462-1473.
- Wang, J., Cota, G.F. and Comiso, J.C. 2005. Phytoplankton in the Beaufort and Chukchi Seas: Distribution, dynamics, and environmental forcing. *Deep-Sea Research Part II-Topical Studies in Oceanography*, 52(24-26): 3355-3368. doi: 10.1016/j.dsr2.2005.10.014.
- Williams, W.J., Carmack, E.C., Shimada, K., Melling, H., Aagaard, K., Macdonald, R.W. and Ingram, R.G. 2006. Joint effects of wind and ice motion in forcing upwelling in Mackenzie Trough, Beaufort Sea. *Continental Shelf Research*, 26(19): 2352-2366. doi: 10.1016/j.csr.2006.06.012.
- Winsor, P. 2001. Arctic sea ice thickness remained constant during the 1990s. *Geophysical Research Letters*, 28(6): 1039-1041.
- Wu, B.Y., Wang, J. and Walsh, J.E. 2006. Dipole anomaly in the winter Arctic atmosphere and its association with sea ice motion. *Journal of Climate*, 19(2): 210-225.
- Zabenskie, S. and Gajewski, K. 2007. Post-glacial climatic change on Boothia Peninsula, Nunavut, Canada. *Quaternary Research*, 68(2): 261-270. doi: 10.1016/j.yqres.2007.04.003.
- Zhang, R. and Vallis, G.K. 2006. Impact of great salinity anomalies on the low-frequency variability of the North Atlantic climate. *Journal of Climate*, 19(3): 470-482.

- Zonneveld, K.A.F. 1997. Dinoflagellate cyst distribution in surface sediments from the Arabian Sea (northwestern Indian Ocean) in relation to temperature and salinity gradients in the upper water column. Deep Sea Research Part II: Topical Studies in Oceanography, 44(6-7): 1411-1443.
- Zonneveld, K.A.F. and Brummer, G.J.A. 2000. (Palaeo-)ecological significance, transport and preservation of organic-walled dinoflagellate cysts in the Somali Basin, NW Arabian Sea. Deep-Sea Research Part II-Topical Studies in Oceanography, 47(9-11): 2229-2256.
- Zonneveld, K.A.F., Versteegh, G.J.M. and de Lange, G.J. 1997. Preservation of organic-walled dinoflagellate cysts in different oxygen regimes: A 10,000 year natural experiment. Marine Micropaleontology, 29(3-4): 393-405.
- Zonneveld, K.A.F., Versteegh, G.J.M. and de Lange, G.J. 2001. Palaeoproductivity and post-depositional aerobic organic matter decay reflected by dinoflagellate cyst assemblages of the Eastern Mediterranean S1 sapropel. Marine Geology, 172(3-4): 181-195.

ANNEXE 1

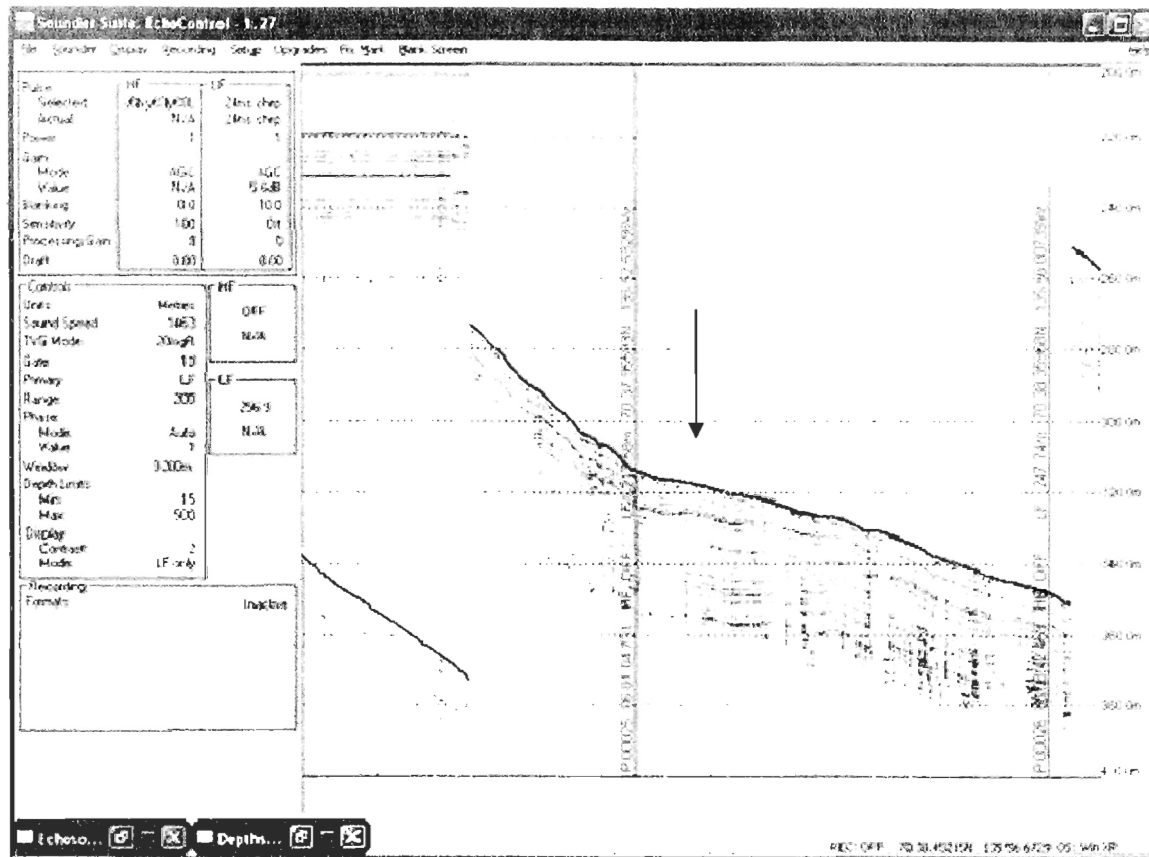


Fig. 7. Image du 3.5 kHz subbottom profiler sur le NGCC Amundsen permettant le choix du site de carottage (station 2004-804-803). À cet emplacement (indiqué par la flèche), l'échosondeur indique une séquence sédimentaire apparemment non-perturbée, c'est-à-dire sans érosion, décrochement, glissement ou coulée gravitaire. (Note : Ne pas tenir compte de la profondeur indiquée).

ANNEXE 2

Table 2. Décomptes des dinokystes dans les carottes sédimentaires de la station 803.

Depth (cm)	Total cysts	Ocen	Pdal	Selo	Bspp	Imin	Imic	Ekar	Eacu	Parc	Other
<i>Core 803BC</i>											
0-1	303	152	54	11	38	30	10	0	1	4	3
1-2	307	198	36	8	31	27	2	0	0	3	2
2-3	315	193	46	7	29	31	3	0	2	4	0
3-4	334	151	110	3	24	36	4	1	3	1	1
4-5	311	119	66	5	44	64	7	0	3	3	0
5-6	301	87	96	8	33	69	4	0	0	3	1
6-7	306	105	92	9	27	63	1	0	1	2	6
7-8	302	119	71	8	45	50	3	0	2	4	0
8-9	306	133	91	8	41	22	4	0	1	3	3
9-10	306	159	61	4	32	39	5	0	1	3	2
10-11	305	147	70	12	21	37	4	6	2	2	4
11-12	303	143	24	9	59	47	3	6	1	8	3
12-13	302	101	86	8	44	48	3	4	1	5	2
13-14	303	91	72	6	54	53	7	12	2	4	2
14-15	303	89	47	11	57	84	3	6	0	6	0
15-16	301	91	49	5	68	66	2	10	0	8	2
16-17	317	80	90	12	20	92	4	7	5	4	3
17-18	307	106	103	10	45	31	4	3	1	2	2
18-19	316	101	95	3	49	41	5	6	2	7	7
19-20	301	109	68	4	74	27	3	5	1	9	1
20-21	305	105	72	11	70	32	5	4	0	4	2
21-22	303	121	85	11	39	32	5	6	1	2	1
22-23	303	105	82	8	71	25	3	4	0	4	1
23-24	310	89	32	4	92	62	6	6	4	15	0
24-25	306	101	62	14	63	47	4	6	2	4	3
25-26	307	60	112	2	40	70	7	9	1	6	0
26-27	303	112	32	7	68	49	14	4	5	11	1
27-28	307	78	67	10	41	86	8	8	2	5	2
28-29	311	75	29	6	76	96	7	8	2	9	3
29-30	303	96	44	15	76	60	6	0	1	4	1
30-31	308	64	51	3	93	65	8	12	0	9	3
31-32	303	73	66	10	48	72	6	19	2	6	1
32-33	302	84	83	6	55	55	7	7	0	3	2
33-34	301	86	96	10	50	40	4	8	3	4	0
<i>Core 803TWC</i>											
0-1	305	98	120	5	21	52	1	5	0	3	0
10-11	307	118	81	12	42	36	5	3	0	3	7
20-21	304	71	58	11	63	75	10	6	0	7	3
30-31	308	87	34	2	67	90	5	10	3	3	7
40-41	305	83	41	10	60	94	1	9	1	6	0
50-51	312	142	66	4	24	57	5	6	3	3	2
60-61	279	73	44	7	44	67	10	7	5	11	11
70-71	303	97	88	3	13	78	6	10	6	1	1
80-81	307	45	105	7	37	68	14	17	3	6	5
90-91	306	73	97	6	42	69	6	4	3	6	0
100-101	307	46	38	2	61	104	16	24	7	5	4
105-106	309	71	77	12	45	70	13	12	2	6	1

ANNEXE 2 (suite)

Depth (cm)	Total cysts	Ocen	Pdal	Selo	Bspp	Imin	Imic	Ekar	Eacu	Parc	Other
<i>Core 803PC</i>											
0-1	302	190	67	13	19	10	1	1	0	1	0
10-11	303	178	48	5	40	24	4	0	0	3	1
16-17	253	80	68	14	58	28	1	2	0	2	0
26-27	307	113	29	6	96	48	2	1	2	7	3
36-37	270	123	22	8	80	30	2	2	0	3	0
46-47	304	125	37	10	69	58	1	2	1	0	1
56-57	280	125	43	19	50	30	3	0	0	10	0
66-67	302	121	48	6	77	44	2	0	0	4	0
76-77	313	74	62	3	42	102	15	8	3	4	0
86-87	303	100	22	4	61	78	18	6	5	5	4
96-97	313	90	59	6	50	79	7	15	5	1	1
106-107	305	67	144	15	21	47	3	3	1	3	1
116-117	306	136	28	12	48	56	6	10	3	6	1
126-127	303	86	18	2	84	85	7	6	7	8	0
136-137	303	114	17	16	57	66	9	14	0	8	2
146-147	313	85	46	5	70	69	9	18	5	3	3
156-157	305	61	89	5	55	85	6	0	1	1	1
166-167	303	114	41	11	51	71	6	3	0	6	0
176-177	309	77	108	3	25	81	8	3	0	3	1
186-187	322	80	30	6	87	90	7	5	1	11	5
196-197	305	127	14	15	116	26	3	0	0	3	1
206-207	309	86	36	11	108	55	2	1	2	7	1
216-217	304	112	23	12	74	56	7	6	3	11	0
226-227	304	97	41	7	73	57	4	12	3	10	0
236-237	309	133	24	11	74	46	5	0	3	13	0
246-247	309	56	22	9	108	85	3	18	0	8	0
256-257	302	124	46	10	86	20	2	5	0	7	2
266-267	316	80	18	14	135	38	2	2	13	13	1
276-277	307	87	21	7	54	109	4	11	5	4	5
286-287	305	118	3	8	137	19	5	9	1	5	0
296-297	316	165	11	11	56	63	1	0	0	9	0
306-307	292	146	32	16	60	19	2	1	0	11	5
316-317	302	71	66	4	87	53	5	2	0	9	4
326-327	309	129	29	18	93	23	2	4	3	6	1
336-337	302	75	96	16	67	25	3	10	0	9	1
346-347	302	182	35	14	33	30	1	4	2	1	0
356-357	336	201	37	13	45	29	3	2	0	3	3
366-367	306	176	36	8	52	27	5	2	0	0	0
376-377	305	200	21	3	36	36	2	3	0	3	1
386-387	306	93	103	7	32	51	11	4	1	4	0
396-397	302	148	76	21	14	26	6	4	0	3	4
406-407	307	80	16	19	81	83	9	3	3	2	11
416-417	307	156	15	6	67	42	10	1	5	5	0
426-427	301	77	8	2	86	96	15	4	4	9	0
436-437	304	132	9	18	82	40	1	10	3	8	1
446-447	306	142	46	13	36	57	2	7	0	0	3
456-457	301	156	76	11	18	22	5	10	0	3	0
466-467	310	115	26	19	99	27	3	11	7	2	1
476-477	305	160	63	16	22	26	6	8	2	2	0
486-487	314	208	26	11	23	32	3	8	2	1	0

ANNEXE 2 (suite et fin)

Depth (cm)	Total cysts	Ocen	Pdal	Selo	Bspp	Imin	Imic	Ekar	Eacu	Parc	Other
<i>Core 803PC (continued)</i>											
496-497	302	136	51	22	38	33	7	10	0	3	2
506-507	304	192	43	11	14	23	2	11	3	3	2
516-517	305	167	16	17	45	28	8	18	4	2	0
526-527	309	106	22	15	64	75	12	5	4	4	2
536-537	302	136	23	2	26	72	15	23	3	2	0
546-547	304	170	15	4	43	34	6	26	2	3	1
556-557	313	105	36	23	38	86	9	13	1	2	0
566-567	304	186	36	10	27	22	6	12	1	4	0
576-577	315	130	143	2	11	19	3	4	0	3	0
586-587	301	99	51	6	70	42	5	16	4	5	3
596-597	303	188	23	9	27	31	4	9	2	2	8
606-607	334	172	94	9	21	19	6	5	3	4	1
613-614	301	211	21	12	31	20	2	2	2	0	0

Ocen = *Operculodinium centrocarpum* sensu Wall & Dale 1966 + *O. centrocarpum*-short processes + *O. centrocarpum*-arctic morphotype; Pdal = cyst of *Pentapharsodinium dalei*; Selo = *Spiniferites elongatus/frigidus*; Bspp = *Brigantedinium* spp. (including *B. simplex* and *B. cariacense*); Imin = *Islandinium minutum*; Imic = *I. minutum* var. *cezare*; Ekar = cf. *Echinidinium karaense*; Eacu = *E. aculeatum*; Parc = cyst of *Polykrikos* spp.-arctic/quadratus morphotypes; Other = rare taxa (*Impagidinium pallidum*, *Spiniferites ramosus*, *S. spp.*, *Nematosphaeropsis labyrinthus*, cyst of *Polykrikos schwartzii* and cyst of *Protoperidinium americanum*) as well as unidentified specimens.

ANNEXE 3

Table 3. Concentrations des principaux palynomorphes dans les carottes sédimentaires de la station 803 (exprimées en individus par centimètre cube de sédiment humide).

Depth (cm)	Pollen grains	Spores	Dinocysts	Foraminifer linings	Copepod eggs	Reworked palynomorphs	Freshwater protists	Tintinnids
<i>Core 803BC</i>								
0-1	526	155	1735	1268	25	4606	107	0
1-2	376	290	4210	1221	392	5459	46	23
2-3	465	154	3543	1076	154	4347	88	0
3-4	246	198	3055	813	330	5690	159	0
4-5	735	144	1366	637	103	5490	101	0
5-6	497	57	1366	720	179	3580	99	42
6-7	512	76	1668	1152	203	5128	191	0
7-8	617	140	1315	1651	47	5257	71	0
8-9	346	90	2049	452	316	4815	149	45
9-10	328	136	877	504	81	2855	47	0
10-11	645	112	1252	936	314	5765	195	4
11-12	453	88	1116	1888	22	3864	81	0
12-13	346	138	950	1889	300	4815	95	0
13-14	410	129	992	1460	109	3620	10	0
14-15	463	310	971	1920	159	5158	126	0
15-16	399	53	495	1071	105	3086	77	0
16-17	333	135	1200	926	65	5085	76	0
17-18	101	65	1393	935	109	2935	90	0
18-19	87	116	1210	766	49	3457	99	0
19-20	333	36	798	1249	11	2516	35	0
20-21	476	113	1748	3027	316	6461	181	23
21-22	321	76	1003	628	23	2289	67	0
22-23	329	122	1143	877	82	4811	183	0
23-24	537	314	990	1293	103	3575	64	0
24-25	522	111	1514	1353	266	5036	116	0
25-26	220	196	1151	1233	255	6030	113	0
26-27	312	18	1223	972	73	2695	61	0
27-28	442	74	791	345	71	4788	89	0
28-29	410	89	780	532	89	2130	72	0
29-30	760	212	711	873	165	2798	35	0
30-31	346	78	680	925	95	6762	132	0
31-32	262	76	943	659	88	2636	57	0
32-33	437	86	829	553	207	3893	129	0
33-34	333	38	869	1192	39	2763	58	0
<i>Core 803TWC</i>								
0-1	229	131	1373	655	37	4493	182	0
10-11	307	56	1414	1619	56	4726	160	0
20-21	240	59	694	2887	236	5715	92	20
30-31	277	70	692	1535	37	5653	75	0
40-41	178	79	1281	2763	109	7399	126	8
50-51	329	51	2746	2209	205	6831	173	20
60-61	213	164	1521	2415	193	6183	256	19
70-71	251	116	870	483	135	4811	116	0
80-81	258	108	1167	1818	103	5226	73	0
90-91	383	124	1760	1463	144	6368	152	0
100-101	332	44	1114	2173	223	4386	125	0
105-106	364	279	1056	1469	362	5674	79	23

ANNEXE 3 (suite)

Depth (cm)	Pollen grains	Spores	Dinocysts	Foraminifer linings	Copepod eggs	Reworked palynomorphs	Freshwater protists	Tintinnids
<i>Core 803PC</i>								
0-1	339	60	1686	524	75	2694	101	0
10-11	222	90	674	796	30	3156	30	0
16-17	244	49	341	472	310	1084	64	7
26-27	108	127	260	272	27	5337	30	0
36-37	146	43	169	266	43	2261	31	5
46-47	206	29	529	540	241	2209	40	0
56-57	228	112	402	739	201	3716	53	22
66-67	613	58	431	323	184	7326	24	46
76-77	193	27	1171	1011	72	1472	126	18
86-87	411	80	1039	1468	147	6241	136	49
96-97	335	99	980	1105	93	2525	123	12
106-107	664	237	1512	1785	489	11027	133	24
116-117	278	80	973	751	24	2905	166	12
126-127	218	20	631	1398	158	1369	111	10
136-137	392	151	853	1053	202	6565	104	0
146-147	457	39	1199	1845	45	1890	173	58
156-157	315	51	859	1371	42	1596	162	33
166-167	306	119	865	1453	331	7825	164	0
176-177	312	56	2144	1055	125	1076	180	21
186-187	332	40	751	944	35	1605	149	9
196-197	487	55	1284	1421	16	2537	55	31
206-207	590	66	1144	1157	44	2654	129	7
216-217	403	27	1124	1168	33	2242	59	20
226-227	262	61	1125	1183	13	1775	78	20
236-237	406	25	811	939	50	1910	71	0
246-247	426	31	358	461	21	1720	44	16
256-257	258	30	580	431	52	2185	88	0
266-267	265	40	683	643	30	1351	108	3
276-277	271	128	565	535	43	4604	62	0
286-287	362	38	511	765	13	2458	30	0
296-297	383	43	1170	944	7	1853	125	0
306-307	272	35	328	282	19	2007	51	0
316-317	372	22	1013	1935	83	2009	121	9
326-327	290	20	782	770	50	2460	110	0
336-337	449	48	719	786	128	2220	72	0
346-347	553	39	1313	440	129	1706	39	0
356-357	477	160	1111	1020	102	5077	122	24
366-367	170	50	765	424	85	1712	38	0
376-377	497	43	1050	752	71	1958	30	0
386-387	327	131	1646	1503	152	6578	212	11
396-397	246	36	1364	355	73	1922	54	9
406-407	421	230	555	899	184	4953	125	46
416-417	331	7	778	431	131	1175	39	0
426-427	367	125	624	234	31	2918	44	16
436-437	356	59	515	912	20	2294	25	10
446-447	582	47	889	752	23	8269	80	0
456-457	234	34	1271	368	7	1453	41	0
466-467	374	13	674	874	9	1952	29	0
476-477	454	179	1818	2507	45	10385	124	0

ANNEXE 3 (suite et fin)

Depth (cm)	Pollen grains	Spores	Dinocysts	Foraminifer linings	Copepod eggs	Reworked palynomorphs	Freshwater protists	Tintinnids
<i>Core 803PC (continued)</i>								
486-487	330	17	754	415	25	1235	23	0
496-497	392	38	1445	1655	19	3501	91	0
506-507	446	39	1701	1909	79	3641	135	0
516-517	611	21	1272	2533	185	3254	177	0
526-527	716	215	1396	1313	69	8087	106	0
536-537	379	0	1410	1033	12	1869	88	0
546-547	810	171	591	640	97	3801	105	0
556-557	1044	115	1210	1613	115	10321	177	46
566-567	1320	76	2899	3616	153	5678	277	0
576-577	864	116	1620	716	77	5708	156	0
586-587	438	12	1169	641	109	2596	80	10
596-597	508	69	732	424	34	2694	46	14
606-607	437	18	4355	942	55	1957	81	0
613-614	841	145	768	559	62	6753	83	6

Reworked palynomorphs consist in pre-Quaternary fossil pollen grains, spores and dinocysts eroded and advected (mostly by the Mackenzie River) at station 803. Freshwater protists include the acritarch *Halodinium*, the colonial green algae *Pediastrum* as well as *Zygnema*-type spores.

ANNEXE 4

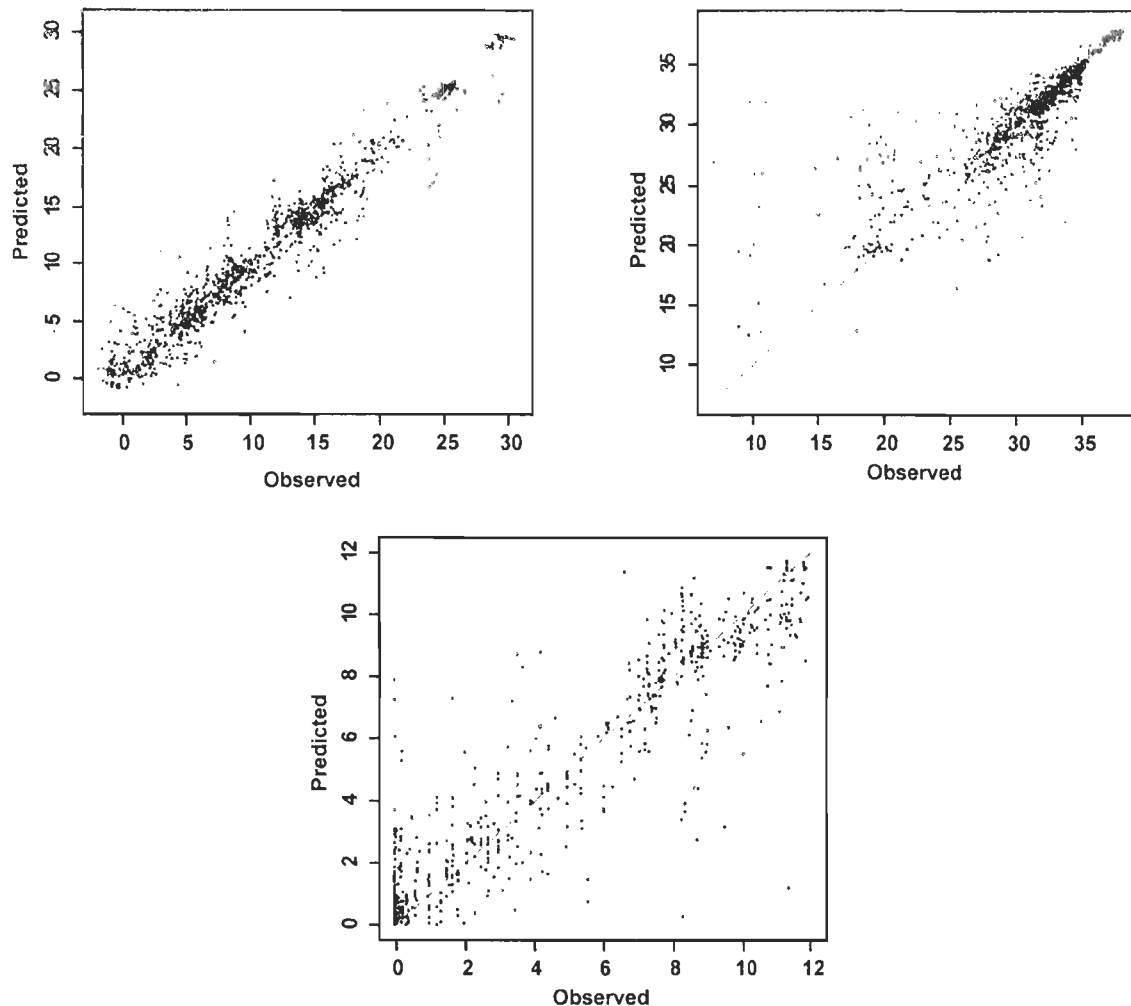


Fig. 8. Résultats des exercices de validation des paramètres reconstitués suivant la technique des meilleurs analogues modernes (MAT), utilisant la base de données de référence « n = 1189 » (voir section 2.3.4; de Vernal et al. 2005b). **A.** Température des eaux de surface en août (°C): $R^2 = 0,957$; RMSE (Root mean square error) = 1,652. **B.** Salinité des eaux de surface en août: $R^2 = 0,742$; RMSE = 2,467. **C.** Durée du couvert de glace (mois par année): $R^2 = 0,904$; RMSE = 1,188.

ANNEXE 5

Table 4. Liste des cinq meilleurs analogues modernes de la base de données de référence comprenant 1189 sites et 63 taxons, pour chacun des assemblages fossiles des carottes de la station 803. Les distances statistiques sont indiquées entre parenthèses.

Depth (cm)	Analogue 1	Analogue 2	Analogue 3	Analogue 4	Analogue 5
<i>Core 803BC</i>					
0-1	F1260 (0.0508)	F1258 (0.1084)	F1259 (0.1185)	F1237 (0.1260)	F1249 (0.1578)
1-2	F1234 (0.0719)	F1258 (0.0768)	F1243 (0.0778)	F1238 (0.0852)	F1257 (0.0918)
2-3	F1234 (0.0926)	F1243 (0.0926)	F1238 (0.1146)	F1257 (0.1162)	F1251 (0.1290)
3-4	F1257 (0.1836)	F1237 (0.1902)	F1238 (0.1976)	Z547 (0.2106)	F1246 (0.2154)
4-5	F1257 (0.1357)	F1255 (0.1367)	F1243 (0.1476)	F1256 (0.1485)	F1258 (0.1526)
5-6	F1237 (0.0735)	F1243 (0.0768)	F1257 (0.0816)	F1256 (0.0935)	F1255 (0.0985)
6-7	F1237 (0.1461)	F1251 (0.1695)	F1243 (0.1995)	F1257 (0.2083)	H1117 (0.2132)
7-8	F1243 (0.1022)	F1257 (0.1136)	F1234 (0.1148)	F1256 (0.1185)	F1255 (0.1304)
8-9	F1237 (0.0663)	F1257 (0.1187)	F1260 (0.1189)	F1243 (0.1229)	F1238 (0.1283)
9-10	F1260 (0.0939)	F1258 (0.1138)	F1237 (0.1307)	F1259 (0.1324)	F1257 (0.1425)
10-11	H1117 (0.1833)	H1115 (0.2346)	H1119 (0.2563)	F1251 (0.2596)	F1258 (0.2789)
11-12	F1260 (0.2445)	H1115 (0.2600)	H1117 (0.3018)	F1258 (0.3050)	F1237 (0.3200)
12-13	H1117 (0.1026)	H1115 (0.1470)	F1251 (0.2050)	F1243 (0.2180)	F1256 (0.2296)
13-14	H1115 (0.2450)	F1258 (0.3107)	Z435 (0.3163)	H1117 (0.3243)	F1249 (0.3708)
14-15	H1115 (0.0857)	H1117 (0.1228)	F1256 (0.1996)	F1255 (0.2138)	F1243 (0.2170)
15-16	H1115 (0.2258)	H1117 (0.2380)	F1237 (0.3229)	F1256 (0.3335)	F1260 (0.3382)
16-17	H1117 (0.2406)	H1115 (0.2756)	H1119 (0.3449)	F1258 (0.3534)	F1251 (0.3694)
17-18	F1237 (0.1678)	H1115 (0.1722)	F1257 (0.2025)	F1260 (0.2140)	H1117 (0.2148)
18-19	F1260 (0.2710)	H1115 (0.2962)	F1258 (0.3072)	F1259 (0.3437)	F1237 (0.3570)
19-20	H1115 (0.2103)	F1237 (0.2472)	F1234 (0.2501)	F1243 (0.2676)	H1117 (0.2704)
20-21	H1115 (0.0932)	F1237 (0.1664)	H1117 (0.1682)	F1257 (0.1814)	F1243 (0.1889)
21-22	H1115 (0.1519)	F1258 (0.2045)	H1117 (0.2057)	F1257 (0.2247)	F1243 (0.2443)
22-23	H1115 (0.0959)	H1117 (0.1411)	F1257 (0.1528)	F1243 (0.1592)	F1238 (0.1593)
23-24	H1115 (0.2594)	F1256 (0.3282)	F1255 (0.3303)	Z435 (0.3581)	H1117 (0.3592)
24-25	H1115 (0.1285)	H1117 (0.1817)	F1243 (0.2590)	F1257 (0.2605)	F1256 (0.2618)
25-26	H1115 (0.2033)	H1117 (0.2913)	F1255 (0.2981)	F1256 (0.3055)	F1243 (0.3135)
26-27	H1115 (0.2580)	F1255 (0.3220)	F1256 (0.3334)	F1258 (0.3487)	F1248 (0.3664)
27-28	H1115 (0.1687)	H1117 (0.2672)	F1255 (0.3119)	F1256 (0.3154)	F1258 (0.3191)
28-29	H1115 (0.2215)	Z435 (0.3001)	H1117 (0.3122)	F1255 (0.3276)	F1256 (0.3327)
29-30	F1258 (0.1183)	F1255 (0.1195)	F1256 (0.1224)	F1257 (0.1341)	F1237 (0.1342)
30-31	H1115 (0.2336)	Z435 (0.2672)	F1260 (0.3173)	F1258 (0.3232)	H1117 (0.3345)
31-32	H1115 (0.2155)	H1117 (0.2980)	Z435 (0.3195)	F1258 (0.3585)	F1256 (0.4145)
32-33	H1117 (0.1496)	H1115 (0.1596)	F1257 (0.2655)	F1251 (0.2669)	H1119 (0.2727)
33-34	H1115 (0.1701)	H1117 (0.2289)	F1243 (0.3001)	F1257 (0.3041)	F1256 (0.3178)
<i>Core 803TWC</i>					
0-1	H1117 (0.1342)	H1115 (0.1760)	F1243 (0.1918)	F1234 (0.1992)	F1257 (0.2196)
10-11	F1260 (0.1041)	F1237 (0.1762)	H1115 (0.1781)	F1258 (0.1958)	F1259 (0.2011)
20-21	H1115 (0.0888)	F1258 (0.1636)	Z435 (0.1982)	H1117 (0.2175)	F1255 (0.2199)
30-31	Z435 (0.3364)	H1115 (0.4025)	F1260 (0.4040)	F1258 (0.4195)	H1117 (0.4207)
40-41	H1117 (0.1558)	H1115 (0.1932)	Z435 (0.3143)	F1256 (0.3148)	F1243 (0.3294)
50-51	F1258 (0.2877)	H1115 (0.2954)	F1249 (0.3095)	H1117 (0.3369)	F1243 (0.3408)
60-61	H1115 (0.2651)	F1258 (0.3403)	Z435 (0.3586)	F1255 (0.3871)	F1256 (0.3892)
70-71	H1115 (0.3650)	H1117 (0.3863)	F1246 (0.3981)	F1257 (0.4145)	Z547 (0.4342)
80-81	H1115 (0.2074)	H1117 (0.3552)	Z435 (0.3861)	F1255 (0.4007)	F1248 (0.4090)
90-91	H1115 (0.1626)	F1256 (0.2489)	F1255 (0.2513)	H1117 (0.2539)	F1243 (0.2542)
100-101	Z435 (0.3980)	H1115 (0.4425)	H1117 (0.5581)	F1258 (0.5597)	F1255 (0.5796)
105-106	H1115 (0.1390)	H1117 (0.2809)	F1255 (0.3185)	F1258 (0.3237)	Z435 (0.3257)

ANNEXE 5 (suite)

Depth (cm)	Analogue 1	Analogue 2	Analogue 3	Analogue 4	Analogue 5
<i>Core 803PC</i>					
0-1	F1238 (0.0774)	F1237 (0.0984)	F1257 (0.1033)	F1245 (0.1036)	F1234 (0.1116)
10-11	F1237 (0.0447)	F1257 (0.0713)	F1238 (0.0741)	F1243 (0.0759)	F1234 (0.0764)
16-17	H1117 (0.0738)	H1115 (0.0972)	F1257 (0.1422)	F1243 (0.1534)	F1234 (0.1670)
26-27	F1237 (0.2378)	F1260 (0.2391)	F1256 (0.2714)	F1234 (0.2845)	F1255 (0.2863)
36-37	H1115 (0.1291)	H1117 (0.1322)	F1257 (0.1562)	F1234 (0.1653)	F1256 (0.1656)
46-47	H1117 (0.1249)	Z547 (0.1686)	H1119 (0.1815)	F995 (0.2004)	H130 (0.2099)
56-57	F1243 (0.0504)	F1234 (0.0518)	F1256 (0.0552)	F1258 (0.0791)	F1255 (0.0837)
66-67	F1257 (0.0763)	F1256 (0.0765)	F1234 (0.0774)	F1243 (0.0776)	F1255 (0.0882)
76-77	H1115 (0.2358)	F1255 (0.3165)	Z435 (0.3232)	F1256 (0.3446)	F1258 (0.3493)
86-87	Z435 (0.3187)	F1258 (0.3498)	H1115 (0.3716)	F1249 (0.4100)	F1255 (0.4253)
96-97	H1115 (0.2978)	H1117 (0.3220)	Z435 (0.3799)	F1257 (0.4121)	Z547 (0.4263)
106-107	H1115 (0.1289)	F1258 (0.1734)	H1117 (0.1781)	F1243 (0.1860)	F1257 (0.2072)
116-117	H1115 (0.2306)	H1117 (0.3075)	Z435 (0.3611)	F1256 (0.3681)	F1255 (0.3707)
126-127	H1115 (0.3727)	Z435 (0.3742)	F1255 (0.4028)	F1256 (0.4194)	H1117 (0.4468)
136-137	H1115 (0.1659)	Z435 (0.2094)	F1258 (0.2762)	H1117 (0.2763)	F1255 (0.3351)
146-147	Z435 (0.3626)	H1115 (0.3770)	F1258 (0.4388)	H1117 (0.4475)	F1249 (0.4989)
156-157	F1257 (0.0864)	Z547 (0.1132)	F1264 (0.1255)	F1255 (0.1262)	F1246 (0.1282)
166-167	H1115 (0.0596)	F1256 (0.1320)	F1255 (0.1344)	F1258 (0.1429)	H1117 (0.1469)
176-177	F1258 (0.1523)	H1115 (0.1604)	F1249 (0.1746)	F1255 (0.1962)	F1257 (0.1979)
186-187	H1115 (0.1472)	F1255 (0.2208)	F1256 (0.2239)	Z435 (0.2336)	H1117 (0.2436)
196-197	F1258 (0.0894)	F998 (0.1302)	F1257 (0.1450)	F1256 (0.1579)	F1255 (0.1586)
206-207	H1115 (0.1677)	F1256 (0.1766)	H1117 (0.1940)	F1255 (0.1953)	F1243 (0.2030)
216-217	H1115 (0.1868)	F1256 (0.2947)	H1117 (0.2972)	F1255 (0.2982)	F1258 (0.3145)
226-227	H1115 (0.2249)	H1117 (0.2899)	Z435 (0.3577)	F1256 (0.3588)	F1255 (0.3699)
236-237	F1256 (0.1495)	F1255 (0.1619)	F1234 (0.1779)	F1258 (0.1798)	F1243 (0.1808)
246-247	H1115 (0.1807)	H1117 (0.2091)	Z435 (0.2377)	F1256 (0.3571)	F1255 (0.3651)
256-257	H1115 (0.1895)	F1258 (0.2143)	H1117 (0.2222)	F1234 (0.2493)	F1243 (0.2655)
266-267	H1115 (0.3920)	F1258 (0.4061)	F998 (0.4145)	F1256 (0.4336)	H1117 (0.4369)
276-277	Z435 (0.3668)	H1115 (0.3866)	H1117 (0.4061)	F1260 (0.4273)	F1258 (0.4640)
286-287	Z435 (0.3082)	H1115 (0.3426)	F998 (0.3759)	H1117 (0.3865)	F1255 (0.4306)
296-297	F994 (0.1049)	F1234 (0.1316)	F998 (0.1332)	F1256 (0.1358)	F997 (0.1413)
306-307	F1260 (0.1520)	F1237 (0.2125)	F1234 (0.2577)	F1258 (0.2609)	F1241 (0.2681)
316-317	F1260 (0.1420)	F1258 (0.1683)	H1115 (0.2015)	F1256 (0.2282)	F1259 (0.2283)
326-327	H1115 (0.2000)	H1117 (0.2250)	F998 (0.2793)	F1234 (0.2797)	F1243 (0.2879)
336-337	H1115 (0.1210)	H1117 (0.1980)	F1258 (0.2497)	F1243 (0.2814)	F1234 (0.2854)
346-347	H1117 (0.1758)	Z547 (0.2395)	H1115 (0.2497)	F1257 (0.2510)	F1238 (0.2687)
356-357	F1258 (0.1112)	F1243 (0.1370)	F1257 (0.1390)	H1115 (0.1403)	F1234 (0.1428)
366-367	Z547 (0.0705)	F1257 (0.1240)	F1264 (0.1573)	H131 (0.1749)	H130 (0.1778)
376-377	F994 (0.1730)	F1234 (0.1738)	F1243 (0.1885)	F1238 (0.1938)	F1257 (0.1943)
386-387	H1115 (0.0991)	F1243 (0.1844)	F1255 (0.1868)	F1257 (0.1886)	F1248 (0.1943)
396-397	F1260 (0.1645)	F1258 (0.1926)	H1115 (0.1985)	F1249 (0.2187)	F1237 (0.2298)
406-407	F1258 (0.2796)	Z435 (0.2833)	H1115 (0.3418)	F1249 (0.3633)	H135 (0.3715)
416-417	F1255 (0.2302)	F1256 (0.2489)	F1258 (0.2545)	H1115 (0.2704)	F1257 (0.2730)
426-427	Z435 (0.3111)	F1255 (0.3585)	H1115 (0.3680)	F1256 (0.3924)	F1258 (0.4191)
436-437	H1117 (0.3265)	H1115 (0.3556)	Z435 (0.3773)	F998 (0.4333)	F1258 (0.4453)
446-447	H1117 (0.1934)	Z547 (0.2047)	H1119 (0.2218)	F1257 (0.2760)	H1115 (0.2870)
456-457	H1115 (0.1268)	H1117 (0.1961)	F1243 (0.2052)	F1238 (0.2202)	F1234 (0.2216)
466-467	H1115 (0.3012)	H1117 (0.3069)	Z435 (0.4299)	F1257 (0.4325)	Z547 (0.4626)
476-477	H1115 (0.1671)	H1117 (0.2340)	F1257 (0.2585)	F1243 (0.2599)	F1238 (0.2750)

ANNEXE 5 (suite et fin)

Depth (cm)	Analogue 1	Analogue 2	Analogue 3	Analogue 4	Analogue 5
<i>Core 803PC (continued)</i>					
486-487	H1117 (0.2338)	H1115 (0.2547)	Z547 (0.2783)	F1257 (0.2881)	F1238 (0.3078)
496-497	H1115 (0.0786)	H1117 (0.1661)	F1243 (0.2333)	F1257 (0.2341)	F1258 (0.2419)
506-507	H1117 (0.3422)	H1115 (0.3423)	F1258 (0.3862)	F1243 (0.3904)	F1234 (0.3921)
516-517	H1115 (0.2910)	H1117 (0.3545)	Z435 (0.3923)	F1257 (0.4465)	F1264 (0.4571)
526-527	H1115 (0.2532)	F1258 (0.2689)	Z435 (0.2765)	F1249 (0.3477)	F1255 (0.3579)
536-537	Z435 (0.3832)	H1115 (0.3847)	H1117 (0.4618)	F1255 (0.4835)	F1257 (0.5041)
546-547	H1115 (0.3361)	Z435 (0.3628)	H1117 (0.3700)	F1255 (0.4695)	F1257 (0.4731)
556-557	H1115 (0.1356)	H1117 (0.2081)	Z435 (0.2675)	F1258 (0.3107)	F1257 (0.3254)
566-567	H1115 (0.1787)	H1117 (0.2554)	F1243 (0.2773)	F1234 (0.2838)	F1238 (0.2949)
576-577	F1238 (0.1615)	F1234 (0.1669)	F1243 (0.1698)	F1257 (0.1952)	F1237 (0.2104)
586-587	H1115 (0.3474)	H1117 (0.4063)	F1260 (0.4579)	F1237 (0.4676)	Z435 (0.4782)
596-597	H1117 (0.2995)	F1251 (0.4203)	H1119 (0.4222)	F1244 (0.4232)	H133 (0.4277)
606-607	H1115 (0.1976)	F1243 (0.2145)	F1238 (0.2206)	F1234 (0.2230)	F1257 (0.2363)
613-614	Z547 (0.1547)	F1257 (0.2318)	F1002 (0.2627)	F1238 (0.2672)	F1264 (0.2685)

The 'n=1189' reference database is available by request from www.geotop.ca. See section 1.2.2 for details on the calculation of the statistical distance of each modern spectrum to the fossil assemblage. The thresholds adopted (1st quartile of random distances) for the BC, TWC and PC are 1.267, 1.312 and 1.300, respectively.

ANNEXE 6

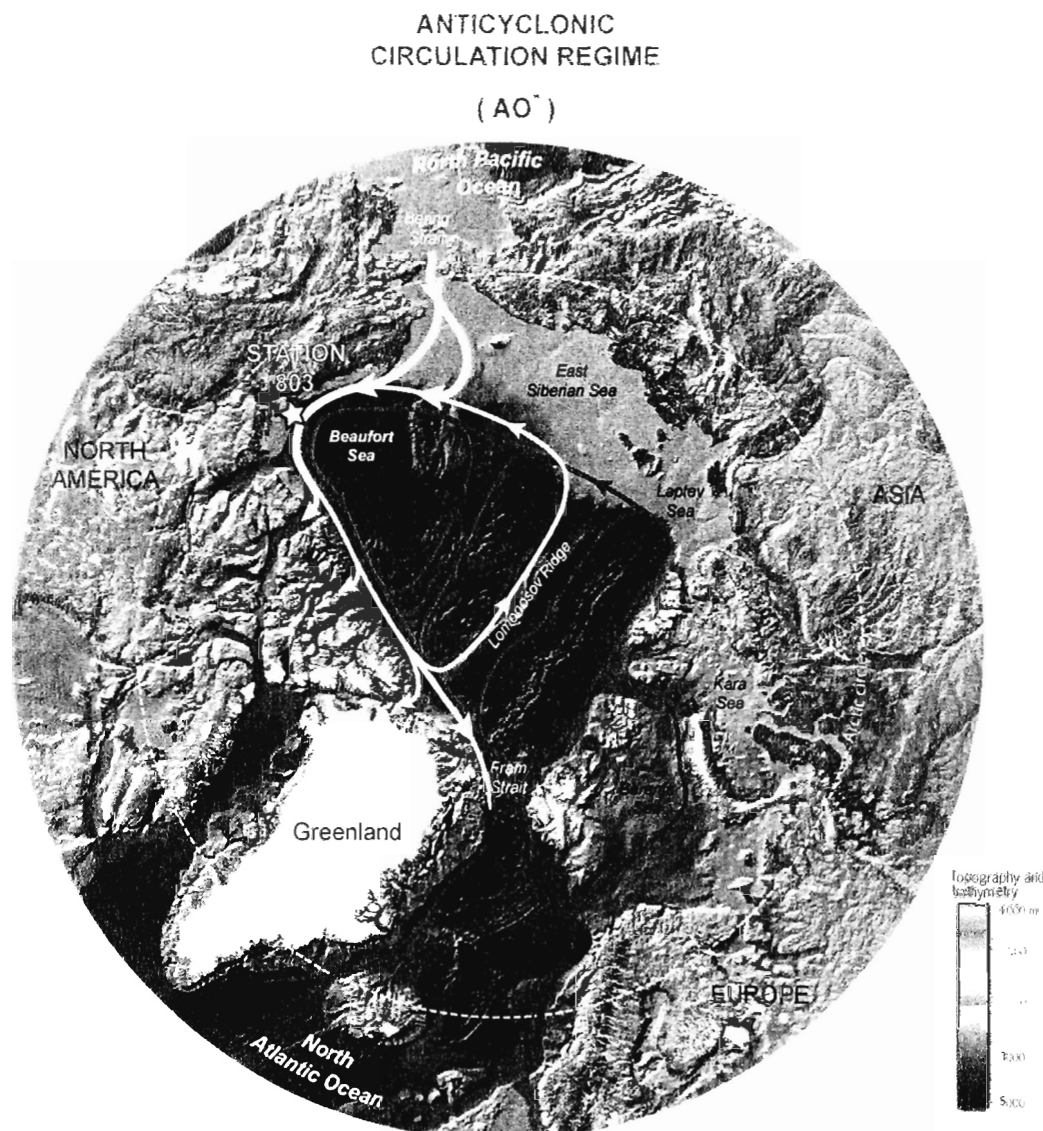


Fig. 9. Circulation des eaux pacifiques (flèches blanches) et atlantiques (flèches rouges) pendant les phases de circulation atmosphérique anticyclonique / phases négatives de l’Oscillation arctique (McLaughlin et al. 2002). L’advection d’eau pacifique dans l’Océan Arctique est maximale. Son influence est accrue à la station 803 et s’étend jusqu’à la dorsale de Lomonosov. La circulation des eaux de surface (e.g., gyre de Beaufort, dérive transpolaire) n’est pas représentée. FSB = *Fram Strait Branch*; BSB = *Barents Sea Branch*.

ANNEXE 6 (suite et fin)

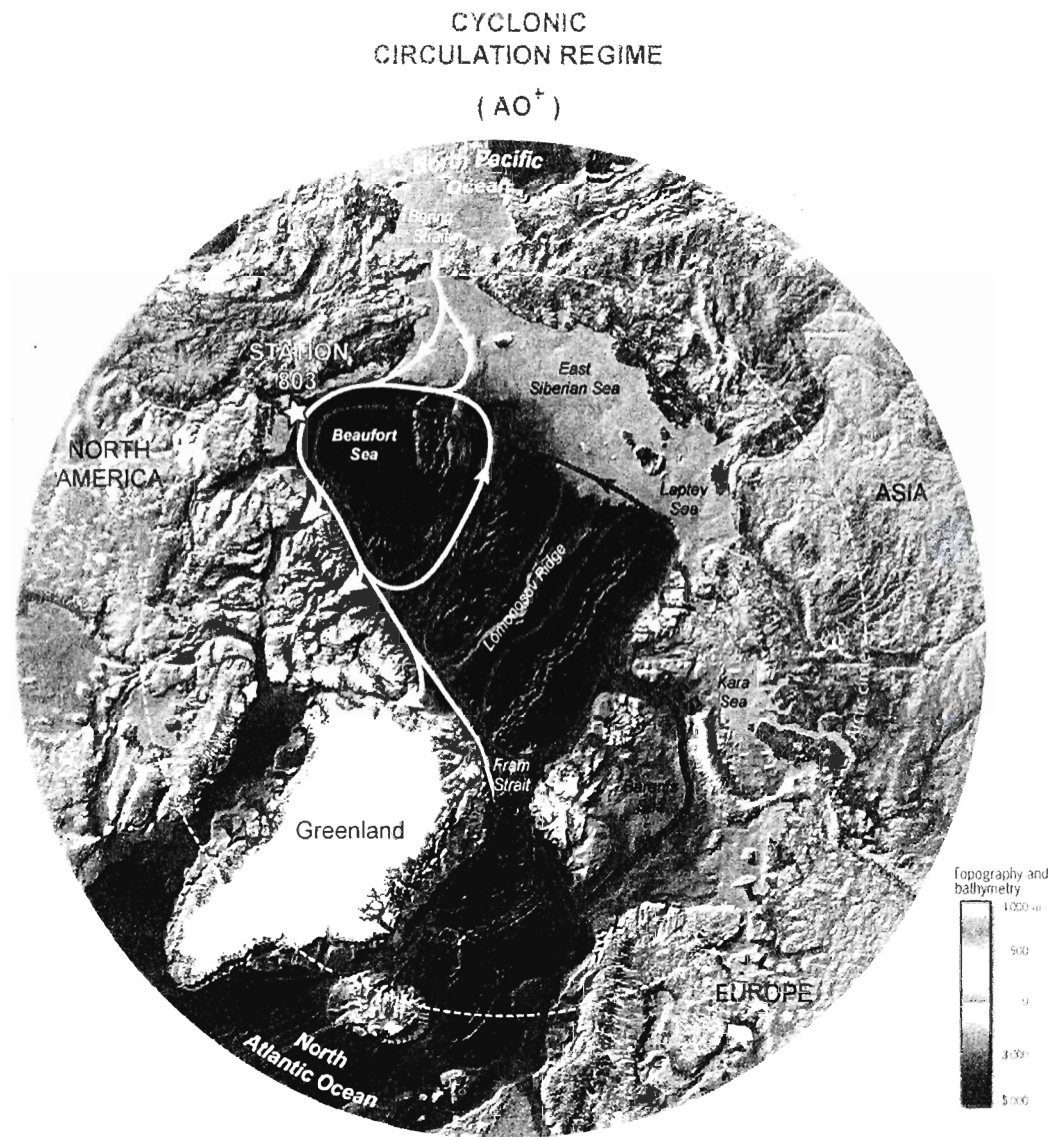


Fig. 10. Circulation des eaux pacifiques (flèches blanches) et atlantiques (flèches rouges) pendant les phases de circulation atmosphérique cyclonique / phases positives de l'Oscillation arctique (McLaughlin et al. 2002). La pénétration d'eau pacifique par le détroit de Béring est moins importante que pendant le régime anticyclonique (AO^-). Son influence est réduite au Bassin Canadien. FSB = *Fram Strait Branch*; BSB = *Barents Sea Branch*.

